APPLICATION OF MINERALOGY IN THE INTERPRETATION OF LABORATORY SCALE ACID ROCK DRAINAGE (ARD) PREDICTION TESTS: A GOLD CASE STUDY

NOLUNTU DYANTYI

Dissertation in fulfilment of the degree of Master of Science in Chemical Engineering

October 2014

DECLARATION

"I know the meaning of plagiarism and declare that all the work in this document, save for that which is properly acknowledged, is my own"

Noluntu Dyantyi

October 2014

ABSTRACT

The mining and beneficiation of gold generates large tonnages of waste, with up to 99% of mined gold ore discharged as waste. The waste generated contains unoxidized sulfides that when exposed to air and water react to form acid, which results in acid rock drainage (ARD). ARD is usually associated with low pH, high sulfate content and elevated concentrations of toxic elements. The mobility of ARD affects our scarce water resources, land and aquatic species. Methods applied to treat ARD do not provide a walk-away solution and they are either expensive or difficult to maintain. The best solution to completely eradicate ARD is to prevent it from the source. However, the effectiveness of ARD prevention depends on the accuracy of predicting future drainage quality. This can be done by using ARD prediction tests, which are generally classified as either static (acid base accounting, ABA, net acid generation, NAG) or kinetic (column leach, humidity cell, biokinetic test). There is no single test capable enough to accurately predict acid generating potential. It is therefore usual practise to conduct more than one test and cross-check results to ensure that the appropriate conclusions are made. In doing so, the reliability of the tests is improved but in some cases the different test results do not correlate. Mineralogy is an analytical technique that can be used to understand the nature of the errors and to better understand the leaching behaviour of minerals in the different tests. This study uses mineralogy to analyse both static and biokinetic test results of a Witwatersrand gold sample in order to improve the understanding of behaviour of mine wastes under different ARD prediction test conditions.

A run-of-mine gold sample from the Witwatersrand region in South Africa was used as a case study to explore the mineral leaching behaviour for different ARD prediction tests. The sample was characterized for chemistry (Inductively Coupled Plasma Optical Emission Spectroscopy, ICP-OES and X-Ray Fluorescence, XRF), sulfur species (Australian Coal Association Research Program sulfur speciation protocol, ACARP), mineralogy and texture (X-Ray Diffraction, XRD and Quantitative Evaluation of Minerals by Scanning electron microscopy, QEMSCAN). The acid generating potential was evaluated using mineralogical techniques (ARD Index and ABA_{MIN}), geochemical static tests (ABA and NAG) and kinetic test (biokinetic test). Different methods to determine acid neutralisation capacity (ANC) were conducted to examine the effects of the test conditions on mineral leaching and on the ANC value. The mineral leaching was evaluated by characterising both solid residues and leachates obtained after the leaching stage of the above-mentioned geochemical tests for chemistry and mineralogy.

The ACARP sulfur speciation protocol showed that the sample had sulfide content (1.3 wt. %) equivalent to the total sulfur (1.3 wt. %) and negligible concentration of sulfates (0.01 wt. %). The gold sample had 5 wt. % sulfides (predominantly pyrite and pyrrhotite), 0.5 wt. % ‘fast dissolving’ carbonates (mainly calcite), no ‘fast weathering’ silicates, 6 wt. % ‘intermediate weathering’ silicates (chlorite and mica), 16 wt. % ‘slow weathering’ silicates (feldspar) and 72 wt. % ‘inert’ (quartz and sphene). The textural results show that sulfide minerals are well liberated (91%) with only a minor

association to quartz (6%), mica (2%) and carbonates (0.02%). The ACARP protocol, bulk mineralogy and texture results all showed that the sample contains negligible secondary minerals (i.e. sulfates and iron oxides/hydroxides) thereby confirming that the sample is unoxidized.

The mineralogy and texture results were further processed to determine the acid rock drainage index, ARDI, which showed that the sample is potentially acid forming (ARDI = 23). The various ANC conducted had different ANC values: Lawrence and Wang ANC method had the lower ANC (4.2 kg H_2SO_4/t) compared to both the AMIRA modified Sobek (14.4 kg H_2SO_4/t) and Skousen Incremental ANC tests (17.4 kg H_2SO_4/t), but relatively comparable to the Paktunc mineralogical ANC (5.0 kg H_2SO_4/t). The ANC values were used to calculate the NAPP (ABA). The chemical and mineralogical ABA in kg H_2SO_4/t (36.5, 26.3, 23.3 and 50.7) in similar order as the ANC above, NAG test (pH = 2.5, accumulative sequential NAG = 51.6 kg H_2SO_4/t) and biokinetic test (final pH = 2.1) showed that the sample is potentially acid forming. The high mineralogical ABA of 50.7 kg H_2SO_4/t was due to overestimation of sulfides by QEMSCAN. The sequential NAG test confirmed that the single-addition NAG test does not always completely oxidize sulfides on samples with sulfide content greater than 1 wt. %.

Similar acid neutralising minerals reacted on all the tests but in differing extents, i.e. carbonates and chlorite. In addition to these, mica reacted under the AMIRA modified Sobek/Skousen ANC tests and the sequential NAG test. Thus revealing that the biokinetic test is less aggressive compared to the AMIRA modified ANC tests and the sequential NAG test. The sulfide minerals were completely oxidised in the sequential NAG and the biokinetic tests. Secondary minerals formed were mainly sulfates such as jarosite.

Deducing from the leaching behaviour, the Lawrence and Wang ANC, and the Paktunc mineralogical ANC tests are more suitable for sample with carbonates and negligible content of silicates. The AMIRA modified Sobek, and Incremental Skousen siderite correction ANC tests are more suitable for sample with carbonates and/or silicates. This study also showed that the single-addition NAG can be used on samples with sulfide content <1 wt. %. The sequential NAG must be used on samples with sulfide content >1 wt. %. This study also showed that mineralogy can be used either as a stand-alone prediction test or as a technique to support/compliment geochemical tests. The biokinetic test results correlated with the static tests, with regards to the acid generating potential.

The mineralogy information acquired in this study enhanced the level of understanding of the controlling reactions involved on the prediction tests conducted. Such as only acid neutralising minerals significantly reacted on the ANC test methods, whereas both sulfides and acid neutralising minerals reacted on the NAG and the biokinetic tests. The extent of mineral leaching revealed that some acid neutralising minerals do not react completely. This study also showed the importance of understanding mineralogy of the sample, as seen that different tests generate different results. In order to improve the level of confidence on the geochemical tests and to optimize their use, sample mineralogy must be studied thoroughly prior to selecting appropriate test method. In that way, errors associated with sample properties, test conditions and interpretation can be minimised.

ACKNOWLEDGEMENTS

To my supervisors Dr Megan Becker and Dr Jenny Broadhurst, thank you for the technical input and professional guidance and for all the time and effort correcting what I feel were sometimes inexcusable mistakes! If this dissertation is even close to what you had in mind when you suggested this project, then I will be very happy.

To Prof Jean-Paul Franzidis, thank you for the professional guidance and financial support through Minerals to Metal Initiative. I truly appreciate it!

This work is based on research supported by: the South African Research Chairs Initiative of the Department of Science and Technology and National Research Foundation, and by the National Research Foundation of South Africa for the grant (Unique Grant 80599). Any opinion, finding, conclusion or recommendation expressed in this material is that of the authors and the NRF does not accept any liability in this regard.

I would like to extend my gratitude to the following people:

- Prof Susan Harrison for your support of the project through CeBER. Emmanuel Ngoma, Dr Rob van Hille and many others from CeBER, thank you for all the time and effort you have put in for me.
- Mymoena van der Fort, Shireen Govender, Lesley Mostert, Sue Jobson, Rosalind Maree and Nelly Dili for all the help you have given me.
- ARD Prevention Discussion Group and Biominerals Group members, as well as all the Minerals to Metal Initiative students for all the support you have given me.
- Stephanie Snoek and colleagues in the analytical lab for their assistance with ICP-OES and LECO S.
- Dr Kistern Corin for her assistance with XRD analysis, Dr Megan Becker, Lorraine Nkemba and Gaynor Yorath for their assistance with QEMSCAN, as well as others from the CMR labs.
- Prof David Reid and colleagues in the Geology Department for their assistance with XRF.

To my son, Bulumko Sixolise, I know that you cannot read this yet, but I hope that someday when you are old enough to understand, you will know that being away from you for many hours at a time was one of the hardest things I have ever had to do. I intend to spend the coming years making it up to you for all the time I spent away from you. Hopefully you will not get sick of seeing my face! ☺ Mommy loves you! I am eternally grateful to my parents for all of their love and support. What you have done for me is nothing short of amazing. Thank you for loving me as you have and thank you for taking care of my son while I toiled away in pursuit of my studies. I hope to make you proud someday.

LIST OF PUBLICATIONS AND PRESENTATIONS

1. Dyantyi, N., Becker, M., Broadhurst, J.L.B., Harrison, S.T.L. and Franzidis, J-P. Use of mineralogy to interpret laboratory-scale acid rock drainage (ARD) prediction tests: A gold case study. Mineral Processing Conference, Southern African Institute of Mining & Metallurgy Western Cape Branch, 2 – 3 August 2012, Cape Town.

2. Dyantyi, N., Becker, M., Broadhurst, J.L.B., Harrison, S.T.L. and Franzidis, J-P. Use of mineralogy to interpret laboratory acid rock drainage (ARD) prediction tests: A gold case study. Process Mineralogy Conference, Mineral Engineering International, 14 – 15 November 2012, Cape Town.

3. Dyantyi, N., Becker, M., Broadhurst, J.L.B., Harrison, S.T.L. and Franzidis, J-P. Use of mineralogy to interpret laboratory-scale acid rock drainage (ARD) prediction tests: A gold case study. World Gold Conference, Australian Institute of Mining and Metallurgy, 26 - 29 September 2013, Brisbane, 1 - 8.

4. Dyantyi, N., Becker, M., Broadhurst, J.L.B., Harrison, S.T.L. and Franzidis, J-P. Application of mineralogy in the interpretation of laboratory scale acid rock drainage (ARD) prediction tests: A gold case study. Mineral Processing Conference, Southern African Institute of Mining & Metallurgy Western Cape Branch, 8 –9 August 2014, Cape Town.

TABLE OF CONTENTS

LIST OF FIGURES

LIST OF TABLES

LIST OF ACRONYMS

ABA	Acid base accounting
ACARP	Australian Coal Association Research Program
AMD	Acid mine drainage
ARD	Acid rock drainage
ARDI	Acid rock drainage index
ANC	Acid neutralizing capacity
ANC_{MIN}	Acid neutralizing capacity based on mineralogy
lld	lower limit of detection
CRS	Chromium Reducible Sulfur method
GARD Guide	Global Acid Rock Drainage Guide
GMT	Geochemistry-Mineralogy-Textural approach
ICP-OES	Inductively Coupled Plasma Optical-Emission Spectroscopy
KOSH	Klerksdorp-Orkney-Stilfontein-Hartebeestfontein area
MPA	Maximum potential acidity
MPA_{MIN}	Maximum potential acidity based on mineralogy
NAF	Non-acid forming
NAG	Net acid generation
NAPP	Net acid producing potential
$NAPP_{MIN}$	Net acid producing potential based on mineralogy
nd	not determined
PAF	Potentially acid forming
QEMSCAN	Quantitative Evaluation of Minerals by Scanning electron microscopy
SPOCAS	Suspension Peroxide Oxidation Combined Acidity and Sulfur method
UC	Uncertain

UCT	University of Cape Town
XRD	X-Ray Diffraction

CHAPTER 1

INTRODUCTION

1.1. Background

Gold mining and beneficiation has been a major contributor to the economy and establishment of infrastructure in South Africa for over a century. However, the same gold mining processes in South Africa are associated with several environmental implications such as acid rock drainage (ARD) formation (Mpephu 2003, Naicker et al. 2003, Oelofse *et al*. 2007, Oelofe 2008). When the sulfide rich waste material generated during mining comes into contact with oxidants such as atmospheric air, they react to form acid that gives rise to ARD. The term acid rock drainage (ARD) will be used instead of acid mine drainage (AMD) since acidic drainage does not arise solely due to mining related activities, but can occur naturally. The sulfide oxidation reaction is influenced by several factors such as whole rock chemistry, mineralogy, geology and microbial content of the waste (Akcil *et al*. 2006, Nengovhela *et al*. 2006, Department of Water Affairs and Forestry 2008). The sulfide oxidation reaction by ferric iron has been reported to be up to 5 orders of magnitude faster than the oxidation by atmospheric air (Blowes *et al*. 1998, Blowes et al. 2005). The generation of ferric iron is facilitated by the presence of naturally occurring iron oxidising bacteria, which oxidize ferrous iron into ferric iron. More acid is generated when reduced sulfur species formed during pyrite oxidation are oxidized by sulfur oxidizing bacteria. In addition to the microbial effect, both the mineralogy and textural properties of the material play a critical role in controlling the reactivity of the acid generating and acid neutralising minerals (Blowes *et al*. 1998, Dold *et al*. 2002, Weber *et al*. 2004b). Textural factors such as mineral association, liberation, morphology, and degree of weathering all control the acid generating potential of the mine waste (Shaw *et al*. 1998, Gunsinger *et al*. 2006a, Moncur *et al*. 2009).

ARD is characterized by low pH, high sulfate contents, and high concentrations of toxic heavy metals (e.g. Mn, Cd etc) that contaminate scarce water resources and subsequently limits their use without treatment (Nordstrom *et al*. 1999, Rosner *et al*. 2001, Lottermoser *et al*. 2010, Jameison 2011, Nordstrom 2011). The mobility of heavy metals may lead to land degradation, water pollution and destruction of aquatic species, which are the primary receptors of the contaminated water (Rosner *et al*. 2001, Mpephu 2003). Unless interventions are put in place, the production of acid rock drainage may continue for many generations following the closure of mining activities. Strategies for the management of ARD can be broadly classified as end-of-pipe treatment methods. The overall

objective of these treatment strategies is to increase the pH to a level that causes the precipitation of metals which can subsequently be recovered. In this way, the mobility of these elements is hindered and there is a potential for recovering saleable minerals/compounds. These treatment methods however, do not completely eradicate the implications associated with ARD and they are costly, and often difficult to implement or sustain. The first and most important step in effectively managing ARD is using simple, inexpensive, robust, reliable and accurate ARD prediction testing procedures to identify ore types with a high potential for ARD generation.

ARD prediction tests are geochemical tests carried out to study the acid generating behaviour of waste and can be classified as either static or kinetic. Static tests include the acid base accounting (ABA) and net acid generation (NAG) tests which classify the acid generating potential of the material over geological time, without providing information on relative rates. Kinetic tests such as humidity cells, column leach and biokinetic tests provide information on the kinetics of the reaction, as well as on the geochemistry of the leachate. ARD prediction test work revolves around the "wheel approach" (Fig 1) established by Morin *et al*. (1998). Even the works published on Global Acid Rock Drainage (GARD) guide online portal (www.gardguide.com) and MEND report by Price (2009) do not completely deviate from the "wheel approach". The wheel approach prediction suite promotes the use of different test methods along with analytical techniques (chemistry and mineralogy) in order to minimize errors encountered when identifying the potential for ARD. Furthermore, analytical techniques on the "wheel" are useful in resolving inconsistencies that may arise when more than one test methods are compared (Morin *et al*. 1998).

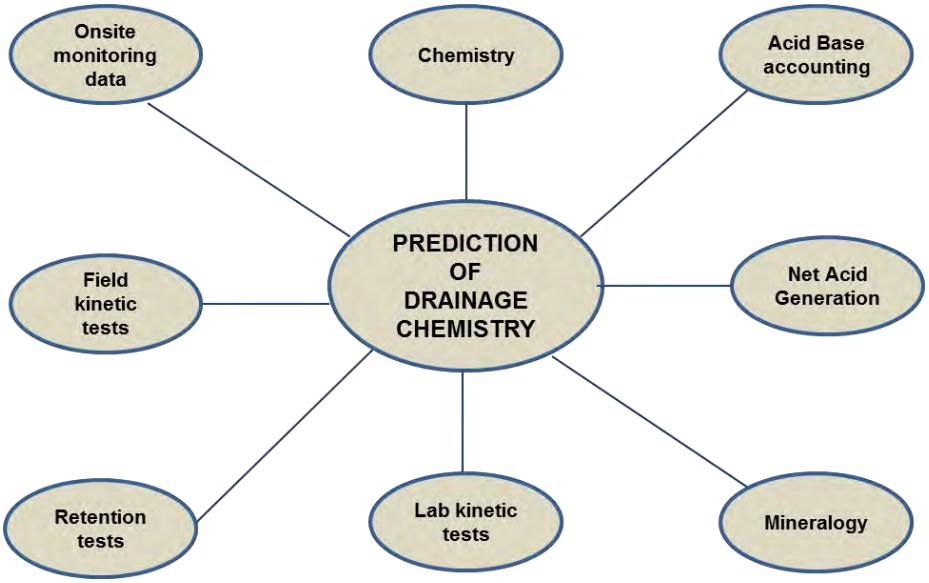

Figure 1: The Wheel approach for predicting drainage chemistry (reproduced after Morin et al, 1998).

Based on its simplicity, short turnaround time and cost effectiveness, the most commonly used static test is Acid Base Accounting (ABA). ABA is a twofold test that includes the estimation of the maximum potential acidity (MPA) based on sulfur content and assessment of acid neutralising capacity (ANC)

through either wet chemistry or mineralogical calculations (Lawrence *et al*. 1989, Lawrence *et al*. 1996, Skousen *et al*. 1997, Paktunc 1999b, Jurjovec *et al*. 2002, Jambor *et al*. 2006, Kaartinen *et al*. 2009). The difference between these two values provides an estimation of the net acid producing potential (NAPP). An additional and commonly used static test is the net acid generation (NAG) test that provides information on the net balance between acid generation and neutralisation potential by allowing both reactions to take place simultaneously. Various modifications have been developed to improve the flexibility of the NAG test methods towards different project objectives and sample properties (Kleinmann 2000, Smart *et al*. 2002, Stewart 2005, Stewart *et al*. 2006, Bucknam *et al*. 2009).

Kinetic tests are long-term tests that are carried out to provide information on the relative rates of the reactions (sulfide oxidation, dissolution of neutralising minerals), as well as the geochemistry of the leachate. Humidity cell and column leach tests are the most widely used tests, but are time-consuming (often conducted for a minimum of 20 weeks but can take up to 1 year to obtain meaningful results) and resource intensive. Moreover, conventional chemical static and kinetic tests do not consider the effect of microbial colonisation on the rates and extents of ARD generation. More recently, a biokinetic test has been developed at the University of Cape Town with a view to enhance and address the shortcomings of traditional static and kinetic tests (Hesketh *et al*. 2010). The biokinetic test generates informative data on the role of the microbial population, relative kinetics and mechanisms of acid rock drainage formation within a reasonable period of ~ 3 months (Hesketh *et al*. 2010). The interpretation of the information obtained from the biokinetic test is, however, currently limited by the complexities involved, particularly in terms of the vast number of simultaneous chemical and microbial reactions that occur, and the influence of ore mineralogy on such (Broadhurst *et al.* 2013).

Mineralogy is one of the analytical techniques that form part of the ‘”wheel” of prediction tests. In addition to the role that mineralogy plays in understanding the acid generating behaviour, it can also be used as an additional stand-alone tool in predicting the acid generating potential of a waste material. Paktunc (1999b) used modal mineralogy to calculate the acid generating potential and neutralising capacity of a material, on the basis of the sulfide and carbonate mineral content respectively. The acid rock drainage index (ARDI), developed by Parbhakar-Fox *et al*. (2011), is a unique mineralogical predictive technique that takes into account five different parameters in predicting the potential acid generating behaviour of a sample: sulfide mineral content, sulfide alteration, sulfide morphology, neutraliser content and the spatial relationship between sulfides and neutralising minerals.

The varying behaviour of mine waste during prediction tests is not only affected by the test conditions, but also by mineralogy. The reactivity of minerals is affected by the availability of the reactive surface of a mineral and that depends on the degree of alteration, liberation and morphology. The presence of secondary mineral precipitates that may armour sulfides or carbonates may adversely affect their reactivity, and subsequently lead to the misclassification of the acid generating potential. Researchers recommend routine use of mineralogy as part of prediction tests, either as part of the screening stage

or when interpreting the results (Morin *et al*. 1998, Paktunc 1999b, Stromberg *et al*. 1999, Price 2009). In practise, this is seldom taken into consideration due to time and financial constraints.

ARD prediction tests are carried out to study the potential of acid generation and play an important role in ARD management and prevention. An understanding of the resultant drainage chemistry will aid in planning for waste management strategies. ARD can be successfully prevented or managed only if the acid generating potential of mine waste is properly understood. However, no single prediction test is capable enough to provide reliable information on future drainage chemistry (Morin *et al*. 1995). It is therefore usual practise to conduct more than one test and cross-check results to ensure that the appropriate conclusions are made. In so doing, the reliability on the tests is improved. In cases where the results from the different tests do not correlate (e.g. Table 1), the representativeness of the different samples, as well as the assumptions behind the test methods will need to be considered. Good interpretation of results relies on an understanding of the limitations of the test, sampling procedures and the techniques employed (Czerewko *et al*. 2003). A clear understanding of the behaviour of mine waste under different test conditions will allow the appropriate usage of these tests and so improve their overall reliability.

Table 1: The comparison of results from different ARD prediction test classifications (Stewart et al, 2009), it must be noted that this table extracted only the non-correlating results.

Sample	Column leach test	ABA as NAPP	NAG
12	UC (NAF)	NAF	PAF
15	NAF	PAF	PAF
100	UC (NAF)	PAF	NAF
125	UC (NAF)	PAF	PAF

ABA- Acid Base Accounting, NAPP- Net Acid Producing Potential, NAG- Net Acid Generation, UC- Uncertain, NAF- Non Acid Forming, PAF- Potentially Acid Forming

1.2. Problem statement

Acid rock drainage is a very real problem in South Africa affecting the local water resources and the environment. The management strategies applied to date are costly and do not completely eradicate ARD. For example, the cost of pumping (i.e. capital and operation) mine water from the Central Basin, in the Witwatersrand region alone, is estimated to be R20 million per annum (Inter-Ministerial Committee on Acid Mine Drainage 2010). In addition to that, a lime neutralisation plant for treating the Central Basin water will cost ~ R 150 million per annum (Inter-Ministerial Committee on Acid Mine

Drainage 2010). Neither the pumping out of mine water from voids into storage facilities nor neutralisation are walk-away solutions to ARD problems. Instead, the prevention of ARD is the solution to avoid the degradation and impairment of the local ecosystem. The first and most important step in effectively managing ARD is by using simple, robust, and precise ARD prediction testing procedures to identify ore types with a high potential for ARD generation. However, there is no single ARD test powerful enough to reliably predict the kinetics of ARD generation and drainage chemistry, but rather a suite of complimentary and consistent test results are needed to ensure the appropriate conclusions are made. In practise, the results of these ARD prediction tests do not always correlate with one another since the reactions (chemical and mineralogical) and assumptions behind the test methodologies are not always well understood.

1.3. Research scope

1.3.1. Overarching research objective

The broader objective is to develop a better understanding of the key waste components and controlling reaction mechanisms involved, and ultimately more accurate and reliable predictions of the ARD risks in a disposal scenario. The objective of the study is to use mineralogy as a tool to assist in interpreting the discrepancies arising from the information obtained through various ARD prediction tests. In order to achieve the objective, the study aimed at:

I. Investigating the effects of various static test conditions and mineralogy on the leaching behaviour of minerals.

II. Evaluating the extent of mineral leaching of the gold sample on the UCT-developed biokinetic test.

1.3.2. Scope of the study

This thesis focuses on the interpretation of a set of laboratory scale ARD prediction tests using a single South African gold ore case study example. The study entails the characterisation of the chemistry, mineralogy, texture, acid neutralising and acid generating potential of the sample prior to and after the various ARD tests. The study is limited to laboratory-scale tests: acid base accounting, net acid generation and the UCT biokinetic test. Mineralogy and texture will be characterized by X-Ray Diffraction (XRD) and Quantitative Evaluation of Mineralogy by Scanning Electron Microscopy (QEMSCAN) while chemistry will be studied through Inductively Coupled Plasma-Optical Emission Spectroscopy (ICP-OES), UV-Vis spectroscopy, Chromium Reducible Sulfur Method, X-Ray Fluorescence (XRF) spectroscopy and LECO Sulfur. The study focuses on both major elements.

Long term kinetic tests such as the humidity cell and column leach test were not conducted. No pilot scale or field prediction tests were carried out in this study. The information generated from this study has assisted in the interpretation of the behaviour of mine waste under different prediction test conditions, ultimately improving the usefulness, accuracy and reliability of laboratory scale ARD prediction tests.

1.4. Thesis structure

This thesis consists of seven chapters: the Introduction in Chapter 1 will provide a background to the study that outlines the problem statement, objectives and scope of the study. Chapter 2 provides a Literature Review which covers the fundamentals of acid rock drainage formation, current prediction tests and their limitations. Mineralogy is also discussed in detail, and thus will lead to the derivation of the hypotheses and key questions of the study. Details of the sample preparation and ARD prediction test methodology is outlined in Chapter 3. Static (ABA and NAG) and kinetic (biokinetic) test results are presented in Chapters 4 and 5, respectively. These results will be presented along with mineralogy and chemistry information obtained from characterising the test residues. A full discussion of the linkage and interpretation of the various tests is given in Chapter 6. Chapter 7 highlights the Conclusions of the study and provides Recommendations for future work. The full set of results is provided in the Appendix. An outline of the thesis is outlined schematically in Figure 2.

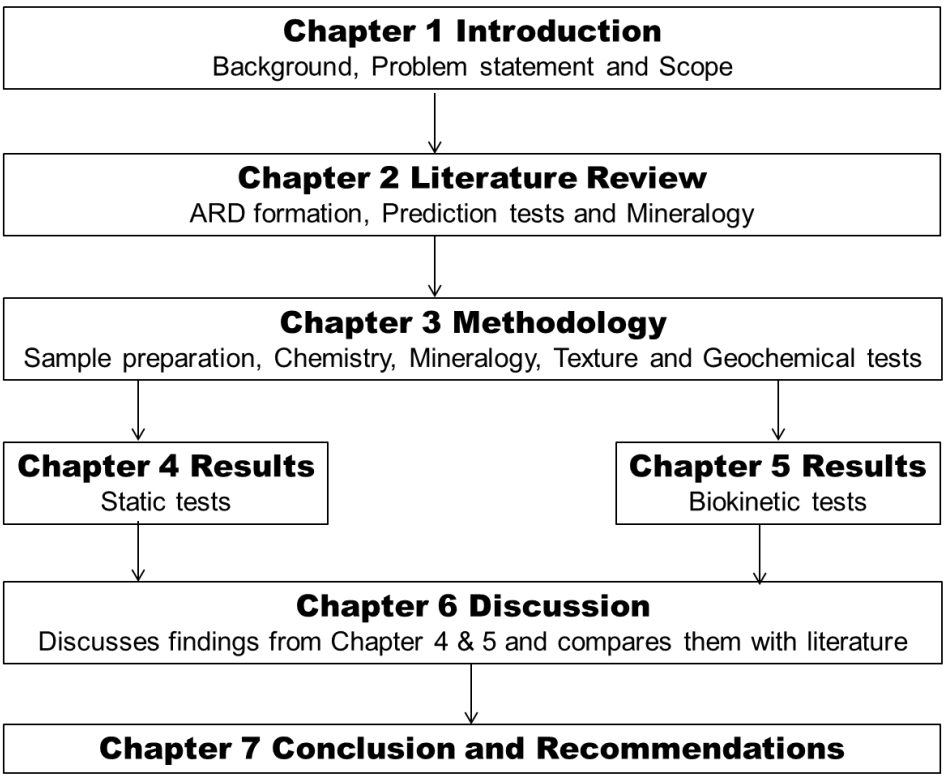

Figure 2: Schematic diagram of the thesis structure.

CHAPTER 2

LITERATURE REVIEW

This chapter presents an overview of the available literature relevant to the processes and factors contributing to ARD generation and prediction tests that are currently employed to study the acid generating potential of mine waste. In line with the objective of the study, geochemical tests and analytical methods commonly applied in prediction test work are discussed in detail highlighting the gaps in the literature that will assist in formulating the hypotheses and key questions to be answered through this study. The chapter concludes with a summary of the literature review before presenting the hypotheses and research key questions.

2.1. Acid Rock Drainage (ARD)

Acid rock drainage (ARD) is an acidic effluent formed through either natural weathering and/or oxidation of sulfides commonly associated with mining. Potential sources of ARD in mining include waste rock dumps, tailings dams, open pits voids and abandoned underground mines. Commercial mining and beneficiation in Johannesburg dates back to 1886 and it was considered as a major contributor to the country's economy (Anhaeusser *et al*. 1987, Janish 1989). Although contribution has changes over the years, the industry in 2014 contributes 6.8% to the global production, 10.7% on foreign currency and 2% in Gross Develop Projects (Chamber of Mines at www.bullion.org.za). As the demand for minerals increases with time, the ore grade decreases (www.bullion.org.za). This leads to ultra-deep mining as to meet the demands. As a result, eight of the ten deepest mines (e.g. depth up to 3 900 m Mponeng and TauTona with 3 400 m) in the world are in South Africa (www.mining-technology.com). In addition to that, beneficiation methods applied require finely ground ore in order to maintain metal extraction that is efficient and economically viable. By so doing, large tonnages of waste ranging from coarse waste rock to ultra-fine tailings are generated (Blowes *et al*. 2005). The waste material generated contains unoxidized sulfide minerals such as pyrite, pyrrhotite and arsenopyrite. When in contact with water and air, the sulfide minerals oxidize to form acid giving rise to acid rock drainage (ARD). ARD is characterized by low pH, high sulfate content, high total dissolved solids and elevated concentrations of heavy metals such as As, Cd, Cu, Pb and Zn (Lappako 2002, Oelofse *et al*. 2007, Jameison 2011). The recorded pH unit for gold tailings in the Johannesburg region is as low as 3.1 and the concentrations of heavy metals as measured in tailings are given in Table 2 as extracted from Rosner *et al.* 2001).

Table 2: Summary of statistics for heavy metal concentrations in tailings dam from the East Rand area (Rosner et al, 2001).

Element	As	Co	Cu	Cr	Ni	Pb	Zn	Th	U
mg/kg	107 ±31	12 ±10	20 ±9	440 ±94	64 ±29	53 ±45	43 ±33	3 ±0	20 ±16

2.3. Geochemistry and mineralogy of ARD

The characteristics of ARD depend on two reactions that play an important role in ARD formation. These reactions are the acid forming and acid consuming reactions that control the dissolution of deleterious elements and precipitation of secondary minerals. The following subsections provide a brief overview of these reactions.

2.3.1. Acid producing reactions

Sulfide oxidation is the principal acid producing reaction that leads to the formation of acid rock drainage. Pyrite is the most common sulfide mineral, followed by pyrrhotite. Other sources of acidity in mine wastes are linked to the dissolution of acidic hydroxysulfate minerals and precipitation of iron and aluminium hydroxides (Price 2009, Lottermoser 2010). The various minerals that form acid are presented in Table 3. Sulfides have differing rates of reaction and acid forming potential, with the latter depending on the metal-sulfide bonding and the crystal structure (Blowes *et al*. 1998, Moncur *et al*. 2009). Table 4 summarises the relative reactivity of sulfides.

Table 3: Acid producing minerals in sulfidic wastes (Lottermoser 2010).

Mineral	Chemical reaction
Sulfides	
Pyrite	$FeS_2 + (15/4)\ O_2 + (7/2)\ H_2O = Fe(OH)_3 + 2SO_4^{2-} + 4H^+$
Pyrrhotite	$Fe_{0.9}S + 2.175O_2 + 2.35H_2O = 0.9Fe(OH)_3 + SO^{2-}_4 + 2H^+$
Chalcopyrite	$CuFeS_2 + 15/4O_2 + 7/2H_2O = Fe(OH)_3 + 2SO^{2-}_4 + Cu^{2+} + 4H^+$
Arsenopyrite	$FeAsS + 7/2O_2 + 3H_2O = FeAsO_4 \cdot 2H_2O + SO^{2-}_4 + 2H^+$
Precipitation of Fe^{3+} and Al^{3+} hydroxides	
Iron hydroxide	$Fe^{3+} + 3H_2O = Fe(OH)_3 + 3H^+$
Aluminium hydroxide	$Al^{3+} + 3H_2O = Al(OH)_3 + 3H^+$
Dissolution of secondary minerals (sulfates and hydroxysulfate salts)	
Melanterite	$FeSO.7H_2O + 0.25O_2 = Fe(OH)_3 + 4.5H_2O + SO^{2-}_4 + 2H^+$
Jarosite	$KFe_3(SO_4)_2(OH)_6 + 3H_2O = K^+ + 3Fe(OH)_3 + 2SO^{2-}_4 + 3H^+$
Alunite	$KAl_3(SO_4)_2(OH)_6 + 3H_2O = K^+ + 3Al(OH)_3 + 2SO^{2-}_4 + 3H^+$

Table 4: Relative resistance of common sulfides to alteration/reactivity (Moncur *et al.* 2009).

Mineral	Formula	Relative reactivity
Pyrrhotite	$Fe_{(1-x)}S$	Low resistance
Galena	PbS	↓
Arsenopyrite	FeAsS	
Pyrite	FeS_2	
Chalcopyrite	$CuFeS_2$	High resistance

Several factors such as oxygen availability, mineralogy, texture and microbiology of the mine waste influence the rate and extent of sulfides oxidation (Blowes *et al*. 1998, Baker *et al*. 2003, Weber *et al*. 2004a, Dold 2005, Akcil *et al*. 2006, Lottermoser 2010,). These factors coupled with the electrochemical nature of sulfides makes it complex to understand the mechanisms involved in its oxidation (Janzen *et al*. 2000, Thomas *et al*. 2000, Cruz *et al*. 2005). The sulfide mineral surface is oxidized predominantly by oxygen at circumneutral pH by bonding to ferrous iron (see Table 3). However the relative kinetics of these reactions are controlled by oxygen availability.

Leptospirillu and *Acidithiobacillus* are acidophilic sulfur- and/or iron-oxidising micro-organisms commonly found in mine waste (Blowes *et al.* 2005). The acidity generated from oxidative dissolution of pyrite creates favourable conditions for the bacteria and thereafter accelerated sulfide oxidation is usually observed. These bacteria oxidize pyrite indirectly through oxidation of ferrous iron into ferric iron according to reaction 2.1. The oxidation of sulfides by ferric iron results is reported to be approximately 5 times of magnitude faster than the atmospheric oxidation (Blowes *et al.* 2005). Reaction 2.2 is the regeneration of catalytic ferric iron in the presence of microbes. The concentration of ferric iron, which depends primarily on acidity, determines the rate of reaction. An acidic pH results in a higher concentration of ferric iron due to the suppressed precipitation of ferric hydroxide. However, if the pH units rise to above 3, the ferric iron precipitation reaction releases acidity (Equation 2.3) which subsequently lowers the pH creating favourable conditions for bacterial activity that enhances sulfide oxidation (Blowes *et al.* 2005).

$$FeS_2 + (7/2)O_2 + H_2O = Fe^{2+} + 2SO_4^{2-} + 2H^+ \quad (2.1)$$

$$Fe^{2+} + (1/4)\ O_2 + H^+ = Fe^{3+} + (1/2)\ H_2O \quad (2.2)$$

$$Fe^{3+} + 3H_2O = Fe(OH)_3 + 3H^+ \quad (2.3)$$

Mineralogy and texture are other important parameters that influence sulfide oxidation. These parameters include: crystal structure, morphology, mineral liberation and mineral association. Morphology also determines the reactivity and rate of reaction of a mineral. As an example (see Figure 3), framboidal pyrite (clusters of mushroom-like structures) has been observed to react faster than euhedral pyrite (well-formed structures with sharp faces) due to the increased available surface area for reaction (Weber *et al*. 2004a, Weisener *et al*. 2010). Sulfide alteration can determine the extent of weathering of mine waste, thus determining the acid generating potential. It is therefore essential to have a clear understanding of the mineralogy and texture of a sample and this can be achieved by using available mineralogical techniques. In addition, knowledge of bulk mineralogy is essential whether when selecting prediction test method or estimating acid generating potential since various minerals reacts differently (e.g. different forms of sulfides and acid neutralising minerals) (Blowes *et al*. 1998).

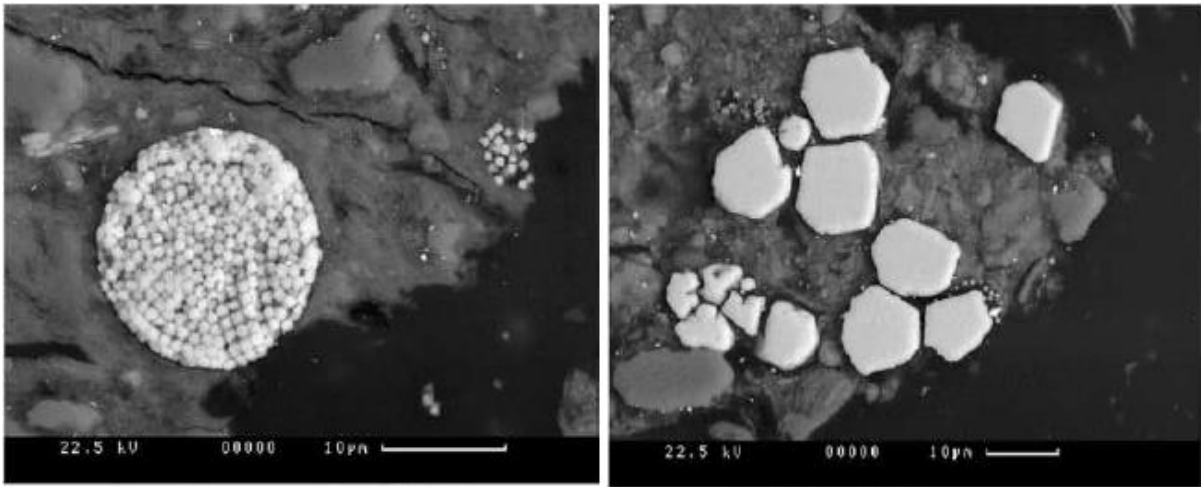

Figure 3: SEM backscattered electron images showing different pyrite morphologies: A framboidal and B euhedral pyrite. Both images are extracted from Weber et al. 2004.

The extent of weathering of sulfide minerals determines their potential to generate acid. Unoxidized sulfide minerals have a higher potential to generate acid compared to altered sulfides (Figure 4). For example, the un-weathered sulfides (Figure 4A) hosted by inert quartz are more likely to oxidize, whereas the remaining sulfides (Figure 4C) are armoured by secondary minerals such as iron oxyhydroxides, hence unavailable for oxidation which is parent to acid generation (Parbhakar 2012).

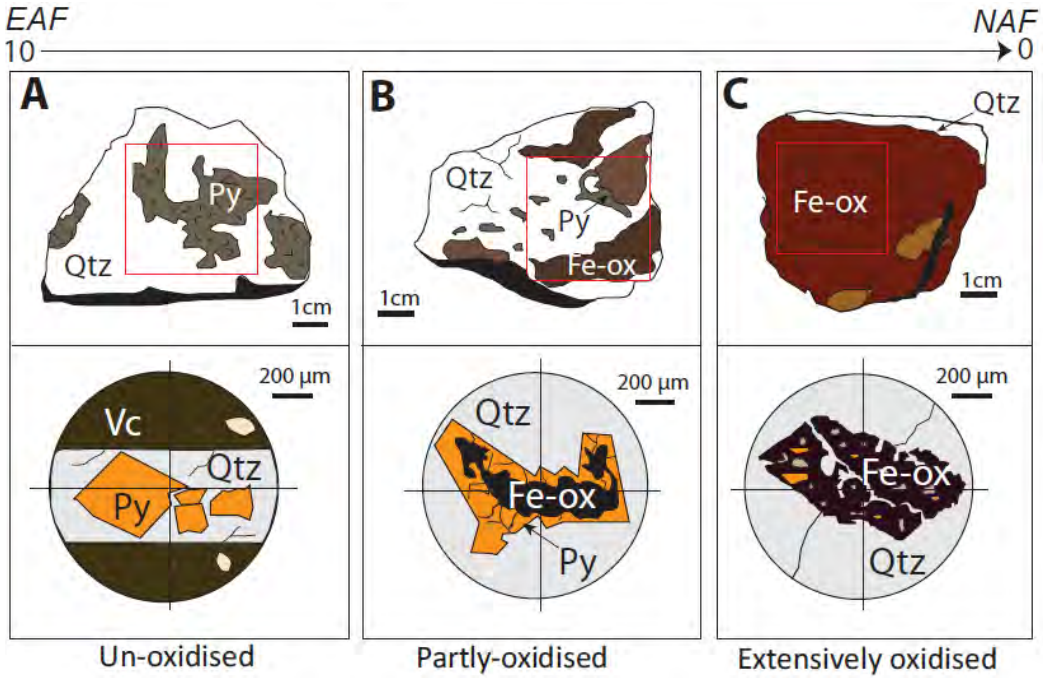

Figure 4: Meso-scale (1 cm) and micro-scale (200 µm) images showing sulfide alteration after Parbhakar (2012). Qtz quartz; Py pyrite; Fe-ox iron oxyhydroxides and Vc volcanic.

Sulfide oxidation is a cyclic process that is difficult to control unless one of the parameters (i.e. sulfide, oxygen or Fe^{3+}) is removed from the system. This continuous process can be shown schematically in Fig 5 ('ARD engine') following the work of Lottermoser (2010). The ARD engine begins with the

'Starter switch' in which oxygen oxidizes pyrite. Ferric iron, oxygen, and pyrite are regarded as the 'fuel' which combust in the 'engine room' and release sulfuric acid, heat, ferric iron, and ferric hydroxide into mine waters through the 'exhaust pipe'. Ferric iron re-enters the 'engine room' as a fuel to oxidize pyrite, continuing the acid producing cycle.

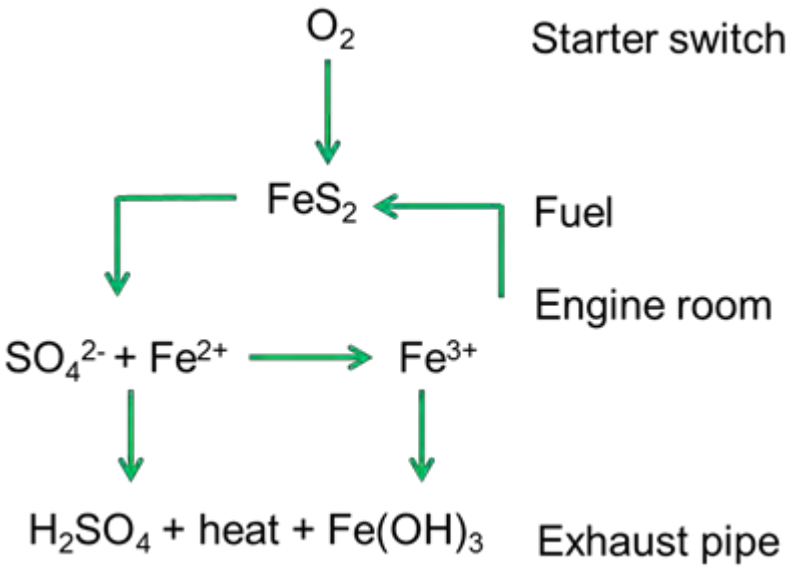

Figure 5: The self-sustaining cyclic destruction of pyrite simplified as the ARD engine (Lottermoser 2010).

2.3.2. Acid neutralising reactions

The net acid rock drainage quality is not only influenced by acid forming reactions, but also acid neutralising reactions. Depending on the mineralogical composition of a waste, the acid formed can be neutralised by acid consuming minerals. The rate of acid consuming reactions is affected by the acidity, the rate of reaction of the inherent mineral/rock and the mineralogical properties of the neutralising minerals (e.g. liberation, alteration). Carbonates, followed by hydroxides are the most effective acid buffering minerals. The stepwise consumption of buffering capacity as depicted in Figure 6 shows the susceptibility of these minerals to dissolution at pH unit as high as 6.3. Figure 6 also shows that calcite is the fast dissolving acid neutralising mineral, followed by aluminium hydroxide since siderite and iron hydroxide have zero net acid neutralising potential.

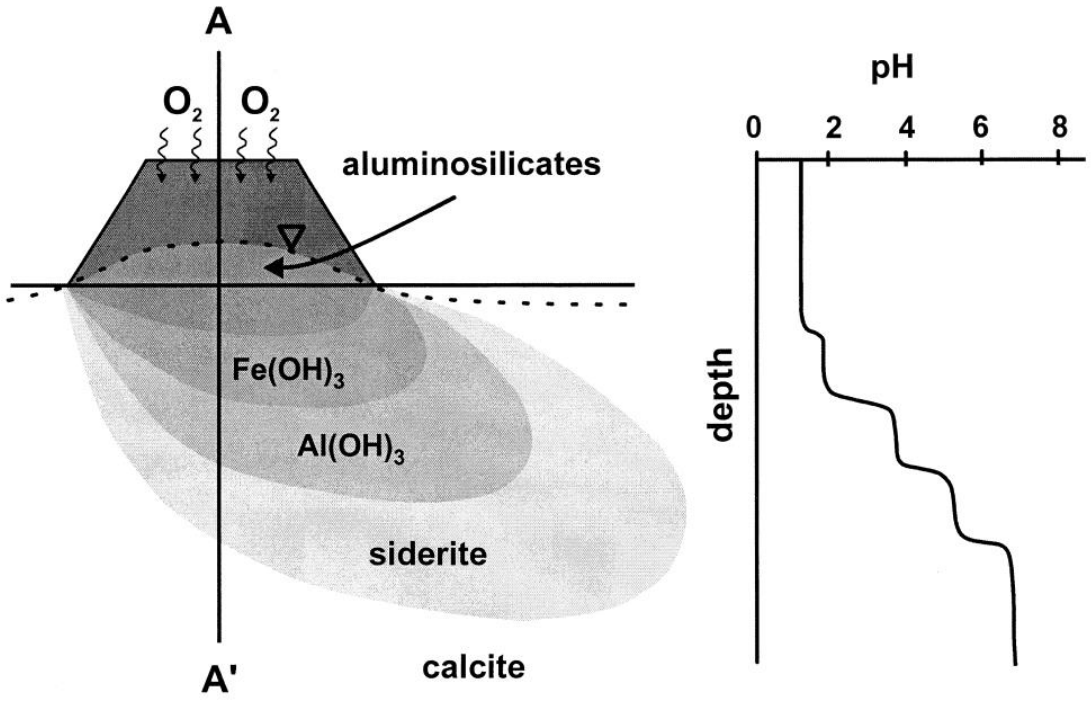

Figure 6: Sketch of a tailings impoundment with a corresponding plume of acidic water and a diagram of pH changes with depth through cross-section AA' (Jurjovec et al. 2002).

Carbonates play a crucial role in acid neutralization due to their reactivity; especially calcite which is the most abundant form. Calcium and magnesium containing carbonates such as calcite ($CaCO_3$), magnesite ($MgCO_3$), dolomite ($CaMg(CO_3)_2$), and ankerite ($CaFe(CO_3)_2$) have high acid neutralising capacity. However iron carbonates such as siderite ($FeCO_3$) have no net neutralisation capacity. The oxidation of Fe^{2+} to Fe^{3+}during siderite dissolution consumes acidity. The acid is subsequently released during precipitation of Fe^{3+} in secondary minerals (Skousen *et al*. 1997). Carbonate minerals can buffer acid at pH as high as 6.3 (Jurjovec *et al*. 2002, Gunsinger *et al*. 2006b, Lottermoser 2010). Depending on the acidity of the environment, carbonate dissolution may generate bicarbonates in weakly acidic (Equation 2.4) or carbonic acid in strongly acidic conditions (Equation 2.5) (Lappako 2002). A study conducted by Jurjovec *et al*. (2002) to examine the carbonate content before and after acid front confirmed that the carbonates are fast dissolving acid buffering minerals. Gunsinger *et al*. (2006b) also observed a rapid increase in pH units from 4.0 to 6.0 that corresponded to the depletion of carbonates, therefore suggesting acid neutralising action of carbonates.

$$CaCO_3 + H^+ = HCO_3^- + Ca^{2+} \quad (2.4)$$

$$CaCO_3 + 2H^+ = H_2CO_3 + Ca^{2+} \quad (2.5)$$

Another potential acid neutralising reaction is the re-dissolution of secondary aluminium hydroxides. The dissolution of aluminium hydroxides (Eq. 2.6), commonly in the form of amorphous $Al(OH)_3$ or gibbsite $Al(OH)_3$, buffers acidity to the pH range of 4.0 – 4.5 units. This is suggested by the rise in pH and increase in Al^{3+} ions in solution after the depletion of carbonates (Blowes *et al*. 2005).

$Al(OH)_3 + 3H^+ = Al^{3+} + 3H_2O$ (2.6)

Silicates are acid consuming minerals with very slow kinetics. Aluminosilicates are known to be reactive at a pH plateau zone of 1.3 (Jurjovec *et al*. 2002, Gunsinger *et al*. 2006b). Depending on the rates of acid generating reactions, silicates may contribute little or no net neutralization potential (Price 2009). At near neutral pH, the most reactive silicates are 7 orders of magnitude less reactive than calcite (Lappako 2002). A study conducted by Jambor *et al*. (2002) on the long-term contribution of silicates and aluminosilicates on the neutralization potential revealed that under acidic pH, fast weathering olivine and wollastonite are 200 times slower than calcite and that they can only raise pH to near neutral. Table 5 with classifications of acid neutralising minerals according to their reactivity also shows that olivine and wollastonite are the fastest weathering silicates. The study by Kalinkina *et al* (2004) showed that sphene is an inert mineral that requires mechanical activation to react.

Table 5: Grouping of minerals according to their reactivity at pH 5 adopted from Lawrence et al. (1996) and Kalinkina *et al* (2004).

Mineral group	Relative reactivity at pH 5	Typical minerals
Dissolving	1.00	Carbonates (calcite, aragonite, dolomite, magnesite, brucite).
Fast weathering	0.40	Feldspar (anorthite), olivine (forsterite), pyroxenes (diopside, hedenbergite, jadeite, spodumene, bronzite), wollastonite, garnets, epidotes, nepheline, leucite.
Intermediate weathering	0.02	Pyroxenes (enstatite, augite), amphiboles (tremolite, actinolite, hornblende, glaucophane anthophyllite), serpentine (chrysotile), mica(biotite), chlorite, talc, hypersthene
Slow weathering	0.01	Feldspar (albite, oligoclase, labradorite), clay (kaolinite, vermiculite, montmorillinite)
Very slow weathering	0.01	Feldspar (K-feldspar),mica (muscovite)
Inert	0.004	Rutile, zircon, quartz, sphene

Silicate minerals neutralise acid through either congruent or incongruent dissolution. By definition, congruent dissolution is the complete dissolution of silicates whereas incongruent is the incomplete dissolution through which silicates are transformed to another phase. Reactions 2.7 and 2.8 demonstrate the different dissolutions of silicates using feldspar as an example (adopted from Lottermoser 2010).

$2KAlSi_3O_8 + 2H^+ + 9H_2O = 2K^+ + Al_2Si_2O_5(OH)_4 + 4H_4SiO_4$ (2.7)

$KAlSi_3O_8 + 2H^+ + 5H_2O = K^+ + Al^{3+} + 3H_4SiO_4 + OH^-$ (2.8)

2.3.3. Secondary minerals

Secondary minerals are formed as precipitates or alteration products of interaction between ions generated during dissolution of sulfides, carbonates and aluminosilicates. The most common, as shown in Table 6, are hydroxysulfates and oxyhydroxides of aluminium and iron, secondary silicates and gypsum. The range and relative extent of the secondary precipitates depends on the pore water conditions such as pH and solutes concentrations. As an example, several studies have observed similar trend of increase in hydroxysulfate content with the extent of weathering or depth of waste deposit (Blowes *et al*. 1998, Hakkou *et al*. 2008, Bogush *et al*. 2011). Jarosite is one of the most commonly encountered hydroxysulfate minerals in acidic oxidized mine wastes. Iron oxides such as: goethite, hematite, ferrihydrite, and lepidocrocite can be alteration products formed during incongruent dissolution of jarosite at pH >3.5 or directly when ions concentrations are low (Bogush *et al*. 2011, Elwood Madden *et al*. 2012). Szomolnokite is a direct precipitate of iron-sulfate commonly found in oxidized mine wastes (Blowes *et al.* 2003). Gypsum precipitation associated with the dissolution of carbonate, forms as a result of interactions between calcite and sulfates (Bogush *et al*. 2011). The precipitation of secondary minerals affects the pH of mine water as their formation either generates or consumes acid. Generally, formation of Al^{3+} and Fe^{3+} oxyhydroxides generates acid, whereas precipitation of hdroxysulfates and sulfates consumes acid. However, the consumption of the acidity is only temporary, as these minerals tend to be soluble and release the stored acidity upon dissolution.

Table 6: Example of secondary minerals found in sulfidic wastes (Lottermoser 2010).

Mineral group	Mineral	Formula
Sulfates	Gypsum	$CaSO_4$
Hydrous sulfates	Szomolnokite	$FeSO_4.2H_2O$
Hydrous sulfates with trivalent cations	Jarosite	$KFe_3(SO_4)_2(OH)_6$
Fe and Al hydroxysulfates	Alunite	$KAl_3(SO_4)_2(OH)_6$
Oxyhydroxides	Goethite	FeOOH
Arsenates	Scorodite	$FeAsO_4.2H_2O$
Silicates	Epidote	$Ca_2Al_3Si_3O_{12}(OH)$

2.4. Gold mining and ARD in South Africa

This section briefly discusses gold mining in South Africa predominantly focussing on the Witwatersrand basin, potential sources of ARD, gold tailings and environmental implications arising as a result of the abandoned mines and improper planning for mine closure.

2.4.1. Gold mining in South Africa

Gold in the Witwatesrand area commonly occurs as native gold associated with quartz and unoxidized sulfides. Gold mining in South Africa has been the pillar of infrastructure establishment and human development from as early as 1886 (Anhaeusser *et al.* 1987 and Janisch 1989). Initially, gold was concentrated either by gravity concentration from coarsely crushed ore prior to extraction using the toxic Hg amalgam until 1915. As the demand for gold mineral increases, the ore grade decreased. The growing demand resulted in deeper mining from just 10 m below surface to more than 3, 000 m below surface. As a result, gold mines in the Witwatersrand are ranking among the deepest mines in the world (e.g. 3, 900 m deep Tautona mine in the Western Witwatersrand basin) (www.mining-technology.com). The decrease in ore grade prompted for other options of mineral beneficiation. The cyanide extraction method (cyanidation) was introduced to replace the Hg amalgam process. The cyanidation method not only improves beneficiation performance, but is also considered as a “greener” option since cyanide decomposes with time compared to the inorganic toxic Hg used in amalgam beneficiation (Stanley 1987). However the cyanide extraction method

requires finely crushed ore that generates large quantities of tailings that are usually disposed of in tailings or slime dams.

To date, there are ten goldfield areas in South Africa with seven regions grouped as part of the Witwatersrand basin (Pulles *et al*. 2005). These goldfields are categorised according to their depositional environment and hydrogeological properties. This study focuses only on the Witwatersrand basin. The Witwatersrand basin consists of Free State Gold Field, KOSH (Klerksdorp/Orkney/Stilfontein/Hartebeestfontein) area, Far West Rand, West Rand, Central Rand, East Rand and Evander Gold Field (Figure 7).

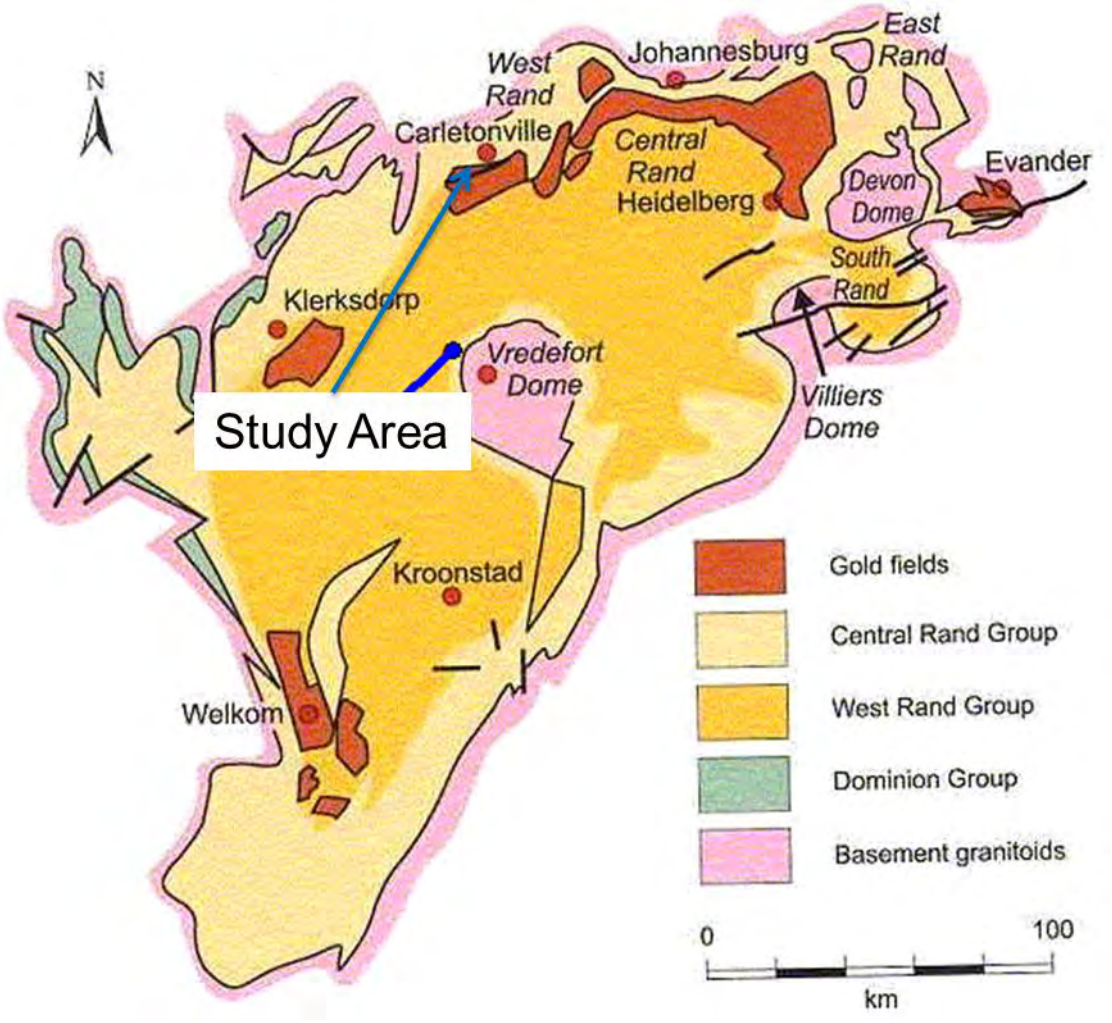

Figure 7: Map of the gold mines in the Witwatersrand region, in South Africa (Frimmel *et al.* 2009).

The Witwatersrand ores contain discrete gold particles distributed along the margins of the host assemblages and are described as free milling gold. Typical Witwatersrand ores are comprised of quartz and unoxidized sulfides (predominantly pyrite) as shown in Table 7 (Anhaenaeusser 1987, Pulles *et al*. 2005). There is only 45 ppm gold in the ore with more than 90% gangue minerals.

Table 7: Bulk mineralogy of a typical Witwatersrand ore (Stanley 1987).

Mineral	Abundance (wt. %)
Quartz	70 - 90
Muscovite and other phyllosilicates	10 - 30
Pyrite	3 – 4
Other sulfides	1 – 2
Grains of primary minerals: chromite, rutile, etc.	1 – 2
Uraniferous Kerogen	1
Gold	~ 45 ppm

2.4.1 Environmental implications of gold mining

One of the problems arising from gold mining is the flood water emanating from ceased mining activities due to ineffective pumping systems. The Western Basin of the Witwatersrand is well known to have a problem of flooding resulting from poor planning of mine closure. The contaminated water pumped from this Basin is estimated to about 60 Ml/day during the wet summer season. Of that, only 12 Ml/day can be treated (Inter-Ministerial Committee on Acid Mine Drainage 2010). In addition, it has been speculated that if the active pumping in the Eastern Basin stops, water will reach the surface of Nigel CBD in East Rand within 30 days (Inter-Ministerial Committee on Acid Mine Drainage 2010). As far as the literature survey of this study extends, there seems to be no back-up plan if these reported threatening circumstances do happen. Figure 8 is a photograph of a dam containing 160 billion litres of water pumped from the KOSH goldfield, where only two thirds of the total volume can be treated (Lifferink 2010).

Figure 8: Mine water pumped from the Eastern Basin of KOSH goldfield (Lifferink 2010).

Gold mining activities generates large tonnages of waste, approximately 99% of gold ore is discharged as waste in the form of mine discharge, waste piles and tailings (Broadhurst *et al.* 2007). Gold mining waste is associated with sulfide minerals (mainly pyrite) that are easily oxidized when exposed to atmospheric air (Janisch 1989). It is in this regard that these same gold mines have left a notorious legacy of acid rock drainage, particularly in the Witwatersrand region where gold mining was pioneered in South Africa. Studies conducted in South Africa to evaluate the extent of ARD generated from mine wastes, as well as its impact on the environment revealed that gold mines are the primary source of waste and pollution, with ARD as a major carrier of toxic pollutants such as As, Cd, Pb etc. (Marsden 1986, Rösner *et al*. 2000, Rosner *et al*. 2001, Mpephu 2003, Naicker *et al*. 2003, Pulles *et al*. 2005, Nengovhela *et al*. 2006, Oelofse *et al*. 2007, Oelofse 2008, Tutu *et al*. 2008, Ogola 2010, Yibas *et al*. 2011).

Geochemical studies carried out in the Gauteng province, South Africa to characterize areas affected by acid rock drainage revealed that acidic conditions have prevailed with a pH unit as low as 3. The acidic pH promotes the dissolution and mobility of toxic elements such as Cd, Ni and Zn. A study conducted by Rosner *et al.* (2001) showed that soil underneath reclaimed gold mine tailings had high concentrations of trace elements: Co, Cr, Cu, Ni, and Zn that exceeded the drinking water standards. Levels of uranium in abandoned gold mine areas near Randfontein, which have been turned into residential, are reported to be 220 times higher than the safe limit, e.g. 0.07 mg in drinking water (Kings 2014). Such soil is deemed unsuitable for agricultural use and is prone to be redistributed to the surrounding area by either wind or erosion. Transportation of the contaminated soil in any form will result in the degradation of the land, water pollution, destruction of aquatic life and distraction on human health that may lead to fatality. One of the major concerns is the contamination of our scarce water systems. It is therefore necessary to assess the extent of the identified risks based on concrete information and reliable scientific facts in order to establish appropriate management plans that are environmentally sound and in favour of the community.

2.5. ARD management strategies

ARD is a self-sustaining cyclic process that is difficult to control once its onset. Currently there are two main options to address ARD: prevention methods and control measures (see Table 8). Unfortunately, the mechanisms involved in the formation of ARD differ from site to site. As a result it is often difficult to develop appropriate prevention methods that are capable of mitigating ARD. ARD prevention and mitigation strategies include water cover, soil cover, blending, backfill etc. Recently, desulfurization has been proposed as an emerging technology to prevent ARD (Hesketh *et al.* 2010). The rate of acid generation can be reduced by minimising oxygen through covers and backfills. ARD generation can be minimised by blending acid-generating and acid consuming materials to produce environmentally benign composites. Alternatively, neutralising ARD raises pH and promotes precipitation of salts.

Table 8: Examples of ARD management methods (Johnson *et al.* 2005).

ARD prevention methods	ARD remediation methods
Flooding/sealing underground mines	Lime neutralisation
Water and soil covers	Wetlands
Backfill	Permeable reactive barriers
Blending	Packed bed iron-oxidation bioreactors
Microencapsulation	
Application of anionic surfactants	

The overall objective of the treatment methods is to increase pH (neutralisation with lime) to a level that causes precipitation of metals which can subsequently be recovered. In this way, the mobility of these elements is hindered and there is a potential for the chance of recovering saleable minerals/compounds (Cheng *et al.* 2011, Chen *et al. 2014*). These treatment methods however, do not completely eradicate the implications associated with ARD and they are costly, and often difficult to implement or sustain. The first and most important step in effectively managing ARD is to use simple, robust, inexpensive, reliable and precise ARD prediction testing procedures to identify ore types with a high potential for ARD generation. Inaccurate results that influence improper decision making may jeopardise the waste management plans such as under-engineering of waste that may cause permanent damage to the environment and become expensive to control.

2.6. Methods of predicting ARD

ARD prediction tests are geochemical tests that are carried out to study the acid generating behaviour of mine wastes and can be broadly classified as either static or kinetic. Static tests include Acid Base Accounting (ABA) and Net Acid Generation (NAG) tests which classify the acid generating potential of the material over geological time without providing information on relative rates. Kinetic tests such as humidity cells, column leach and biokinetic tests provide information on the kinetics of the reaction as well as on the geochemistry of the leachate. These tests are essential in identifying ores with a potential for ARD so that appropriate management strategies can be put in place.

2.6.1. Acid base accounting (ABA)

ABA test is a two-fold test that includes the estimation of the maximum potential acidity (MPA) based on the sulfur content, and the assessment of the acid neutralisation capacity (ANC) using either wet chemistry or mineralogy (Sobek *et al*. 1978, Lawrence *et al*. 1996, Paktunc 1999a, Jambor *et al*. 2002, Jurjovec *et al*. 2002, Kaartinen *et al*. 2009). The difference between the two values (i.e. ANC and MPA) provides an estimation of the net acid producing potential (NAPP) as shown on Eq. 2.8. ABA is the most commonly used test due to its simplicity, low-cost and short time taken to generate information.

$$NAPP = MPA - ANC \quad (2.8)$$

2.6.1.1. Maximum potential acidity (MPA)

The maximum potential acidity (MPA) is determined by measuring the sulfur content of a sample based on the assumption that all sulfur species are in the form of reactive sulfides (mainly pyrite) and are completely oxidized (Sobek *et al*. 1978, Smart *et al*. 2002, Schumann *et al*. 2012). Reaction 2.9 stoichiometry shows that one mole of pyrite will produce 2 moles of sulfuric acid.

$$FeS_2 + (15/4)\ O_2 + (7/2)\ H_2O = Fe(OH)_3 + 2H_2SO_4 \quad (2.9)$$

The MPA (Eq. 2.10) is calculated as the %S multiplied by 30.6 (98.1÷32.1×10) where 10 is a factor used to represent the results as a part per thousand (ppt) which is equivalent to the kg H_2SO_4 generated per tonne of waste (Smart *et al*. 2002, Stewart 2005). Total sulfur is determined by LECO Sulfur that uses high temperature combustion and Infrared spectroscopy.

$$MPA = \%S_{total} \times 30.6 \quad (2.10)$$

The assumptions may result in overestimation of MPA in cases where there are other forms of sulfides that are not acid generating such as elemental, sulfate and organic sulfur. The presence of such sulfur species commonly found in base metal and coal mine wastes may result in overestimation

of the acid generating potential as they do not contribute to the actual MPA (Stewart *et al.* 2009, Kotelo 2013). Hence Stewart *et al*. (2009) developed the ACARP sulfur speciation protocol (Figure 9) that differentiates sulfide sulfur from other forms of sulfur thereby allowing the calculation of MPA based on "pyritic" sulfur (sulfides).

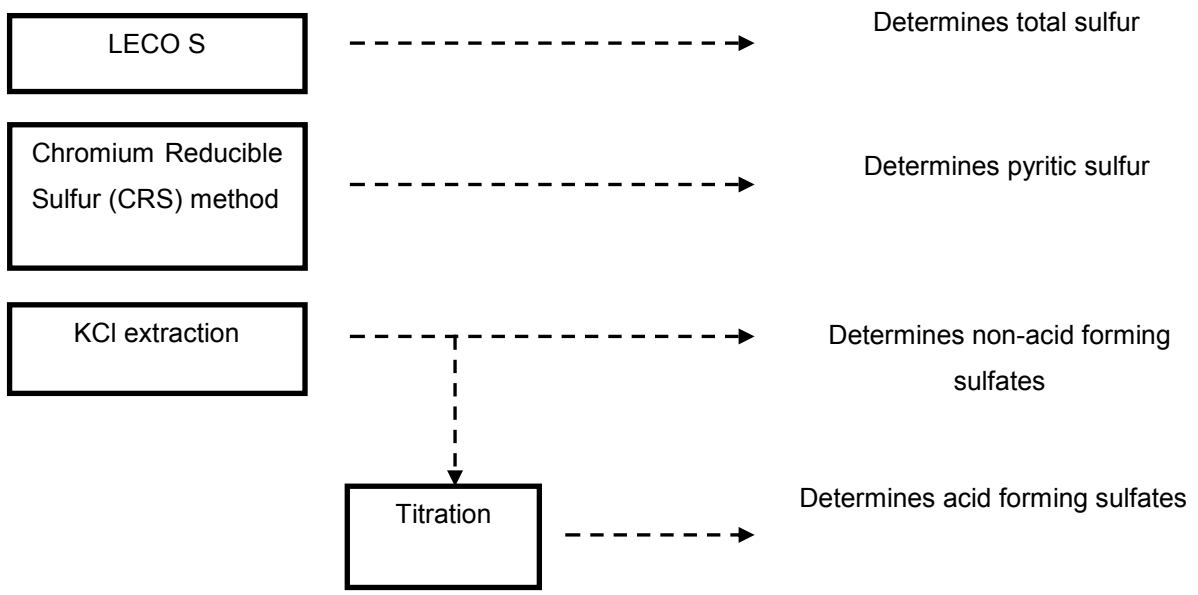

Figure 9: ACARP sulfur speciation protocol developed by Stewart et al. (2009).

The Chromium Reducible Sulfur (CRS) method used in the ACARP protocol to estimate sulfide sulfur content was initially proposed as a chromium reduction method to determine reduced the inorganic sulfur forms (pyrite, acid volatile sulfur and elemental sulfur) of sea sediments and rocks. In the chromium reduction method, reduced inorganic sulfur is decomposed into H_2S in hot acidic $CrCl_2$ solution and collected by trapping it in zinc acetate solution as ZnS. The ZnS solution is titrated with iodate solution to determine the content of reduced inorganic sulfur (i.e. sulfide sulfur). Several studies have been undertaken to modify the CRS method in order to improve its efficiency in terms of test duration, accuracy and reproducibility (Canfield *et al*. 1986, Ahern *et al*. 2004, Sullivan *et al*. 2004, Burton *et al*. 2008 Stewart *et al*. 2009, Schumann *et al*. 2012). The most commonly applied method is the one established by Sullivan *et al*. (2004) which includes an acetone extraction step to remove the elemental sulfur prior to hot acid digestion. However, work done by Stewart *et al*. (2009) to evaluate this method revealed that the acetone extraction step is not mandatory since elemental sulfur commonly occurs in minute concentrations that have no significant effect on sulfide concentration/determination.

The content of sulfates, the most oxidized form of sulfide species, depends on the extent of oxidation of mine waste. Ahern *et al*. (2004) in the SPOCAS report presented a three-stage extraction method: KCl/argon-purged water extraction to dissolve soluble sulfates, roasting to remove pyrite and HCl extraction to recover jarosite. Li *et al*. (2007) modified the HCl/KCl extraction by reducing the duration of the extraction. The drawback of this extraction is the critical temperature for roasting, as it may

result in loss of sulfur as SO_2. However jarosite is grouped with low risk sulfur due to its slow kinetics and contribution to the net acid production. Hence the HCl/KCl extraction method was replaced by the KCl extraction method developed for ACARP by Miller (2008). The KCl extraction method involves treating the sample with a KCl solution under inert conditions at ambient temperature and splitting the aliquots into two parts, one for chemistry to measure elemental composition (S, Fe, Ca, Mg, Na) and the other for assessing the acidity of the sulfates through back-titration with NaOH to pH 7 units. The elemental composition data is used to differentiate between acid generating and non-acid generating forms of sulfate species present in the sample. Organic sulfur classified as low-risk sulfur (Eq. 2.11) can also be determined using the difference of the sulfur species obtained from this protocol.

$$\text{Low risk S} = \text{Total S} - (\text{CRS} + \text{KCl S}) \quad (2.11)$$

$$S_{acid} = \text{CRS} + \text{Acidic Sulfates} \quad (2.12)$$

$$\text{MPA} = \%\ S_{acid} \times 30.6 \quad (2.13)$$

Equations 2.12 and 2.13 allow calculation of acid generating potential based on only acid forming minerals. Thus addresses the discrepancies that may arise due to conservative assumptions. Mineral composition can be used in conjunction with the ACARP protocol when interpreting information in order to optimise its efficiency.

2.6.1.2. Acid neutralization capacity (ANC)

The acid neutralisation capacity is determined chemically by treating the sample with a standard acid followed by titration with a standard base. The amount of base added to neutralise the unreacted acid is measured and converted to a kg H_2SO_4 per tonne in order to simplify comparison. The sample investigated is subjected to a 'fizz rating', which is a test that evaluates the presence of carbonates prior to acid treatment. The fizz rating determines the amount and concentration of the acid needed to leach the samples, as well as the base for back-titration to pH units of 4.5 and 7.0. The leaching conditions of commonly used tests and the respective references are summarised in Table 9. The minerals expected to dissolve is a courtesy of Department of Water Affairs and Forestry (2008). The amount of the base used to titrate to pH 4.5 is used to estimate the neutralization potential that results from the dissolution of carbonates such as calcite and, dolomite; the precipitation of aluminium hydroxides from dissolution of aluminosilicates and the precipitation of Cu, Zn, Pb, Fe hydroxides from sulfide oxidation. Back-titration to pH 7.0 is used to estimate the free acid remaining unreacted in the solution.

Table 9: Commonly used ANC test methods and the minerals expected to dissolve.

ANC test	Leaching conditions	Minerals dissolved
Sobek (Sobek *et al.* 1978)	Heat for 1 – 2 hours (hrs) at 80 – 90^{0}C Boil for 1 minute	Carbonates, fast, intermediate and slow weathering silicates[#]
Lawrence and Wang (Lawrence *et al.* 1997)	Shaking at room temperature for 24 hours	Carbonates, fast weathering silicates
AMIRA modified Sobek (Smart *et al.* 2002)	Heat for 1 – 2 hrs at 80 – 90^{0}C Add 2 drops of 30% H_2O_2 after back-titrating to pH 4.5	As per Sobek excluding Fe and Mn carbonates, slow weathering silicates
Incremental Skousen siderite correction (Stewart *et. al.* 2009)	Heat for 1 – 2 hrs at 80 – 90^{0}C Incrementally add 30% H_2O_2 after back-titrating to pH 4.5 until pH stabilises	As per Sobek excluding Fe & Mn carbonates, slow weathering silicates

[#]see Table 2.1

The first ANC test was developed by Sobek *et al*. (1978) to assess the neutralisation potential of mine overburden. The Sobek ANC test involves a boiling step to facilitate the dissolution of neutralising minerals such as carbonates and reactive silicates. Many researchers reported that the Sobek ANC test overestimates the neutralisation capacity due to the boiling step that promotes the dissolution of minerals that are slowly-reacting or inert under normal environmental conditions (Lawrence *et al*. 1989, Skousen *et al.* 1997 Jambor *et al*. 2002, Plante *et al*. 2012).

Subsequently, Lawrence *et al*. (1989) proposed a modified Sobek ANC test (named Lawrence and Wang ANC test in this study) that involves the acid digestion of a sample at ambient temperature for 24 hours. The Lawrence and Wang ANC method addresses the shortcoming of dissolving minerals that have little or no contribution to the acid neutralisation (i.e. silicates) in a real case scenario while allowing sufficient time for reactive minerals (viz. carbonates) by operating for 24 hours instead of 2 hours from the Sobek test. Lawrence *et al*. (1996) re-evaluated the Lawrence and Wang ANC test and further refined it to improve its efficiency. The refined Lawrence and Wang ANC test includes a 2-step addition of acid and shaking at room temperature for 24 hours. The Lawrence and Wang test returned ANC values less than those from Sobek test.

Various neutralising minerals have different reaction rates and they react differently under different test conditions (Jambor *et al.* 2002). Carbonates have higher neutralisation potential relative to other

minerals due to their fast dissolution rates even at near-neutral pH, unlike the silicates that only dissolve under acidic conditions. Carbonates associated with oxidisable cations such as Fe^{2+} may have no net neutralisation capacity as shown by Skousen *et al.* (1997) and Paktunc (1999b) using siderite as an example. The dissolution of siderite consumes acid which is later released during precipitation of ferric iron as hydroxide following the mechanism outlined in reactions 2.14 – 2.16.

$$FeCO_3 + 2H^+ = Fe^{2+} + CO_2 + H_2O \quad (2.14)$$

$$Fe^{2+} + 1/4O_2 + H^+ = Fe^{3+} + 1/2H_2O \quad (2.15)$$

$$Fe^{3+} + 3H_2O = Fe(OH)_3 + 3H^+ \quad (2.16)$$

Both the Sobek and Lawrence and Wang ANC tests do not account for or address this limitation. The Sobek test may dissolve siderite, but the time period of the test is not sufficient to allow all 3 reactions to occur. This may result in an overestimation of the acid neutralisation potential for samples with significant amounts of siderite. The ambient temperature condition of the Lawrence and Wang ANC test reduces reaction kinetics and that makes 24 hours insufficient for these reactions to take place. Evans *et al.* (1995) proposed different modifications on the Sobek ANC test such as filtering, boiling for longer, and addition of hydrogen peroxide. All the tests returned information with no appreciable differences. Skousen *et al.* (1997) carried out four different ANC tests with the modifications stated above at 3 different laboratories. The ANC test that includes a peroxide addition step had less ANC values compared to the Sobek test and this was due to oxidation of ferrous iron into ferric iron by peroxide followed by the formation of ferric hydroxide that releases the consumed acidity. Skousen *et al*. (1997) concluded that the Sobek ANC does not accurately reflect the actual neutralization potential for samples with content of siderite, Skousen *et al.* (1997) recommended the incorporation of the peroxide addition step, nowadays known as Skousen siderite correction ANC test. Smart *et al*. (2002) developed an AMIRA modified Skousen siderite correction test that includes addition of 8 drops of H_2O_2 after back-titrating to pH 4.5. The H_2O_2 added however, may be decomposed prior to complete oxidation of ferrous iron. Stewart *et al.* (2009) developed an Incremental Skousen siderite correction method that continually adds H_2O_2 after back-titrating to pH 4.5 until the pH stabilises at 4.5 units (complete oxidation). The Sobek fizz rating depends on human physical judgements and has been reported to be one of the sources of errors associated with ANC (Lawrence 1989, Paktunc 1999, Weber 2004). Hence Smart *et al* (2002) introduced the AMIRA fizz rating which consists of wider categories and expected pH ranges to ensure that the appropriate acid concentration is used.

The reproducibility of ANC test strongly relies on the methodology of the test and mineralogy of a sample. Understanding the sample mineralogy and content of neutralising minerals plays a critical role in selecting the suitable method, thus minimising errors as all tests have their inherent advantages and disadvantages. ABA tests assume complete reactivity of sulfides and dissolution of neutralising minerals but no study has been carried out to thoroughly quantify the differing reactivity of these various minerals under different test conditions. It is well recognised that the reactivity strongly

depends on system properties such as temperature, pH, duration, and most importantly on sample mineralogy and textural properties.

The ANC can also be evaluated using calculations based on the bulk mineralogy of the neutralising minerals (Lawrence *et al*. 1997, Paktunc 1999b, Plante *et al*. 2012). Lawrence *et al*. (1997) established an equation to calculate ANC using the dissolution rates at pH 5 units (see Table 5) and mineralogical composition calculated from the chemistry analysis of major oxides (Al, Ca, Mg, Na and K) analysed on digestion leachate. This equation does not account for the neutralization of carbonates associated oxidisable cations such as siderite, which are known to have no net neutralization potential. Silicates that are included in this equation do not usually provide significant neutralisation that can counterbalance sulfide oxidation due to their slow kinetics especially under near-neutral pH conditions. This method of estimating ANC may lead to misclassification of the neutralisation potential since the mineral composition was not directly measured. Paktunc (1999b) further developed an equation that includes only carbonates with their differing contribution towards ANC, while taking into account oxidisable cations. Plante *et al*. (2012) evaluated these equations (Table 10) on different five hard rocks, while comparing them with the Lawrence and Wang ANC test, the one carried out at room temperature for 24 hours.

Table 10: Mineralogical ANC methods (Plante et al. 2012).

Method	Formulation	Characteristics
Lawrence and Scheske (1997)	$ANC = 1000 \times M_{CaCO3} \times \sum_{i=1}^{n} \frac{C_{Mi} \times R_i}{M_{Mi}}$	Takes into account carbonate and neutralising silicates Does not account for Mn + Fe carbonates
Paktunc (1999)	$ANC = \sum_{i=1}^{k} \frac{10 \times X_i \times w_a \times c_i}{w_i \times n_{Mi}}$	Takes only carbonates into account Accounts for Mn + Fe carbonates
(Plante *et al*., 2012)	$ANC = 1000 \times M_{CaCO3} \times \sum_{i=1}^{n} \frac{C_{Mi} \times R_i \times c_i}{M_{Mi}}$	Accounts for Mn + Fe carbonates Includes carbonates and silicates

Plante *et al*. (2012) did not conclude on which method is superior but recommended the use of mineralogy in selecting the appropriate ANC method (see Figure 10) and further proposed a Lawrence-Scheske-Paktunc ANC method that incorporated properties of the Lawrence and Wang, and Paktunc methods. The Lawrence-Scheske-Paktunc ANC method however uses the dissolution rates at pH 6 and calculated mineralogy that are not precisely mineralogical properties. Hence, as far as the literature survey extends, only the Paktunc ANC method was considered as the mineralogical ANC method.

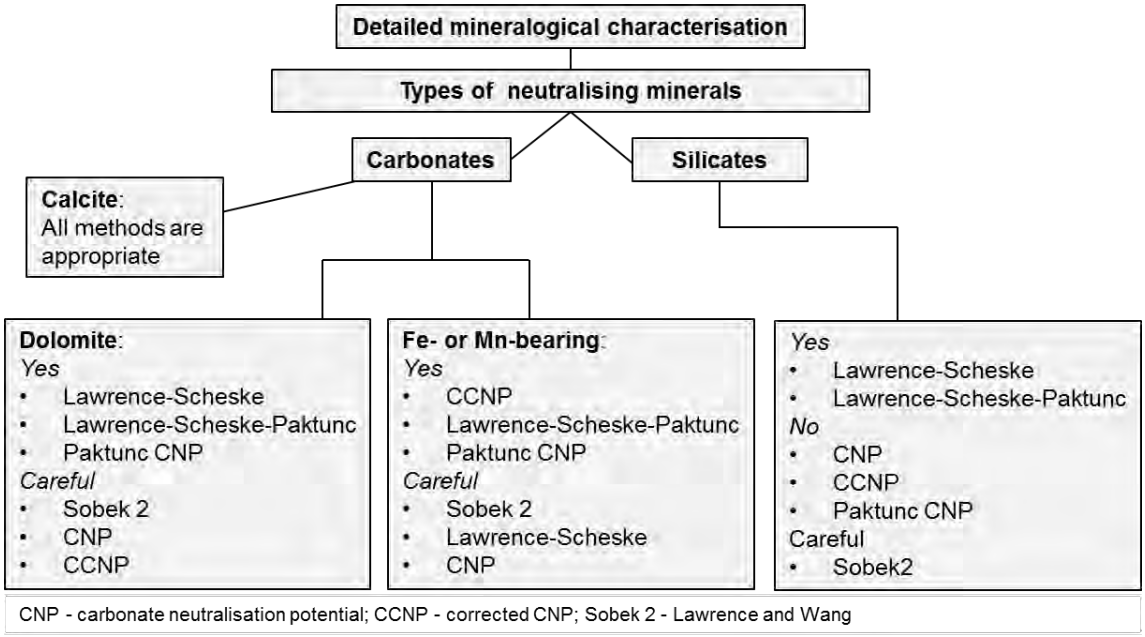

Figure 10: ANC tests selection flowchart (Plante *et al.* 2012).

2.6.2. Net acid generation (NAG) test

The net acid generation test is a laboratory-scale geochemical test that assesses the acid generating potential of a sample by chemically quantifying the interaction between acid generating and acid consuming minerals. The NAG test was initially developed by Sobek *et al*. (1978) as a method that uses hydrogen peroxide to estimate the acid generating potential of overburden samples and was later modified by Finkelmann *et al*. (1986) as a hydrogen peroxide test that determines the pyrite content of coal-related wastes. The hydrogen peroxide used is a strong oxidising agent that promotes rapid complete oxidation of sulfides (Sobek *et al*. 1978) as demonstrated in reaction 2.17. Acidity generated from sulfide oxidation stimulates reactive neutralising minerals, thus allowing sulfide oxidation and mineral dissolution reactions to take place simultaneously.

$$FeS_2 + 15/2H_2O_2 = Fe(OH)_3 + 4H_2O + 2SO_4^{2-} + 4H^+ \quad (2.17)$$

Lawrence *et al*. (1989) applied the same principle on hard rock samples to determine the acid generating potential through net acid production (name used for NAG) test but the information obtained was highly inaccurate. O'Shay *et al*. (1990) then modified the method by Finkelmann *et al*. (1986) and improved the reproducibility of the test. Modifications including treating the sample with 15% H_2O_2 on 1:1 ratio of grams of the sample: millilitres of H_2O_2, heating the solution for an hour and filtering were then applied to NAP test by Lappako *et al*. (1993). The modified NAP test results showed complete oxidation of sulfides (99%) and correlated with the results of acid base accounting.

The NAG test suffers from several limitations such as the decomposition of hydrogen peroxide prior to the complete oxidation of sulfides and/or oxidation of minerals other than sulfides that may lead to

misclassification of the acid generating potential of a sample (Lawrence *et al*. 1989, Smart *et al*. 2002). Hydrogen peroxide decomposition may be attributed to either the presence of carbonaceous materials and sulfates or to the rapid rise of temperature as a result of the exothermic sulfide oxidation reactions (Sobek *et al*. 1978). Thorough research has been done in order to optimise the reliability on these tests. This has led to developments of modified testing procedures that account for the limitations encountered in single-addition NAG test. These methods are: sequential-, kinetic- and multi-NAG tests.

Multi-NAG (mNAG) test which uses the same volume of hydrogen peroxide as the single-addition NAG, but added stepwise (i.e. 250 ml added once in single-addition is added as 100 ml twice and then 50 ml later in the multi-addition NAG test) was proposed in order to minimise peroxide decomposition. Studies undertaken by Stewart (2005) and Parbhakar-Fox (2012) revealed that there is no significant difference between single-addition and mNAG test. Hence the aforementioned researchers concluded that the peroxide decomposition is time-independent.

Smart *et al*. (2002) proposed a sequential-NAG (sNAG) test that aims at minimising the decomposition of hydrogen peroxide prior to the complete oxidation of the sulfides. The sequential-NAG test involves multi-stage series of single-addition NAG test on the same sample until the after-boil pH stabilizes at 4.5 units. Stewart (2005) applied the sequential-NAG test on coal mine waste and concluded that is suitable for samples with sulfide content >1 wt. %. A study conducted by Price (2009) to evaluate both the single-addition and sequential NAG tests showed that the single-addition NAG is suitable for samples with a sulfide sulfur content <1% and low concentration of metals, such as copper, that may promote the decomposition of H_2O_2. Parbhakar-Fox *et al*. (2012) reported that sequential-NAG can take up to seven steps before the pH stabilizes or becomes greater than 4.5 and this consumed about 1.75 litres of H_2O_2. Hence Parbhakar-Fox *et al* (2012) recommended use of the mNAG for samples with sulfide content >0.3 to 3 wt. % and for samples dominated by sulfides other than pyrite, but the results must be cross-checked with single-addition NAG test. For samples containing >3 wt. % sulfide content dominated by pyrite, mNAG underestimated the acid generating potential hence suggested use of sNAG test. These observations highlight the importance of understanding the sample mineralogy when selecting the appropriate method(s) and interpreting the results.

2.6.3. Interpretation and presentation of static test results

The discussions in sections 2.6.1 and 2.6.2 have shown that each test has both its own advantages and disadvantages. The acid generating potential can be properly characterized by employing more than one static ARD prediction test to improve the confidence in the results obtained. ABA and NAG tests are commonly carried out together as part of screening stage. ABA (NAPP) and NAG (NAG pH) are usually presented concurrently to classify the acid generating potential using the guidelines summarised in Table 11. In many cases, assumptions (e.g. complete oxidation of sulfides irrespective of mineral liberation and surrounding environment, and all sulfur forms present are acid generating)

are made based on site specific information but end up applied globally. These assumptions can only be explained and appropriately implemented by understanding the mineralogy of the samples investigated.

Table 11: Classification guidelines for the static test results (Stewart et al. 2006).

ARD tests	Results (kg H_2SO_4/t)	Classification
Acid base accounting (ABA)	NAPP > 0 NAPP < 0	Potentially acid forming Non-acid forming
Net acid generation (NAG)	NAG pH < 4 and NAG_{pH7} > 10 NAG pH > 4.5 and 5 < NAG_{pH7} < 10	Acid forming Non-acid forming
Combined NAG and ABA	NAG pH < 4.5 & NAPP > 0 NAG pH > 4.5 & NAPP < 0	Potentially acid forming Non-acid forming
If either of these criteria fail, the results are considered uncertain and further testing is required for classification		

2.6.5. Chemical kinetic tests

Humidity cell and column leach tests are the commonly used laboratory-scale kinetic tests. As a result, only these two will be discussed in this section. The humidity cell test simulates weathering by aerating a sample (typically 1 kg) with dry and humid air and flushing weekly with deionised water to wash out the primary reaction products (Sobek *et al*. 1978, Frostad *et al*. 2002, Benzaazoua *et al*. 2004 and Sapsford *et al*. 2009). Humidity cells are widely used to estimate the relative kinetics of weathering and the lag time to ARD onset, but they are resource intensive and can take up to several years to generate meaningful results (although minimum time is 20 weeks). Worth noting that lag time refers to the time taken by microbes to colonise, usually at pH level below 4. This takes time due to the slow kinetics of pyrite oxidation by oxygen. Several studies carried out on the humidity cell tests addressed questions such as: how long, how many, whether sample pre-treatment is necessary or how to interpret data (Morin *et al*. 1999, Bowell *et al*. 2006, Gonzalez-Sandoval *et al*. 2009, Sapsford *et al*. 2009, Villeneuve *et al*. 2009, Waples *et al*. 2009). Consequently, the humidity cell test was standardised as the ASTM-D5744-96 method (Morin *et al*. 1998, Villeneuve *et al*. 2009). The minimum recommended time to carry out the humidity cell test is 40 weeks (Morin *et al*. 1998, Price 2009), but some researchers have found that it is necessary to continue the test for up to 173 weeks (Herell *et al*. 2009). The studies conducted by Benzaazoua *et al*. (2004), Sapsford *et al*. (2009), Villeneuve *et al*. (2009), Bouzahzah *et al*.(2010) showed that the results obtained from the humidity

cell tests are sensitive to the test conditions and the method of interpretation (e.g. oxidation-neutralisation curve).

Column leach tests are conducted in the same manner as the humidity cells, except that they are flushed monthly and dried with heat lamps. Free draining column leach tests involves the intermittent irrigation of a sample (roughly 2-3 kg) throughout the test period ((Benzaazoua *et al*. 2004, Smart *et al* 2002). Column leach tests provide information on the release rate of elements that are formed as products of sulfide oxidation, dissolution of neutralising minerals and the precipitation of secondary minerals (Smart *et al*. 2002, Sapsford *et al*. 2009). Unlike humidity cells, column leach tests are not yet standardised.

Humidity cell test conditions are regarded as more aggressive than normal environmental oxidation conditions and the wetting and drying cycle is reported to disrupt oxidation (Frostad 2002, Benzaazoua *et al*. 2004). Column leach tests are more suitable for the determination of drainage quality (geochemistry) whereas humidity cell tests are suitable for assessing long term acid generating potential (Benzazzoua 2004). Each method has both limitations and advantages. Hence the choice of the test will depend on the project hypothesis and objectives. It is recommended to always consolidate mineralogy and chemistry in selecting and interpreting the geochemical tests in order to minimise any complications arising due to the heterogeneity experienced in mine wastes (Morin *et al*. 1998).

2.6.6. Biokinetic test

The biokinetic test is a microbial shake flask test developed at the University of Cape Town (UCT) by Hesketh *et al.* (2010) to study the effect of bacteria population on the acid generating potential. The first test developed to evaluate the effect of microbes on acid generating potential was the British Columbia Research Confirmation (BCRC) test. The BCRC test however, suffers limitations such as initial acidification of the sample prior to testing and the use of only one oxidizing species. As a result the BCRC test is considered as not representative of natural oxidation (Lawrence *et al*. 1989). Unlike the BCRC test and biokinetic test, microbial activity occurred accidentally in column leach and humidity cell tests. In the UCT biokinetic test, a non-acidified sample is inoculated with mixed cultures of sulfur- and iron-oxidising bacteria (*Acidithiobacillus ferrooxidans, Leptospirillum ferriphilum, Acidithiobacillus caldus and Sulfobacillus benefaciens*). Unlike the BCRC test and biokinetic test, microbial activity occurred accidentally in column leach and humidity cell tests. Parameters measured as a function of time to determine whether the sample has a potential to generate acid are pH, redox potential and iron concentration.

The biokinetic test is specifically designed to provide information on the relative rates of the acid forming and acid neutralising reactions under conditions of microbial colonisation. The test is relatively simple to operate and produces meaningful data in a relatively short space of time. As such it addresses many of the short-comings of the chemical kinetic tests discussed in Section 2.6.5. Studies

at the University of Cape Town have extended the application of this test to a number of wastes: coal fines, coarse coal discards, copper sulfide tailings and waste rock, as well as pyrrhotite-rich tailings from the processing of nickel sulfide ores (Kazadi Mbamba 2011, Chimbganda 2012 and Kotelo 2013). In general, the pH-time profiles in Figure 11 for the biokinetic tests are characterized by an initial increase in pH, due to the acid dissolution of relatively reactive carbonate minerals. As these minerals become depleted and the rates of acid generating sulfide oxidation reactions increase, the pH decreases and wastes become net acid generating. In sulfide-lean tailings, such as those generated through the desulfurisation flotation of conventional processing wastes, no decline in pH was observed, and the samples remained net acid neutralising for the duration of the test. A comparison of results shows variations in pH profiles, with the rates and extents of increases and subsequent decreases in pH being dependent on ore type and mineralogy. A lot of work has been done on microbial leaching of sulfides (Sasoki *et al.* 2009, Chi *et al. 2006*). However, no detailed studies have been conducted to better understand mechanisms of the key reactions involved in ARD formation under the biokinetic test conditions.

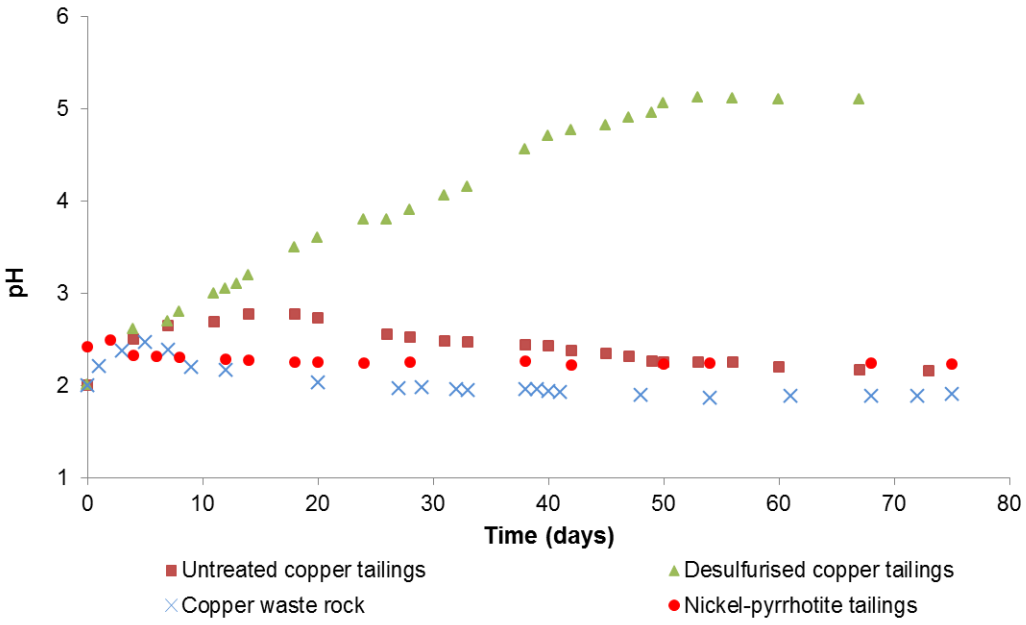

Figure 11: Biokinetic test results for wastes from processing of hard-rock ores (Broadhurst *et al.* 2013).

2.6.7. Acid rock drainage index (ARDI)

Parbhakar-Fox *et al*. (2011) developed an acid rock drainage index (ARDI) that predicts the acid generating potential based on the modal mineralogy and textural properties of the material such as liberation, degree of alteration, association and morphology. The ARDI forms part of the screening stage of the geochemistry-mineralogy-texture (GMT) approach. One of the advantages of the ARDI is that it does not only consider the bulk mineralogy, but the textural properties of the mine waste that

have direct influence on ARD formation (Parbhakar-Fox *et al*. 2012). The five parameters investigated include: sulfide content (A), sulfide alteration (B), sulfide morphology (C), neutraliser content (D) and spatial relationship between sulfide and neutraliser content (E). Figure 12 is a schematic showing the scoring of the parameters describing sulfide morphology taken from Parbhakar-Fox (2012).

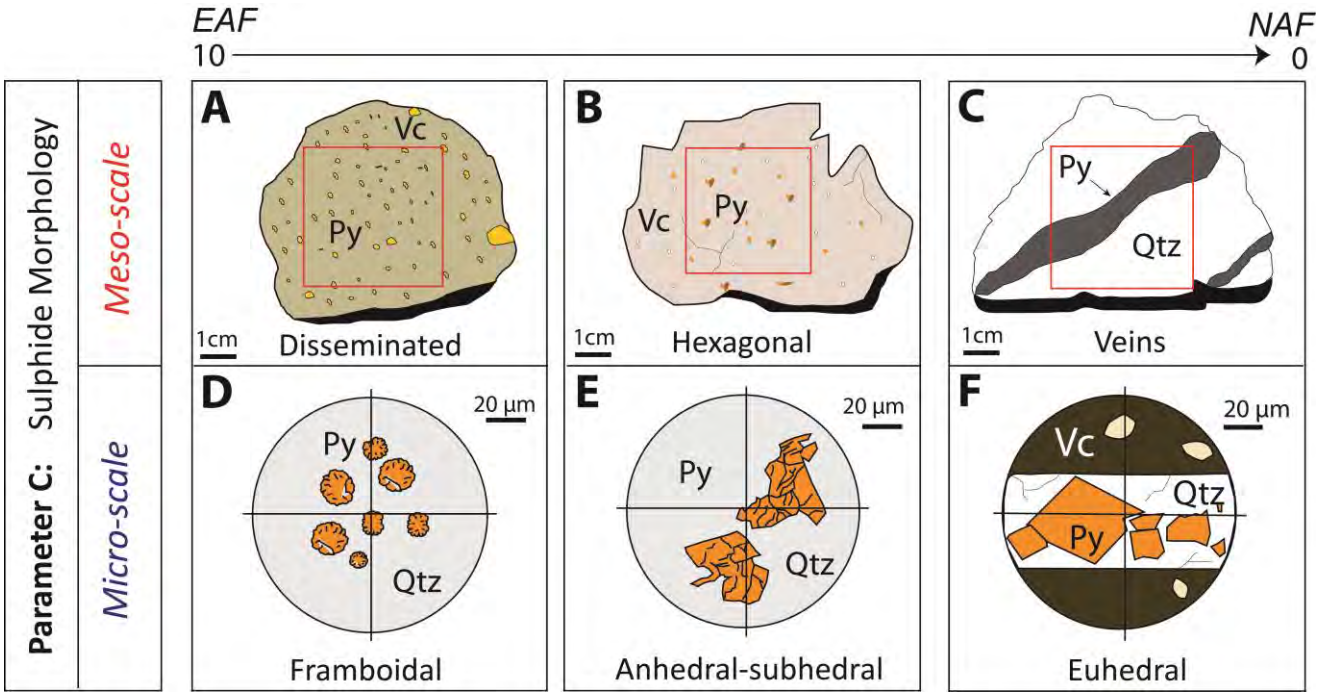

Figure 12: Diagrammatic examples of ARDI evaluation for morphology on meso-scale (1 cm) and micro-scale (20 µm) (Parbhakar-Fox 2012). EAF: Extremely acid forming, NAF: not acid forming.

Figure 12 shows that disseminated sulfides (EAF) are more susceptible to oxidation due to their greater surface area whereas the pyrite inclusions in inert quartz veins (NAF) make it unavailable for oxidation (Parbhakar-Fox 2012). Euhedral pyrite is less reactive than framboidal pyrite (Weber *et al. 2004*). Using the bulk mineralogy and texture, the acid generating potential can be estimated based on the knowledge of reactivity of minerals appearing in such forms. Each parameter is scored out of 10, with the highest value indicating a higher potential to generate acid. The negative value indicates that the sample is non-acid forming and is potentially acid neutralising. The scores from all the parameters are summed up to a total of 50. The final ARDI value is used to classify the acid generating potential according to Table 12.

Table 12: ARDI classification guidelines from (Parbhakar-Fox et al. 2011).

Final ARDI Value	ARD Classification
50 to 41	Extremely acid forming
40 to 31	Acid forming
30 to 21	Potentially acid forming
20 to 11	Not acid forming
10 to 0	Not acid forming/ acid neutralising capacity
-1 to -10	Acid neutralising capacity

2.6.8. Effect of mineralogy on the interpretation of ARD prediction tests

Recommendations have been made by several researchers to incorporate mineralogy into ARD prediction suite (Lawrence *et al*. 1997, Morin *et al*. 1998, Paktunc 1999b, Parbhakar *et al*. 2009b, Akabzaa *et al*. 2012). In practise, this is seldom taken into consideration due to time and financial constraints. The study conducted by Parbhakar-Fox *et al.* (2013) shows the costs for methods that involve the study of mineralogy (e.g. wheel approach and GMT). Information obtained from the mineralogical characterization can be used in selecting sample specific tests, to interpret the results from the geochemical tests and as a stand-alone prediction technique. Mineralogy and chemistry are used in studying mechanism of reactions that contribute to the drainage chemistry. The presence of precipitating secondary minerals that can armour sulfides and/or carbonates may alter the reactivity of these minerals thereby compromising conclusions drawn based on the prediction test results. Outcomes such as results leading to the misclassification of acid generating potential (Figure 13) have motivated researchers (i.e. Parbhakar *et al.* 2009b, Plante *et al.* 2012) to incorporate mineralogy in ARD prediction suites.

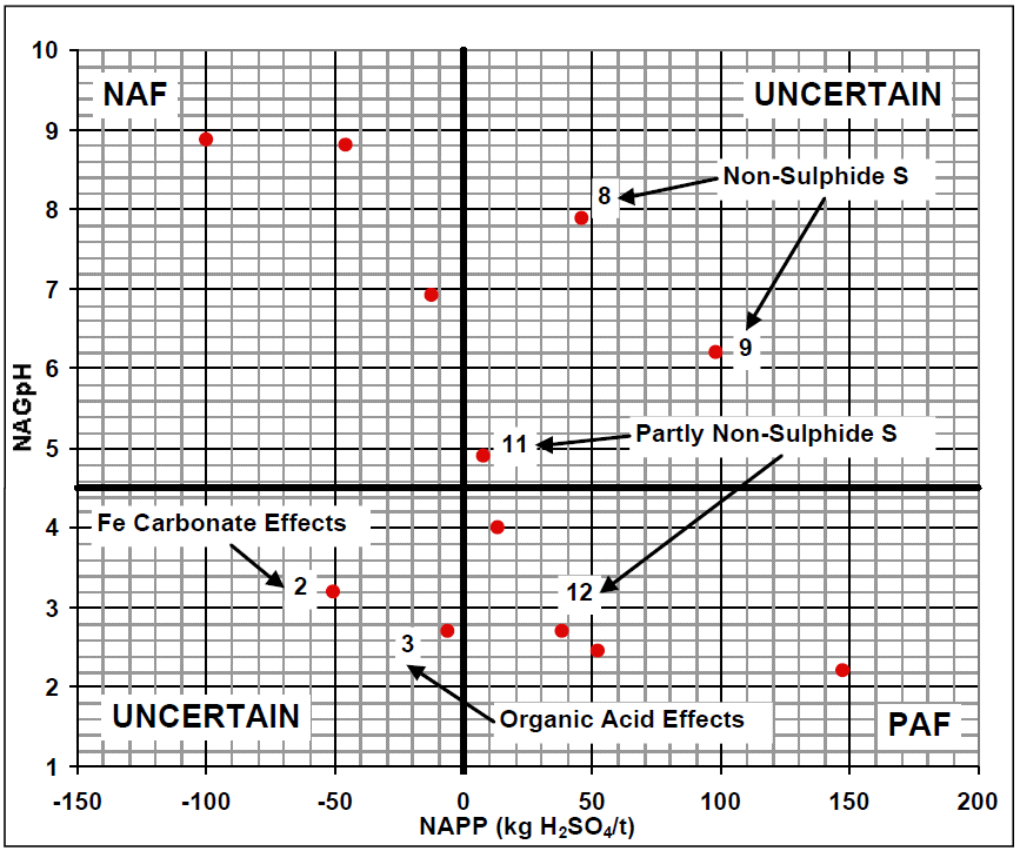

Figure 13: ARD classification plot for a case study sample set from Stewart et al (2006).

Figure 13 shows a comparison of static tests (i.e. Acid Base Accounting, ABA and Net Acid Generation NAG). This figure shows the contradictions encountered when comparing ABA and NAG results, which can be attributed to ore characteristics, specifically mineralogical compositions. As expected, samples with non-sulfide sulfur (non-acid forming sulfur species) result in an overestimation of NAPP during the ABA test. The presence of Fe carbonates, on the other hand, underestimates NAPP, since in ANC tests without siderite correction, these compounds are net-acid consuming. The presence of organic matter in coal wastes has been shown to overestimate the acid generating potential during NAG tests, due to the formation of solid organic acids from oxidation of carbonaceous material.

2.7. Summary of the literature review

Gold mining and beneficiation has been a major contributor to the economy and establishment of infrastructure in South Africa for over a century. However, the same gold mines in South Africa are associated with several environmental implications such as acid rock drainage (ARD) formation (Mpephu 2003, Naicker *et al*. 2003, Oelofse *et al*. 2007, Oelofse 2008). The ARD is characterized by low pH, high sulfate content and elevated concentrations of heavy metals. The mobility of heavy

metals may lead to land degradation, pollution of our scarce water resources and destruction of aquatic life. Unless interventions are put in place, the production of ARD may continue for many generations following the closure of mining activities. The first important step in effectively managing ARD is using simple, reliable and inexpensive ARD prediction testing procedures to identify ores with a high potential for ARD generation. The overall objective of these testing procedures is to evaluate the balance between the acid generating reactions and acid neutralising minerals.

Mineralogy plays a key role in the acid rock drainage formation. Various sulfides and neutralising minerals react differently and have varying contribution to the net acid generation. In the case of acid base accounting, determination of acid generating potential is standardised to be estimated based on sulfide content. The neutralisation potential however, has captured the interest of many researchers as it is not standardised and susceptible to a variety of inconsistencies. The Sobek ANC method is known to be aggressive when compared to other methods due to its higher ANC values. The boiling step in Sobek ANC allows the dissolution of the inert or slow reacting minerals, while the Lawrence method, carried out at room temperature, is considered to be more representative of the natural environment. The argument may have arisen on whether a method (Lawrence method) returning lower ANC values should be considered more accurate or whether it underestimates the neutralisation potential. Limitations of the NAG test have been identified and dealt with through the development of modified methods that address such shortcomings.

The conventional kinetic tests (i.e. humidity cell and column leach) carried out to study the long term acid generating behaviour of mine waste are resource extensive and may take up to several years to generate meaningful results. In addition to that, these kinetic test methods are sensitive to test conditions and methods of interpretation, and scale-up is highly uncertain and often controversial. The results obtained from kinetic test are complex to interpret without a thorough understanding of the mineralogy and geochemistry. Furthermore, neither the static nor the standard kinetic tests provide any information on the effect of microbiology on ARD formation. The UCT biokinetic test is a kinetic test developed to address the limitations of current static and kinetic tests. The biokinetic test provides information on the effect of microbial population on ARD formation, relative reaction kinetics within shorter period of ~90 days. However interpretation of the information obtained from biokinetic test is limited due to complex interactions such as chemistry, mineralogy and microbiology. Mineralogy is a technique that can be used as a stand-alone test and as a tool to study behaviour of mine waste under different ARD prediction test conditions. This will enhance the level of understanding of the controlling reactions, subsequently simplify interpretation of results and ultimately improve reliability on these tests.

2.8. Hypothesis and research questions

The key findings from the literature review highlighted the importance of understanding the mineralogical characteristics of a sample when assessing the acid generating potential of mine wastes. It has been acknowledged that application of the ARD prediction tests in research practices is different from real-world practices. The AMIRA modified Sobek ANC was selected over the Sobek ANC based on the wider fizz rating scale. It was also noted that there is no ANC method superior to the other (Morin *et al.* 2009). The hypotheses formulated based on literature review of research practices are:

I. The AMIRA modified Sobek ANC method overestimates ANC relative to the Lawrence and Wang method due to the high-temperature leaching conditions that allow the dissolution of slow weathering silicate minerals.

II. The prolonged test duration of the biokinetic test allows complete oxidation of sulfides and dissolution of carbonates and reactive silicates.

Research questions to be addressed are as follows:

I. What are the mineralogical factors associated with the changes of empirical ANC under different ABA test conditions and how does the empirical ANC compare to the mineralogical ANC?

II. What is the extent of mineral leaching during conventional static and the novel biokinetic geochemical tests for ARD prediction?

III. How do the results of the mineralogical and above-mentioned geochemical tests compare in terms of characterising ARD potential?

IV. In what way can mineralogical analysis be used to enhance the interpretation of ARD characterisation?

CHAPTER 3

MATERIALS AND METHODS

This chapter presents the experimental work carried out in this study. The experimental work includes sample preparation, characterisation of the sample for mineralogy, chemistry and ARD potential as shown in Figure 14. This chapter also explains different test methods used to characterize the ARD potential and analysis performed on the solid residues and leachates sampled after the leaching stage, before back-titration.

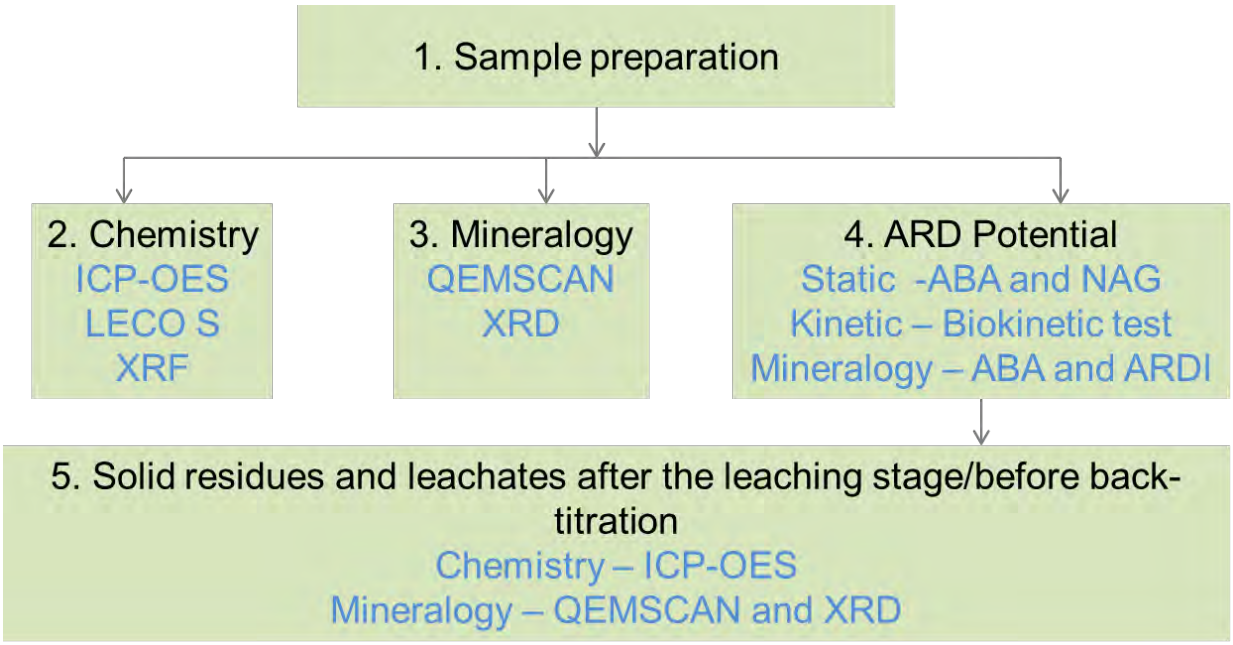

Figure 14: Flow diagram of experimental work and methods.

3.1. Sample preparation

A bulk composite sample of run of mine (ROM) ore obtained from an active South African gold mine, near Carletonville (see Figure 7) on the Witwatersrand in South Africa was used as a case study

(since actual tailings was not available at the time of study). The bulk sample consisted of 80% stock pile ore and 20% underground channel sampling gold ore. The gold sample was crushed using the high pressure grinding rolls (HPGR) at a pressure of 120 bar and then split into 1 kg portions following the representative sampling protocol (Nwaila 2014). The product was then dry screened and particles from the +4/-5.6 mm, and -1 mm size classes were selected for use in this study. The +4.0 mm sample was used to characterize unbroken textures for ARDI evaluation. The weighed 1 kg portions of -1.0 mm sub samples were further split using a rotary splitter in order to obtain 300 g samples for screening. The 300 g sample was dry screened on a stack of sieves from 1 mm down to 38 µm in order to obtain a bulk -150 µm sample. Representative subsamples of the -150 µm were further pulverized to 100% passing 75 µm in order to meet the requirements for the ARD prediction tests. Both the -150 µm and pulverized -75 µm samples were dried by leaving them open at room temperature until a stable mass reading was measured. Taking into to account the importance of representative sampling as emphasized by Brough *et al.* (2013), the samples were split using the "blend and split" principle on different scales of rotary splitters into smaller portions as required for the various analysis and tests.

3.2. Mineralogical and Chemical Characterization

3.2.1. Chemical characterization

The chemical composition was evaluated using both Inductively Coupled Plasma Optical Emission Spectroscopy (ICP-OES) and X-Ray Fluorescence (XRF) at the University of Cape Town. The feed sample was analysed for both major and minor elements: Al, Ca, Cr, Fe, K, Mg, Mn, Na, Ni, P, S, Si and Ti. The data obtained from XRF was used to select elements of interest throughout this project. The elements selected were studied to evaluate reactions of interest concerning the objectives of this study: sulfide oxidation, dissolution of acid neutralizing minerals, formation of secondary minerals and trace elements deportment. Some elements were not studied due to their low concentrations (below detection limit) on the feed. The elements analysed on the solid residues and liquors sampled after the leaching stage from the ARD prediction tests are: Al, Ca, Fe, K, Mg, S and Si. Both residues and leachates were supposed to be analysed with ICP-OES. However there was little confidence in the in-house digestion method of ICP-OES and the fusion discs of XRF were more reliable for both the feed and residues. The XRF fusion discs also provide fully quantitative results.

The solid feed samples of -38 µm, -53/+38 µm, -75/+106 µm, -106/+150 µm and bulk -150 µm sizes were submitted for XRF analysis. The solid residues generated from geochemical tests were washed with deionized water and dried in air prior to submission to the Geology Department at UCT for XRF analysis. Preparation of samples for XRF analysis involves roasting at high temperatures and mixing the roasted sample with flux (Willis 1999). The liquor samples obtained after the leaching stage were

filtered through 0.45 µm cellulose membrane and preserved with 2 drops of concentrated nitric acid prior to submission for ICP-OES.

The gold sample was further studied to determine the different forms of sulfur species using the ACARP sulfur speciation protocol that includes use of LECO S for total sulfur, Chromium Reducible Sulfur (CRS) method for sulfide sulfur and KCl extraction for sulfates (Smart *et al.* 2002). LECO S is an analytical instrument at UCT that uses high temperature combustion and infrared spectroscopy to measure total sulfur. The Chromium Reducible Sulfur method was conducted based on the procedure outlined in Ahern *et al.* (2004), which includes the hot acid digestion of the sample so that the sulfides react with zinc acetate solution to form ZnS that is measured by either titration or spectrophotometry. Detailed methodology of the KCl extraction method carried out in this study is described by Smart *et al.* (2002) and presented in Appendix A.3. Leachates generated from the KCl extraction were taken for ICP-OES to determine sulfate content.

3.2.2. Mineralogy

The mineralogy and textural properties of the feed sample were studied using QEMSCAN on a LEO 1450 SEM at the University of Cape Town. The feed sample was wet screened into the following fractions: +106, +75, +38, -38 µm before the QEMSCAN analysis. Each fraction was split into 3 x 1.0 g in triplicates to prepare into 30 mm blocks for QEMSCAN. The preparation of blocks includes mixing Epofix resin and hardener in a 10: 1 ratio, vacuuming for 10 minutes, curing in pressure pot overnight and polishing. The analysis was carried out using either the Bulk Mineralogical Analysis (BMA) to quantitatively determine bulk mineralogy or the Particle Mineralogical Analysis (PMA) routine to evaluate mineral association and liberation (Goodall 2008). A subset of coarse particulates (+4/-5.6 mm particles) was analysed using the QEMSCAN field image analysis routine to determine unbroken mineral textures and mineral associations. Analysis for solid residues from geochemical tests was conducted on unsized blocks due to the very low solids masses available.

In addition to the QEMSCAN, bulk mineralogy was validated using X-Ray Diffraction (XRD) at the University of Cape Town. The gold sample was milled with a McCrone micronizer to approximately 10 µm. The micronized sample was analysed using a Bruker D8 diffractometer with Vantec detector and mineral phases were quantified with Topas Rietveld refinement software.

Limitations of both methods have been acknowledged on sulfides analysis. The detection limit for XRD and Auto SEM (including QEMSCAN) is 2 wt. % and 0.01 wt. % respectively. The accuracy of sulfide results from QEMSCAN may be due to sulfur-containing trap phases more than the detection limits. However, the XRD results may be affected by the detection limit. Hence the ACARP sulfur speciation protocol was used to measure different forms of sulfur and MPA was calculated based on these results.

3.3. ARD Prediction Tests

3.3.1. Acid Rock Drainage Index (ARDI)

The mineralogy results obtained from QEMSCAN were used to evaluate the ARD potential of the gold sample using the acid rock drainage index (ARDI) developed by Parbhakar-Fox *et al.* (2011). The ARDI evaluation was done at the micro-scale level instead of micro and meso scale levels (cf. Parbhakar-Fox *et al.* 2011). Parameters investigated in determining the ARDI are sulfide content (parameter A), sulfide alteration (parameter B), sulfide morphology (parameter C), neutralizer content (parameter D), and acid former/neutralizer spatial relationship (parameter E). According to the ARDI methodology, each of the parameters is given a score out of 10, where a score of 10 indicates high acid producing potential and negative or zero score indicates low acid producing potential. Detailed information on allocating the score is given in appendix A.1. The sum of these individual scores was then calculated to determine the acid rock drainage index for the meso phase. The acid generating potential was classified according to the guidelines in Table 12.

3.3.2. Acid Base Accounting (ABA)

Acid base accounting, expressed as Net Acid Producing Potential (NAPP), is the balance between the maximum potential acidity (MPA) and the acid neutralizing capacity (ANC). The MPA and ANC are determined separately as discussed in the following subsections. The results obtained from both MPA and ANC are then used to estimate the NAPP as shown in Equation 3.1.

$$NAPP = MPA - ANC \tag{3.1}$$

3.3.2.1. MPA

The MPA was estimated based on the sulfide sulfur content obtained from Chromium Reducible Sulfur (CRS) method. A stoichiometric factor of 30.6 was used to calculate the resultant MPA in kg H_2SO_4 produced per ton (Eq. 3.2) assuming that H_2SO_4 is the primary product for all sulfide oxidation reactions taking place. Equation 3.2 also implies that all sulfides are pyrite, the sample however has pyrrhotite. Hence the Paktunc formula was used to calculate MPA that accounts for both pyrite and pyrrhotite. Further information on CRS method is presented on appendix A.2. The bulk mineralogy data was used to calculate a mineralogical NAPP using the equation (Eq. A.2) formulated by Paktunc (1999).

$$MPA = 30.6 \times S_{sulfide} \tag{3.2}$$

3.3.2.2. ANC

The ANC was calculated using both wet chemistry methods that include acid digestion and back-titration with a standard base, and modal mineralogy calculations. Various ANC methods were selected to examine the leaching behaviour of the sample under the different test conditions. These ANC methods were based on the AMIRA modifications of the standard Sobek, Skousen and, Lawrence and Wang test methods. These adaptations were based on extensive test work conducted by various researchers under the auspices of AMIRA during 2002, with the aim of improving the consistency and reliability of the static ABA test methods. Table 13 highlights the different leaching conditions of the wet chemistry ANC methods conducted in this study.

Table 13: The leaching conditions of the ANC test methods conducted in this study.

ANC test	Leaching conditions	References
AMIRA modified Sobek	Heat for 1 – 2 hours at 80 – 90^{0}C Add 2 drops of 30% H_2O_2 after back-titrating to pH 4.5	Smart *et al.* 2002
Modified Lawrence and Wang	Shaking at room temperature for 24 hours	Lawrence and Wang 1996
AMIRA Incremental Skousen Siderite correction	Heat for 1 – 2 hours at 80 – 90^{0}C Incrementally add 30% H_2O_2 after back-titrating to pH 4.5 until pH stabilizes	Maluleke 2006

The AMIRA modified Sobek method omitted the boiling step originating from standard Sobek method, as it promotes dissolution of minerals that contribute little or no net neutralization and subsequently overestimates effective ANC. The Lawrence and Wang method follows the same principle as AMIRA modified Sobek except that leaching was conducted on an orbital shaker at room temperature for 24 hours. As discussed in Section 2.6.1, these leaching conditions were specifically designed to address drawbacks associated with the boiling step from the Sobek method. The Skousen siderite correction test was initially designed to correct samples containing siderite. Later, the AMIRA modified Skousen siderite correction test that adds H_2O_2 stepwise was developed to prevent the decomposition of H_2O_2 prior to complete oxidation of ferrous iron into ferric iron. The ANC tests were conducted in several replicates: some were stopped after the leaching stage and the other set was back-titrated to determine the acid neutralization capacity. The solid residues and liquors taken down after the leaching stage were submitted for chemistry (ICP-OES and XRF) and mineralogy (QEMSCAN and XRD). The total volume of base used to back-titrate was used to calculate the ANC (kg H_2SO_4/t) value using Equation 3.3. Errors on duplicates were calculated as standard deviation. Detailed procedures are documented in appendix A.4.

$$ANC = \frac{(V_{HCl} - V_{NaOH} \times C) \times 49.0 \times M_{HCl}}{W} \quad (3.3)$$

Where V_{HCl} (ml) is the volume of HCl, V_{NaOH} (ml) is the volume of NaOH, C is the ratio of acid to base added in blanks, 49.0 is a conversion factor for kg H_2SO_4/t, M_{HCl} (M) is the concentration of acid and W (g) is the mass of the sample.

3.2.3.3. Mineralogical ANC

The mineralogical ANC was estimated based on the modal content of carbonates obtained from QEMSCAN since there were no significant fast weathering acid neutralizing silicate minerals identified. Calcite was the only carbonate mineral abundant in the sample. Hence the ANC was calculated using the equation (Eq. 3.4) established by Paktunc (1999). Unlike the methods developed by Lawrence and Scheske, and Plante, that considers both carbonates and acid neutralizing silicates contents and their relative reactivity, the Paktunc ANC method takes into account the content of only carbonates and the non-oxidisable cations that are considered as having no net ANC.

$$ANC = \sum_{i=1}^{k} \frac{w_a \times 10 \times X_i \times c_i \times n_s}{n_i \times w_i} \quad (3.4)$$

Where w_a is the molecular weight of H_2SO_4,10 is the conversion factor, X_i is the content of mineral in wt. %, c_i is the number of non-oxidisable cations in one formula unit of neutralised mineral i, n_s is the moles of sulfuric acid formed by the oxidation of one mole of sulfide mineral s, n_i is the moles of mineral required to consume n_s, and w_i is the molecular weight the neutralising mineral.

3.3.3. Net Acid Generation (NAG)

3.3.3.1. Single-addition NAG test

A 2.50 g of pulverized sample was leached with 15% H_2O_2 at room temperature for 24 hours. After 24 hours, the leached solution was boiled until no audible effervescence (approx. 2 hours). The solution was filtered and back-titrated to pH 4.5 and pH 7.0. The cumulative volume of base used to back-titrate to pH 4.5 and 7.0 was used to calculate $NAG_{4.5}$ and $NAG_{7.0}$ (kg H_2SO_4/t) using Equation 3.5. Errors on duplicates were calculated as standard deviation. Additional information on the procedure is given in appendix A.5.

$$NAG = \frac{49 \times V \times M}{W} \quad (3.5)$$

Where 49 is a conversion factor for kg H_2SO_4/t, V (ml) is the volume of NAOH, M (M) is the molarity of NaOH and W (g) is the mass of the sample.

3.3.3.2. Sequential NAG test

The sequential NAG test is a series of single-addition NAG tests conducted until the NAG pH stabilizes at 4.5 units. Similarly to the ANC tests, solid residues and liquors taken down after the leaching stage were further studied for chemistry and mineralogy while other duplicates were back-titrated to evaluate the NAG, which was calculated as per in single-addition NAG test.

3.3.4. Biokinetic Test

7.5 g sample (-150 µm) was inoculated with mixed cultures of sulfur- and iron-oxidizing bacteria in an acidic (pH 2 units) autotrophic basal salt medium. The flasks were maintained in 37^0C orbital shaker for 63 days, as shown in Figure 15. Three different sets of biokinetic tests were conducted: abiotic, pH controlled (biotic) and non-controlled pH (biotic). These tests were conducted in five replicates to generate sufficient material for analysis of residues. The biotic tests were inoculated with 7.5 ml volume of $1.0x10^6$ cell/mL population of the mixed cultures as described in Hesketh et al. (2010). The abiotic test was neither inoculated with cultures nor sterilised of naturally occurring microbes and was conducted as a control. The species used are *Acidothiobacillus ferroxidans, Leptospirillum ferriphilum, Acidothiobacillus caldus* and *Sulfobacillus benefaciens*. The pH controlled test was maintained at pH 2 by titrating with H_2SO_4 and/or NaOH. Redox potential and pH were measured using a Crison ELP 21 Eh meter against a silver/silver chloride reference electrode (+199 mV) and a Metrohm 713 pH meter respectively in intervals of 2 to 4 days. Leachates were sampled on a weekly basis, vacuum filtered through 0.45 µm cellulose membrane, preserved with concentrated nitric acid prior to submission for chemical analysis (ICP-OES). The solid residues from biokinetic tests were also submitted for chemistry (XRF) and mineralogy (QEMSCAN and XRD). Detailed procedures on growth and adaptation of cultures and, biokinetic test method are discussed in appendix A.6.

Figure 15: Biokinetic test flasks on an orbital shaker at the Centre for Bioprocessing Engineering Research (CeBER) Unit at the Department of Chemical Engineering.

CHAPTER 4

RESULTS: STATIC TESTS

One of the aims of this study is to investigate the effects of various static test conditions and mineralogy on the extent of mineral leaching of a gold sample. This chapter presents the results obtained from the characterization of the chemical composition, mineralogy, textural properties and acid generating potential. The static tests conducted in this study to determine whether the sample has a potential to generate acid are Acid Base Accounting (ABA) and Net Acid Generation (NAG) tests. In addition, the ARD Index and mineralogical NAPP ($NAPP_{MIN}$) were applied to characterize the acid generating potential. The leached residues generated from ABA and NAG tests were further characterized for chemistry and mineralogy. The information generated on leached residues was used to assess the extent of mineral leaching. The full set of data is presented in the appendix.

4.1. Feed sample characterization

4.1.1. Chemical composition

The elemental composition results presented in Table 14 were acquired using XRF and LECO S. Both major and minor elements were determined using XRF, except for S that was evaluated using LECO S. Data validation of the chemical analyses was performed by comparison of the actual chemistry derived by XRF and LECO S against the calculated chemistry obtained from the QEMSCAN bulk modal analysis (Figure 15).

Table 14: Chemical composition of the feed sample obtained from XRF and LECO S.

Element	wt. %
Al	4.4
Ca	0.6
Fe	3.0
K	1.2
Mg	0.5
Mn	< 0.05
Na	0.3
S	1.3
Si	37.1
Cr	< 0.05
P	< 0.05
Ni	< 0.05
Ti	0.2

The major elements studied were selected to represent oxidation of sulfides and dissolution of acid neutralising minerals. Table 14 shows that Si (37 wt. %) is the dominant element. Other elements identified with contents greater than 1 wt. % are Al, K and Fe. The total sulfur determined using LECO S is also greater than 1 wt. %. The elements Ca, Mg and Na each comprise less than 1 wt. % of the sample. Trace elements such as Cr and Ni identified by XRF were in low concentrations of less than 0.05 wt. % except Ti (0.2 wt. %).

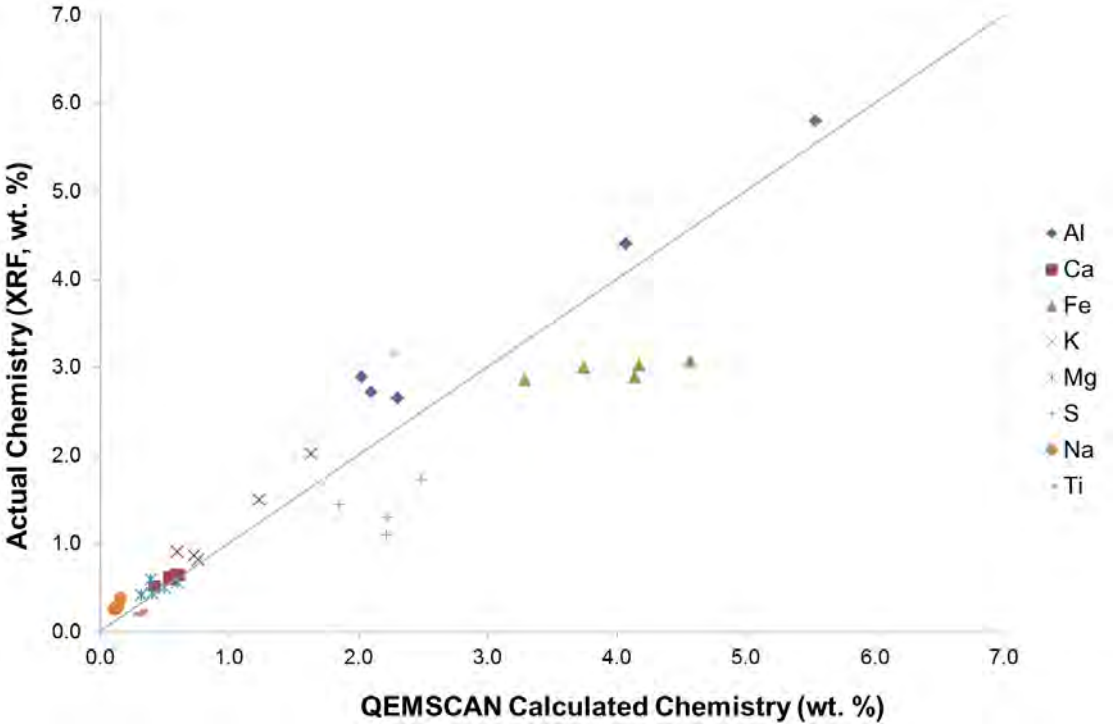

Figure 16: Graph showing the correlation between XRF chemical assay and QEMSCAN data for the major elements present in the feed sample. The x=y shows 1:1 relation. Note that graph axes do not include Si.

The correlation between the actual and the calculated chemistry of the feed sample to the various ARD tests was generally deemed acceptable in spite of the minor deviations of Al, Fe and S. The Fe and S elements were relatively higher for QEMSCAN on all the samples compared to XRF. One of the possible reasons for the low similarity in Fe content is that the exact Fe content of the Fe oxyhydroxides is unknown and also likely to be highly variable.

4.1.2. Bulk mineralogy

The bulk mineralogy of the gold sample is shown in Table 15 and the parity chart on Figure 16. The 'inert' quartz (as classified in Table 5) is the dominant mineral (71 wt. %) followed by the 'intermediate weathering' chlorite and mica (18 wt. %), the 'very slow weathering' K-feldspar (3 wt. % which includes its intermediate weathering alteration product, epidote) and the 'slow weathering' Fe oxides/hydroxides (2 wt. %). Pyrite (2 wt. %) and pyrrhotite (2 wt. %) were the only major sulfide minerals identified. Only very low contents of the neutralising carbonate minerals (0.5 wt. %) were present (predominantly calcite) and the 'inert' sphene (0.8 wt. %). The bulk mineralogy of the sample fits the profile of a typical Witwatersrand gold ore (see Table 7). Good correlations exist between the QEMSCAN and XRD data as shown in Figure 17, with differences on sulfide content (pyrite, pyrrhotite). Comparison with LECO S suggests overestimation of sulfides by the QEMSCAN.

Table 15: Bulk mineralogy of the feed sample acquired from QEMSCAN and XRD.

Mineral	Ideal formula	QEMSCAN (wt. %)	XRD (wt. %)
Pyrite	FeS_2	2.3	0.9
Pyrrhotite	$Fe_{(1-x)}S$	2.5	1.6
Other sulfides	$CuFeS_2$, PbS	0.2	<0.1
Carbonates	$CaCO_3$, $CaMg(CO_3)_2$	0.5	0.3
Quartz (silica)	SiO_2	70.7	68.0
Sphene	$CaTiSiO_5$	0.8	0.3
Feldspar	$KAlSi_3O_8$	3.1	3.9
Mica	$KMg_3(AlSi_3O_{10})H_2O$	12.8	17.3
Chlorite	$Mg_3Fe_2Al_2Si_3O_{10}(OH)_8$	5.0	5.1
Fe oxide/hydroxide	FeOOH	1.6	nd
Sulfates (jarosite)	$KFe_3(SO_4)_2(OH)_6$	<0.1	<0.1
Others (uraninite, zircon)	UO_2, $ZrSiO_4$	0.4	2.3

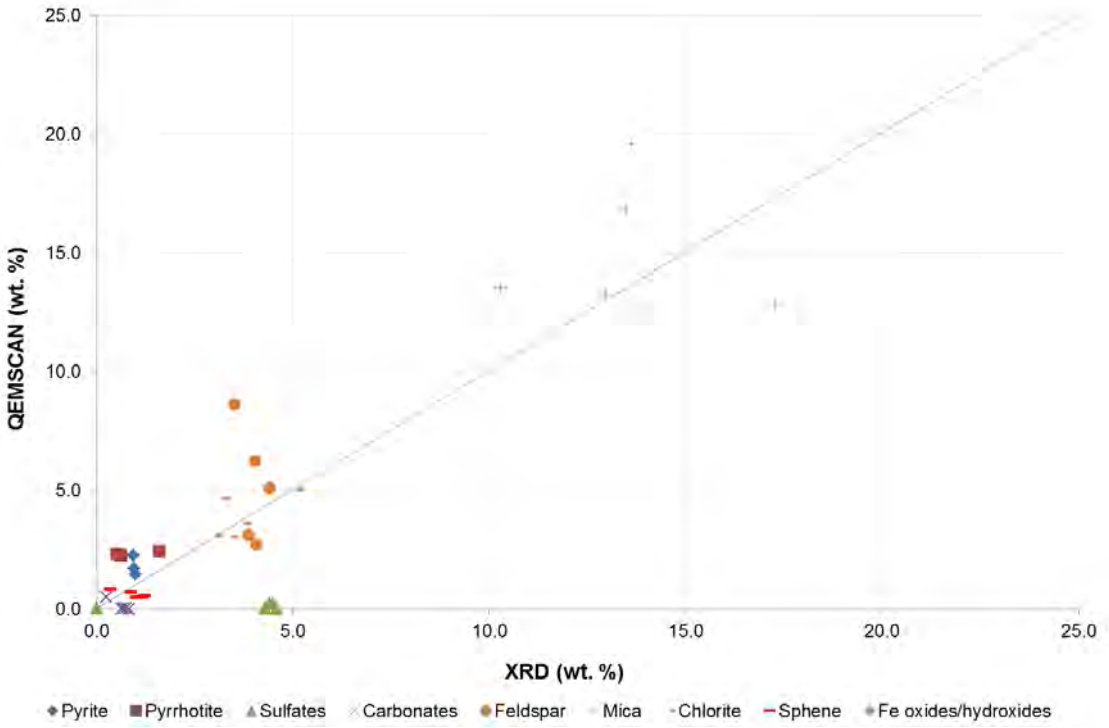

Figure 17: Graph showing the correlation between QEMSCAN bulk mineralogy and XRD data for the major mineral phases present on the static tests solid residues. The x=y shows 1:1 relation.

The QEMSCAN data was further processed to determine the elemental deportment which allows the identification of the host minerals to certain elements as shown in Figure 17 (see Appendix for actual data). Note that the mineral compositions used when calculating the element deportment are typical for each mineral type, and were not actively quantified using specialised mineralogy techniques in this study (e.g. electron probe micro analysis). The information acquired is used to evaluate the leaching behaviour of the minerals.

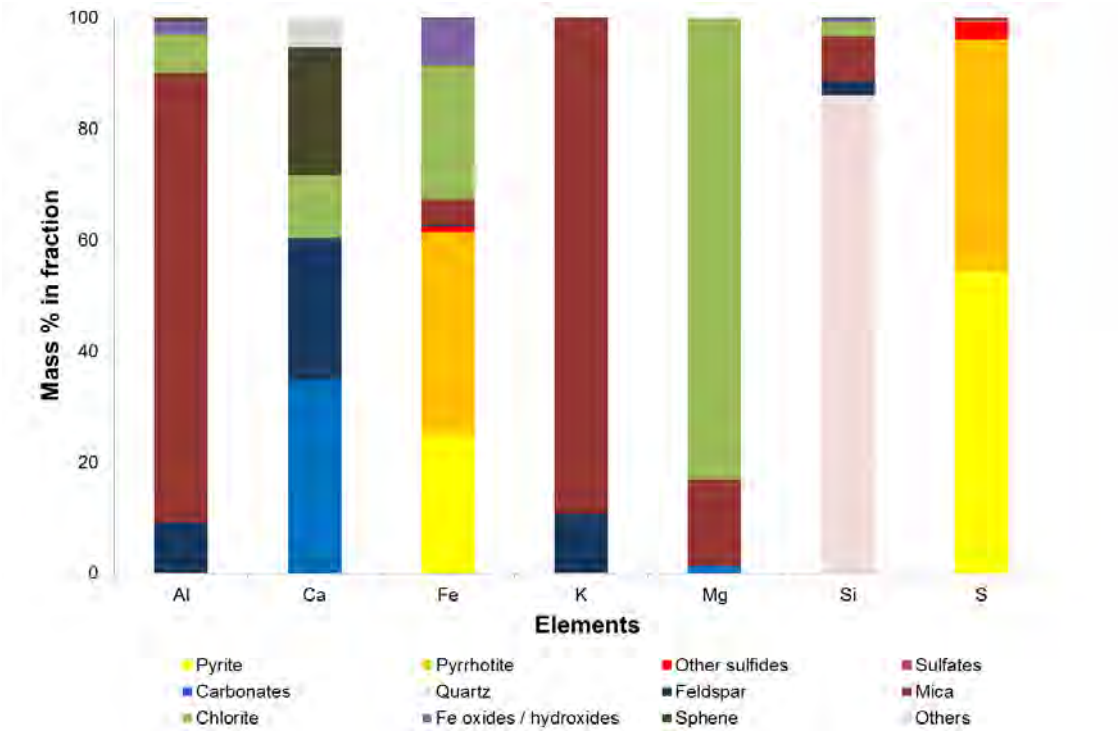

Figure 18: Elemental deportment of major elements obtained from QEMSCAN.

Al and K are mainly hosted by mica implying that changes in the concentration of these elements reflect the leaching of mica. Ca is mainly hosted by the carbonates, feldspar (including epidote) and sphene. The majority of the Mg is hosted by chlorite with a small fraction hosted by mica. Iron is mainly hosted by the sulfides and iron oxides. Sulfur is hosted by only sulfides with no notable sulfates identified. The lack of sulfates confirms the unoxidized nature of the sample.

4.1.3. Textural properties

The textural properties studied using QEMSCAN are the sulfide liberation and mineral association where sulfide liberation is indicated by the area % of sulfides in a particle (liberated ≥90% area). The association of unliberated sulfides was then quantified as binary particles with quartz, mica, chlorite, carbonates and others. The results obtained show that sulfide minerals are well liberated (91%) with only a minor fraction associated with quartz (6%) and mica (2%) as presented in Figure 18. Only 0.02% of the sulfides showed an association to the carbonates. Selected particles shown for illustration in Figure 19 confirm the good liberation of the sulfide minerals and poor association to the acid neutralising minerals (composite particles containing sulfides and carbonates).

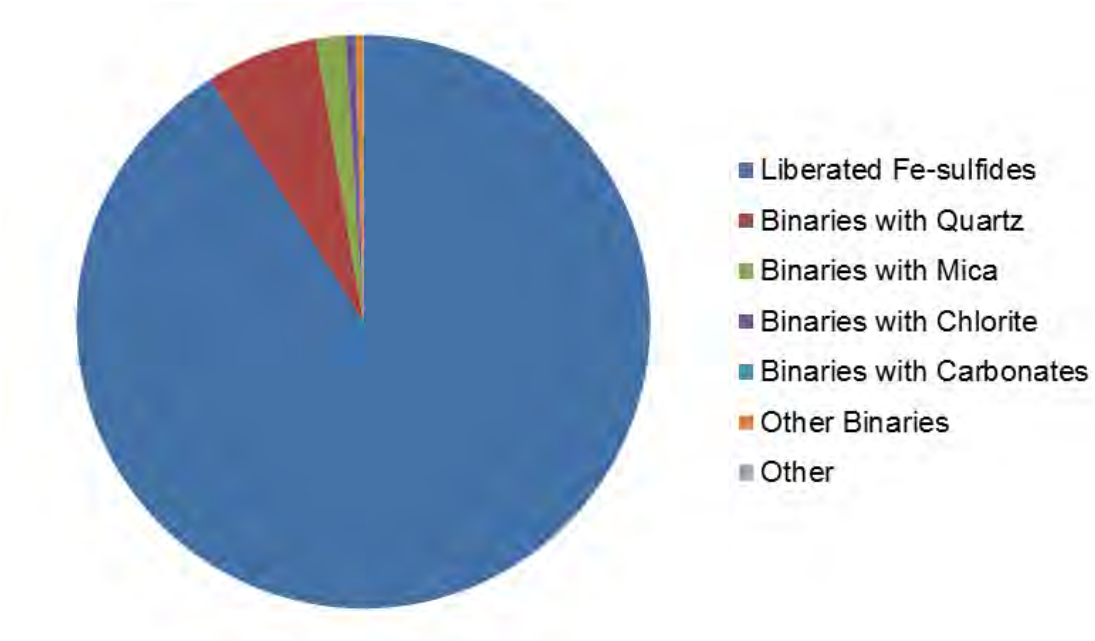

Figure 19: Sulfide liberation and association. Liberated indicates particles where the sulfide area is >90%. The association of unliberated sulfides (<90% sulfide in particle) is also quantified.

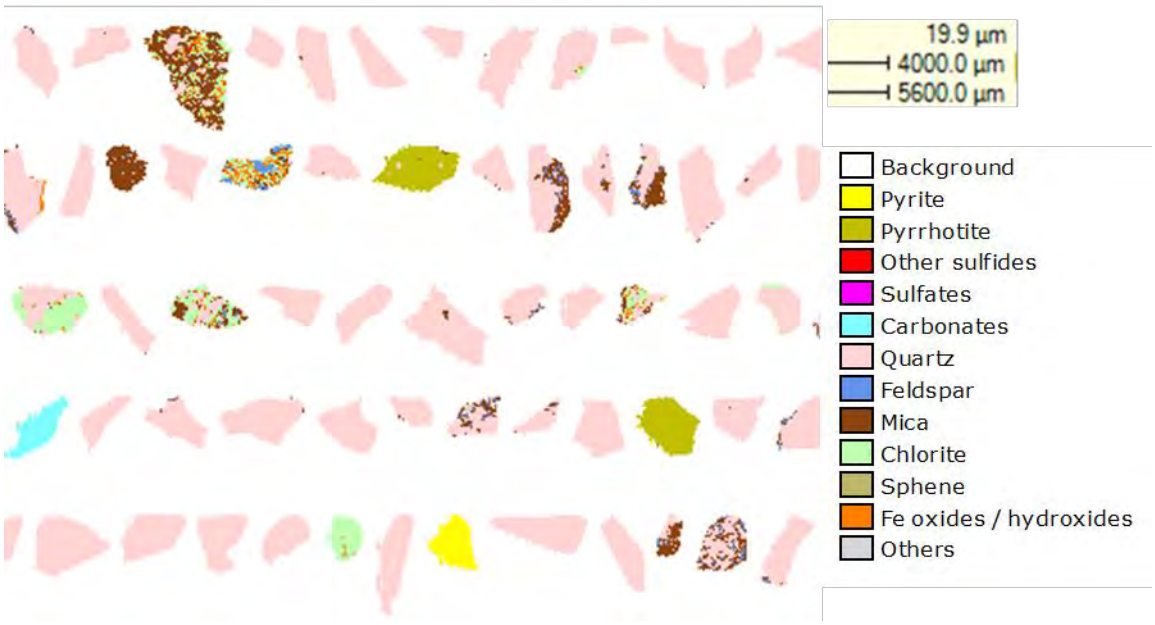

Figure 20: QEMSCAN particle view of the feed sample showing various minerals.

4.2. Acid Rock Drainage Index (ARDI)

The ARD Index developed by Parbhakar-Fox *et al.* (2011) was calculated on the micro-scale using coarse particles with unbroken textures (+4 mm) as shown in Figure 20. The evaluation could not be performed on the same size fractions used for conventional static tests (<150 µm), where the primary textures would have been destroyed through milling (c.f. liberated sulfides present in Figure 18 and 19)

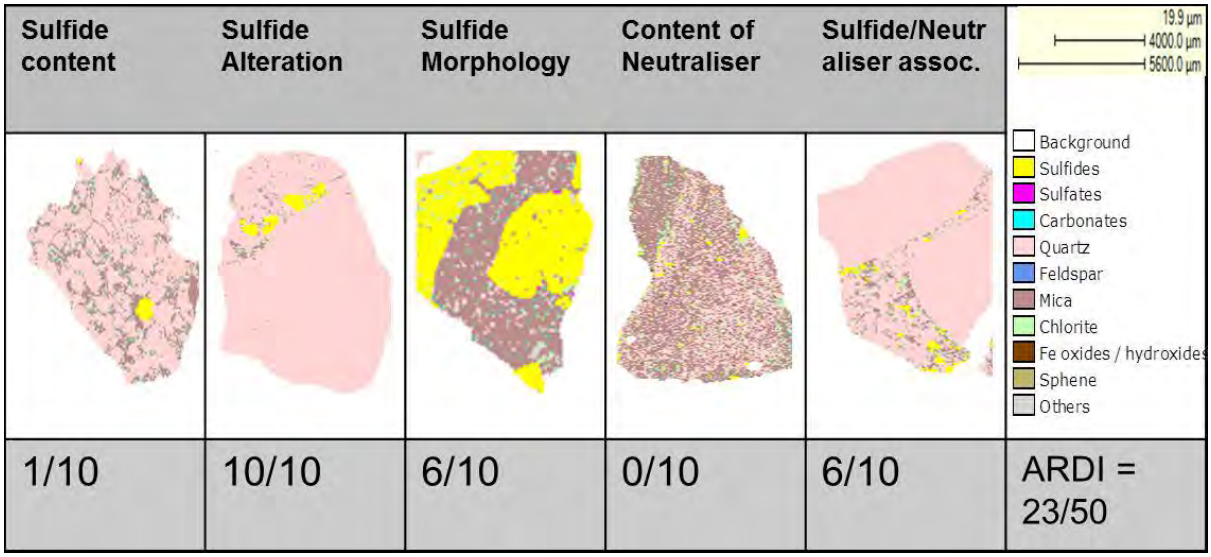

Figure 21: Illustration of the ARDI classification performed on coarse (+4.0 mm) particles with unbroken textures.

The bulk mineralogy showed that the total composition of all Fe-sulfides identified in the gold sample is less than 10 wt. % hence it was allocated a score of 1 for sulfide content. Both bulk mineralogy and texture showed that the sample contains negligible secondary minerals (i.e. sulfates and iron oxides/hydroxides) thereby confirming that the sample is unoxidized and consequently a score of 10 was allocated for the sulfide alteration category. The sulfide morphology category was given a score of 6 due to the subhedral-anhedral nature of sulfides observed. The carbonate content in proximity with sulfides as revealed by Fe-sulfides liberation (Figure 18) was also less than 10 wt. % leading to the score of 0 for the content of neutraliser category. As it can be seen in Figure 19 and 20, the sulfides are associated with 'inert' quartz with a negligible amount in direct contact with 'fast dissolving' carbonates and 'intermediate weathering' chlorite and 'very slow weathering' mica. Figure 19 also shows that individual sulfide grains are associated with each other. Thus the sulfide/neutraliser association category was allocated a score of 6. The final ARDI value of 23 reveals that the sample is potentially acid generating (Figure 20).

4.3. Acid Base Accounting

The net acid producing potential (NAPP) was determined using a two-fold method that includes evaluating the sulfide sulfur content for MPA and assessing ANC by using wet chemistry test methods. The MPA is the estimate of the extent of sulfide oxidation that results in acid formation whilst ANC is the ability of acid buffering minerals to neutralise the acid formed. The mineralogical data acquired from QEMSCAN was also used to calculate a mineralogical NAPP ($NAPP_{MIN}$).

4.3.1. MPA

Different forms of sulfur (i.e. sulfide and sulfate) were determined using the ACARP sulfur speciation protocol. LECO S measured the total S concentration of 1.33 wt. %, which is equivalent to a sulfide S content of 1.33 wt. % obtained from CRS method. There were no acid generating sulfates identified by the KCl extraction method. Sulfur speciation results revealed that there are no secondary minerals formed implying that the sample is unoxidized. This is consistent with the bulk mineralogy which showed that only acid forming sulfides (pyrite and pyrrhotite) were identified. Therefore, the MPA was calculated based on sulfide sulfur content obtained from the ACARP sulfur speciation protocol. The bulk content of sulfides identified in the gold sample (i.e. both pyrite and pyrrhotite) was used to calculate a mineralogical MPA (MPA_{MIN}) using the equations established by Paktunc (1999). Table 16 summarizes sulfur speciation results and MPA values.

Table 16: ACARP sulfur distribution and MPA for the gold sample.

Total S (wt. %)	Sulfide S (wt. %)	Sulfate S (wt. %)	MPA (kg H_2SO_4/t)	MPA_{MIN} (kg H_2SO_4/t)	
1.33 ± 0.033	1.33 ± 0.042	0.011 ± 0.003	40.70 ± 1.310	64.24	Py = 36.89 Po = 27.35

Py – pyrite; Po - pyrrhotite

The MPA_{MIN} which takes into account the content and the contribution of the different forms of sulfide minerals towards acid formation had a higher MPA compared to the chemical MPA which assumes that all sulfides present are pyrite and will be completely oxidized to form sulfates. The higher MPA_{MIN} is due to the overestimation of sulfides by QEMSCAN (see Table 15).

4.3.2. ANC

There are several methods available in the literature to determine acid neutralisation capacity. These methods include wet chemistry tests that involve acid digestion and back-titration, and mineralogical

calculations. The methods selected to evaluate ANC in this study are limited to the Paktunc mineralogical ANC (ANC_{MIN}), AMIRA modified versions of the original Sobek and Incremental Skousen siderite correction, and the modified Lawrence and Wang tests. The Paktunc method was used solely to determine mineralogical ANC since the methods developed by Lawrence and Scheske (1997), and Plante *et al.* (2012) does not necessarily include mineralogical properties (i.e. no actual bulk mineralogy used). Figure 21 presents ANC values obtained from the chemical tests and the mineralogical calculations.

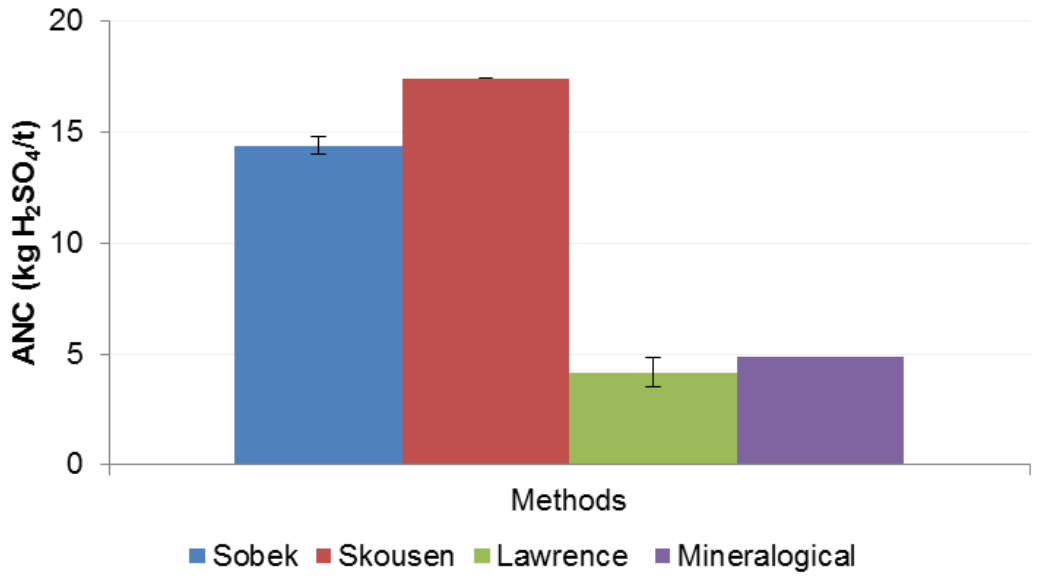

Figure 22: ANC values from chemical tests and mineralogical calculations. Standard deviation is shown as error bars.

The ANC calculated from the cumulative amount of base used to back-titrate had a higher value for the AMIRA Incremental Skousen siderite correction test (17.4 kg H_2SO_4/t) compared to the AMIRA modified Sobek test (14.4 kg H_2SO_4/t). The modified Lawrence and Wang test, conducted at room temperature, returned the lowest value of 4.2 kg H_2SO_4/t. This ANC value is comparable to the calculated mineralogical ANC value of 4.9 kg H_2SO_4/t, which accounts for only carbonates. The differences in ANC obtained from the various tests shows the dependence of the ANC value on dissolution conditions of the method. The effects of test conditions on the ANC values are further discussed in Chapter 6.

4.3.3. NAPP

Similarly to ANC and MPA, the NAPP (difference between ANC and MPA) was calculated based on both chemical tests and mineralogical calculations as shown in Table 17. According to the ARD classification guidelines from Stewart *et al.* (2006), a NAPP greater than 0 kg H_2SO_4/t implies that a sample is potentially acid forming. All chemical tests revealed that the sample is potentially acid

forming despite the difference in values that reflects the varying leaching behaviour of minerals under the different test conditions. The $NAPP_{MIN}$ with is considerably higher relative to the other NAPP calculations due to the overestimation of sulfides by QEMSCAN. All the NAPP results are consistent with the ARDI classification that the sample is potentially acid generating.

Table 17: NAPP values obtained from chemical tests and mineralogical calculations.

ANC method	ANC (kg H_2SO_4/t)	MPA (kg H_2SO_4/t)	NAPP (kg H_2SO_4/t)
Sobek	14.39 ± 0.39	40.70 ± 1.31	26.31 ± 0.65
Skousen	17.43 ± 0.00		23.27 ± 0.92
Lawrence	4.17 ± 0.66		36.53 ± 0.46
Mineralogical	4.89	64.24	59.35

4.3.4. Leaching behaviour for ANC tests

Solid residues and leachates generated after the leaching stages of the modified Lawrence and Wang, and AMIRA modified Sobek ANC methods were further characterized for their chemical and mineralogical changes. The residues were obtained under leach conditions consistent with the AMIRA modified Sobek and Skousen Incremental siderite correction ANC methods. The extent of mineral leaching was assessed by monitoring certain elements and mineral phases before and after leaching. XRD confirmed the presence of various sulfate minerals not easily identified with QEMSCAN. The small residue sample masses and changes in mineral chemistry due to leaching means that quantitative mineralogical analyses of the residues (QEMSCAN and QXRD) were challenging. In many cases, the QEMSCAN classification SIP (species identification protocol) file needed to be tailored for the different ARD test methods to obtain parity between the measured and calculated chemical assays (this in itself is evidence of incongruent leaching in the ARD prediction tests). Hence the extent of leaching is interpreted on the basis of general trends in terms of mineralogical and chemical changes during leaching, using the following categories: reacted (>10 wt. %) and reacted - then further classified as slightly (<30 wt. %), moderately (31 - 60 wt. %) and strongly reacted (>60 wt. %)), formed as secondary minerals (<0 wt. %) or unreacted (0-10 wt. %). Instead of 'reacted', 'extracted' was used for elements since there were no individual elements in the feed. Detailed results of the residues and leachates, as well as the calculations, are documented in the appendix. The summary of the calculations and therefore the leaching behaviour is presented on Tables 18, 19 and 20.

Table 18: Extent of minerals leaching for different ANC test methods. Only the major mineral groupings are shown.

Mineral group	Modified Lawrence and Wang	AMIRA modified Sobek
Sulfides	Slightly reacted	Slightly reacted
Carbonates	Strongly reacted	Strongly reacted
Quartz (silica)	Unreacted	Unreacted
Feldspar (incl. epidote)	Formed	Formed
Mica	Unreacted	Slightly reacted
Chlorite	Moderately reacted	Moderately reacted
Fe oxide/hydroxide	Slightly reacted	Moderately reacted
Sulfates (jarosite)	Formed	Formed

Unreacted: ~0 wt. %, slightly reacted: 0 – 30 wt. %, moderately reacted: 31 – 60 wt. %, strongly reacted: >60 wt. % and formed: <0 wt. %

The results in Tables 18 showed that sulfides were only slightly oxidized and that the carbonates completely reacted for both the modified Lawrence and Wang, and AMIRA modified Sobek/Skousen tests. The 'intermediate weathering' chlorite reacted moderately for all the ANC methods. Mica and feldspar appear to show relatively inconsistent behaviour between the tests. XRD analyses indicated the formation of the secondary sulfate minerals jarosite and szomolnokite in all the methods.

Table 19: Extent of elements leaching for the solid residues from the ANC test methods.

Element	Lawrence and Wang	Sobek/Skousen
Al	Slightly extracted	Slightly extracted
Ca	Moderately extracted	Moderately extracted
Fe	Slightly extracted	Slightly extracted
K	Slightly extracted	Slightly extracted
Mg	Slightly extracted	Moderately extracted
Si	Not-extracted	Not-extracted

Not-extracted: ~0 wt. %, slightly extracted: 0 – 30 wt. %, moderately extracted: 31 – 60 wt. % and strongly extracted: > 60 wt. %

Table 20: Extent of elements dissolution into the leachates for the ANC test methods.

Element	Lawrence and Wang	Sobek/Skousen
Al	Slightly extracted	Slightly extracted
Ca	Slightly extracted	Moderately extracted
Fe	Slightly extracted	Moderately extracted
K	Slightly extracted	Slightly extracted
Mg	Slightly extracted	Slightly extracted
Si	nd	nd

The elemental composition of the residues and leachates, and elemental deportment results were used to validate leaching behaviour of minerals. The results in Tables 19 and 20 showed that there was slight net extraction of Al for all the test methods. Al is hosted by mica and chlorite. Ca was moderately extracted on both residues and leachates, except for the leachate from the Lawrence and Wang method. The minerals hosting Ca are carbonates, sphene and feldspar. The bulk mineralogy results showed that carbonates reacted strongly in the low pH media of ANC leach conditions. Mg and K slightly reacted for all the methods. The bulk mineralogy however, showed that mica slightly reacted in the AMIRA modified Sobek/Incremental Skousen siderite correction ANC test and K-containing secondary mineral jarosite was formed (formation of jarosite confirmed by QXRD) in all the tests. This accounts for the insignificant change in total K concentration on both the leach residues

and leachates. The chemical analysis of the residues indicated negligible net extraction of Si. This is consistent with the simultaneous extraction and precipitation reactions occurring.

4.4. Net Acid Generation

4.4.1. ARD characterisation

The NAG test was carried out as an additional static test to further characterize the acid generating behaviour of the sample. The single-addition NAG test was conducted to determine the after-boil pH used in conjunction with the MPA to classify the acid generating potential. Since the sample has a sulfur content greater than 1 wt. %, it was further subjected to the sequential NAG test to ensure complete oxidation of sulfides that provides a more accurate NAG prediction (Smart *et al*. 2002). The cumulative NAG values for each step of sequential NAG test are presented in Figure 22 with the standard deviation shown as error bars.

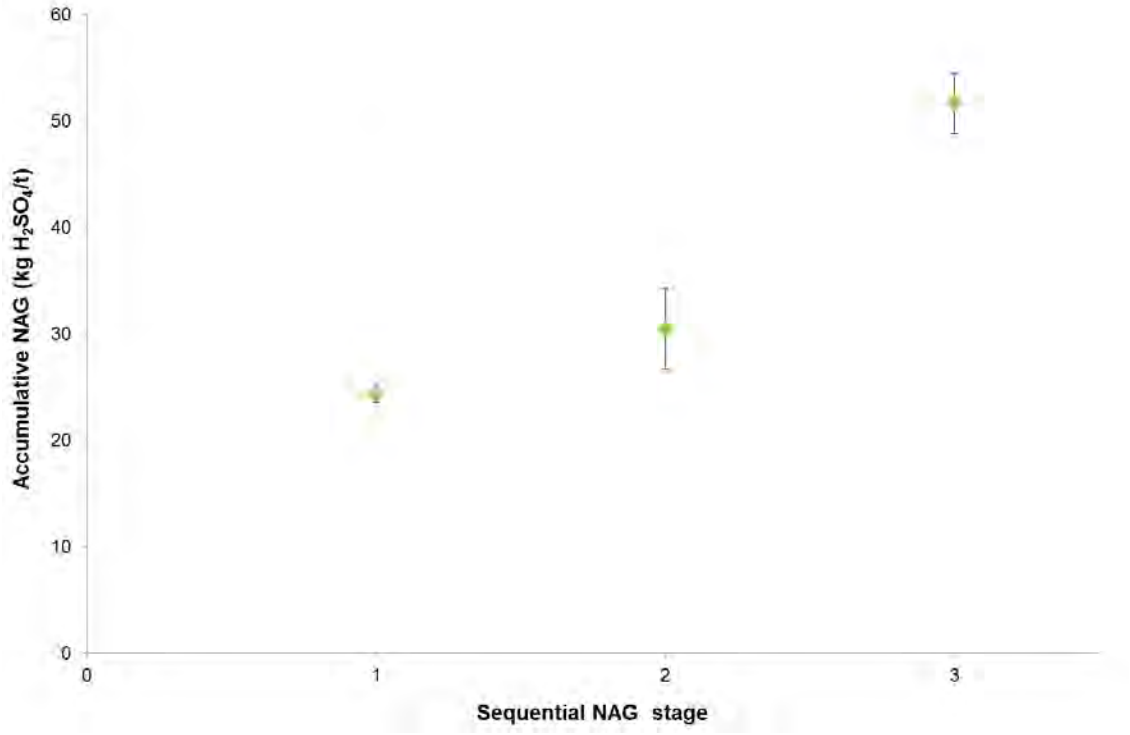

Figure 23: Sequential NAG test results. Standard deviation is shown as error bars.

In the sequential NAG, a series of single-addition NAG tests were conducted on the same sample until the pH was stable at greater than 4.5. The NAG value and pH obtained from the single-addition test are 24.84 ± 0.84 kg H_2SO_4/t and 2.5 ± 0.03 (which is less than 4.5). The sample took a suite of three single-addition NAG tests to reach pH greater than 4.5, resulting in the accumulative NAG and final pH of 51.64 ± 2.80 kg H_2SO_4/t and 4.54 ± 0.02 respectively. The single-addition NAG test

confirmed that the sample is potentially acid forming according to the ARD classification guidelines as stipulated in Table 11 (pH <4.5). The sequential NAG proved that a sample with sulfide content greater than 1 wt. % can be incompletely oxidized using the single-addition NAG test.

4.4.2. Leaching behaviour for NAG tests

Similarly to the ANC tests, the solid residues and leachates generated after the leaching stage on the sequential NAG test were further characterized to determine their elemental composition and bulk mineralogy in order to evaluate the extent of mineral leaching. Tables 21 and 22 summarise the extent of leaching using the protocol described in Section 4.3.4.

Table 21: Extent of minerals leaching for sequential NAG test. Only major mineral groupings are shown.

Mineral group	Sequential NAG test
Pyrite	Strongly reacted
Pyrrhotite	Strongly reacted
Carbonates	Strongly reacted
Quartz (Silica)	Slightly reacted
Feldspar (incl. epidote)	Slightly reacted
Mica	Slightly reacted
Chlorite	Slightly reacted
Fe oxide/hydroxide	Formed
Sulfates	Formed

Table 22: Extent of elements leaching for sequential NAG test.

Element	Solid residues	Leachates
Al	Slightly extracted	Slightly extracted
Ca	Moderately extracted	Moderately extracted
Fe	Slightly extracted	Slightly extracted
K	Moderately extracted	Slightly extracted
Mg	Slightly extracted	Slightly extracted
Si	Not-extracted	nd

The results summarised in Tables 21 show that the sulfides were strongly oxidized and the carbonates were depleted on the sequential NAG test. Chlorite, mica, and feldspar all reacted but only slightly. The secondary minerals formed as identified by QEMSCAN are the hydroxysulfates, as well as iron oxides and hydroxides. The XRD results also confirmed the formation of sulfates such as jarosite anglesite and szomolnokite (see Appendix). The leaching behaviour of the elements is relatively similar to that of the ANC leaching conditions: all the elements were slightly to moderately extracted except for Si. The difference in K extraction may be linked to precipitation of jarosite into solid residues. The iron was extracted only slightly compared to the strongly reacted iron sulfide which may be due to precipitation of iron-containing secondary minerals such as ferric hydroxides.

CHAPTER 5

RESULTS: BIOKINETIC TESTS

This chapter explores the effects of the UCT-developed biokinetic test conditions on leaching behaviour and on the extent of mineral leaching of the gold sample. This was done by evaluating the changes in mineral phases in terms of elemental composition and bulk mineralogy as observed during the course of the biokinetic tests. This chapter presents results of the three sets of biokinetic tests: abiotic (not inoculated and unsterilized), biotic pH controlled and biotic non-controlled pH. The changes in chemical parameters such as pH, redox potential and iron concentration that reflect the role of the microbial population on sulfide oxidation were monitored in order to characterize the acid generating potential and estimate qualitative relative kinetics of sulfide oxidation and dissolution of neutralising minerals. All three sets of biokinetic tests were run in five replicates. The full set of the mineralogy and chemistry data presented in this chapter is documented in the appendix.

5.1. ARD Characterisation

Biokinetic tests were run for 63 days to study the acid generating behaviour of the gold sample. The presence of bacteria catalyses the oxidation of ferrous iron into ferric iron, that subsequently promotes sulfide oxidation. The microbial effect on ARD formation was studied by monitoring pH and redox potential.

5.1.1. The pH

The pH profile shown in Figure 23 is indicative of the change in H^+ concentration, which is a product of sulfide oxidation and acid neutralisation. The results are divided into four time intervals to simplify presentation.

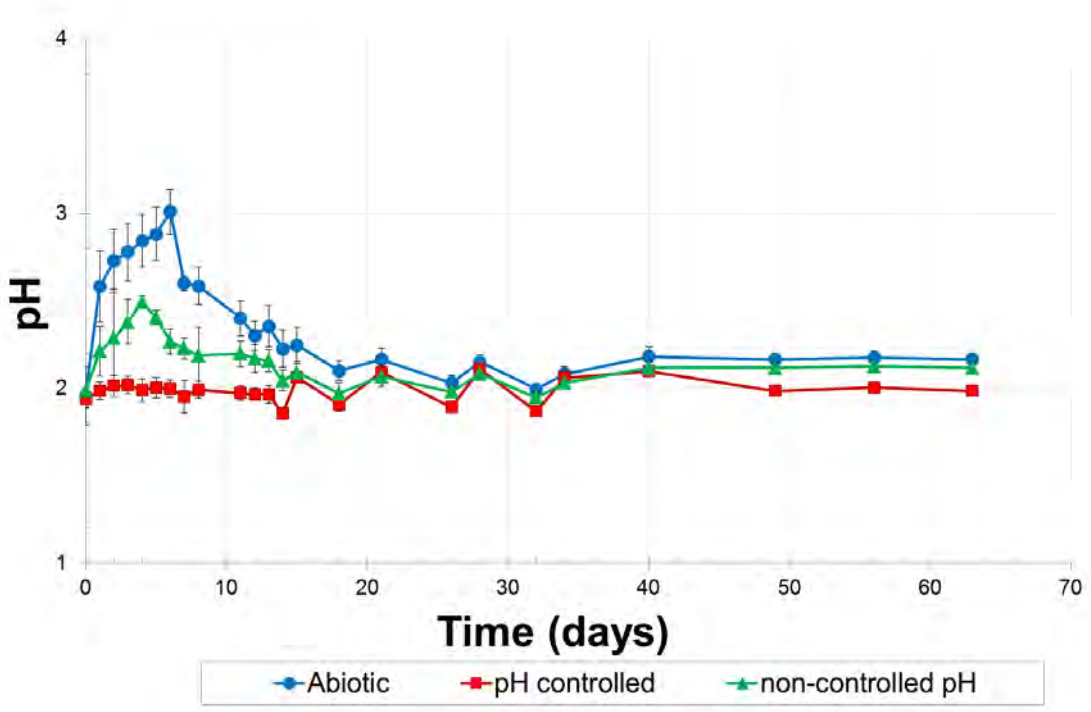

Figure 24: Change in pH with time for the biokinetic tests for the gold sample. Error bars shown represent the standard deviation. The pH controlled test shows the initial pH before adjusting it to pH 2.0.

The time intervals that showed distinct changes in pH with time were: 1 (first 6 days), 2 (6 to 18 days), 3 (18 to 32 days) and 4 (after 32 days). In region 1, the pH increased up to 2.6 units immediately after day 1 for the abiotic test, whereas it only reached 2.2 units for the biotic non-controlled pH tests. The rapid continually increased pH until day 4 and 6 for the non-controlled pH and abiotic tests respectively may be due to dissolution of 'fast dissolving' acid neutralising minerals. A steady drop in pH was observed in region 2 reaching a minimum of approximately 2.2 units and 2.0 units after 18 days for the abiotic and non-controlled pH tests respectively. This showed that the sulfide oxidation reactions dominated over this period. A slight gradual rise and fall in pH was observed for all tests in region 3 which most likely indicates the dissolution of the 'slow weathering' acid buffering minerals. The pH levelled off at approximately 2.1 units (< 4.5 units) in region 4.

5.1.2. Redox potential

The redox potential measured against a Ag/AgCl standard electrode is assumed to show only the potential at which the conversion of ferrous iron into ferric iron occurs, which is indicative of the bacterial activity. Figure 24 presents the redox potential time course profile for three different sets of biokinetic tests, divided into four time intervals following the trend of the pH profile (Figure 23).

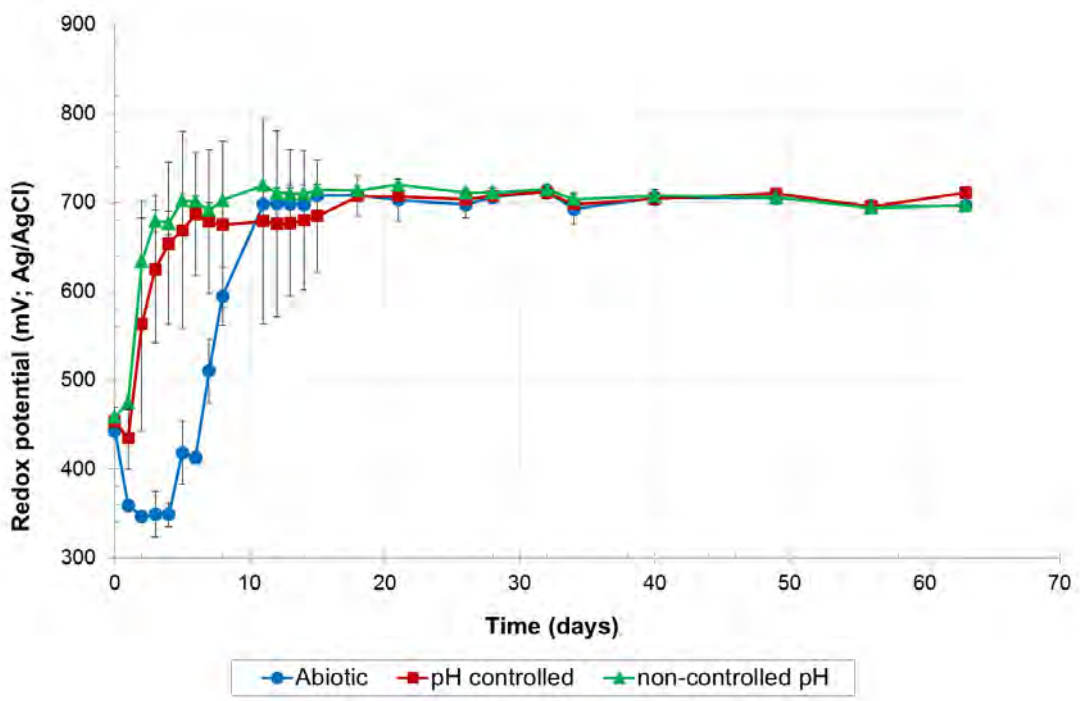

Figure 25: Change in redox potential with time for the biokinetic tests for the gold sample. Error bars shown represent the standard deviation.

The redox potential increased rapidly in the first few days, reaching values of greater than 600 mV after 3, 4 and 8 days for the pH-controlled, non pH-controlled and abiotic tests respectively. The redox potential for the abiotic test continued to increase in region 2 until it stabilized at ~700 mV, corresponding with the biotic pH controlled and non-controlled pH tests. This showed the lag time for microbial activity in the abiotic test since a redox potential between 600 and 700 mV is indicative of the rapid oxidation of Fe^{2+} into Fe^{3+} (accelerated sulfide oxidation) in the presence of bacteria instead of 485 mV for sterile media. The redox potential stabilised at above 700 mV in region 3. The redox potentials level off for all tests at around 700 mV in region 4. This shows that the microbial sulfide oxidation reaction dominated in all the tests for the rest of the test duration.

5.2. Leachate chemistry

Leachates were assayed weekly to evaluate changes in chemical composition using ICP-OES from day 7. In accordance with the pH results this was after the sample became net acid generating and the concentration of reactive carbonates was depleted. The choice of elements and mineral phases monitored was based on the bulk mineralogy of the feed, elemental deportment information and reactions of interest (i.e. sulfide oxidation and dissolution of acid buffering minerals). Major elements presented in this section are Al, Ca, Fe, K, Mg and Si. Results obtained for day 21 were unreliable and were omitted. It was not possible to conduct repeats since only the minimum volume of 1 ml was sampled to avoid disruption on microbial activity.

5.2.1. Iron

Changes in iron concentration can be attributed to dissolution of iron-containing sulfides and precipitation of iron oxides and sulfates. The changes in ferrous iron concentration evaluated using 1-10 phenanthroline assay on UV-Vis spectroscopy (Komadel *et al.* 1988) reflects the conversion of Fe^{2+} into Fe^{3+}. Figure 25 presents results for total iron (A) and ferrous iron (B).

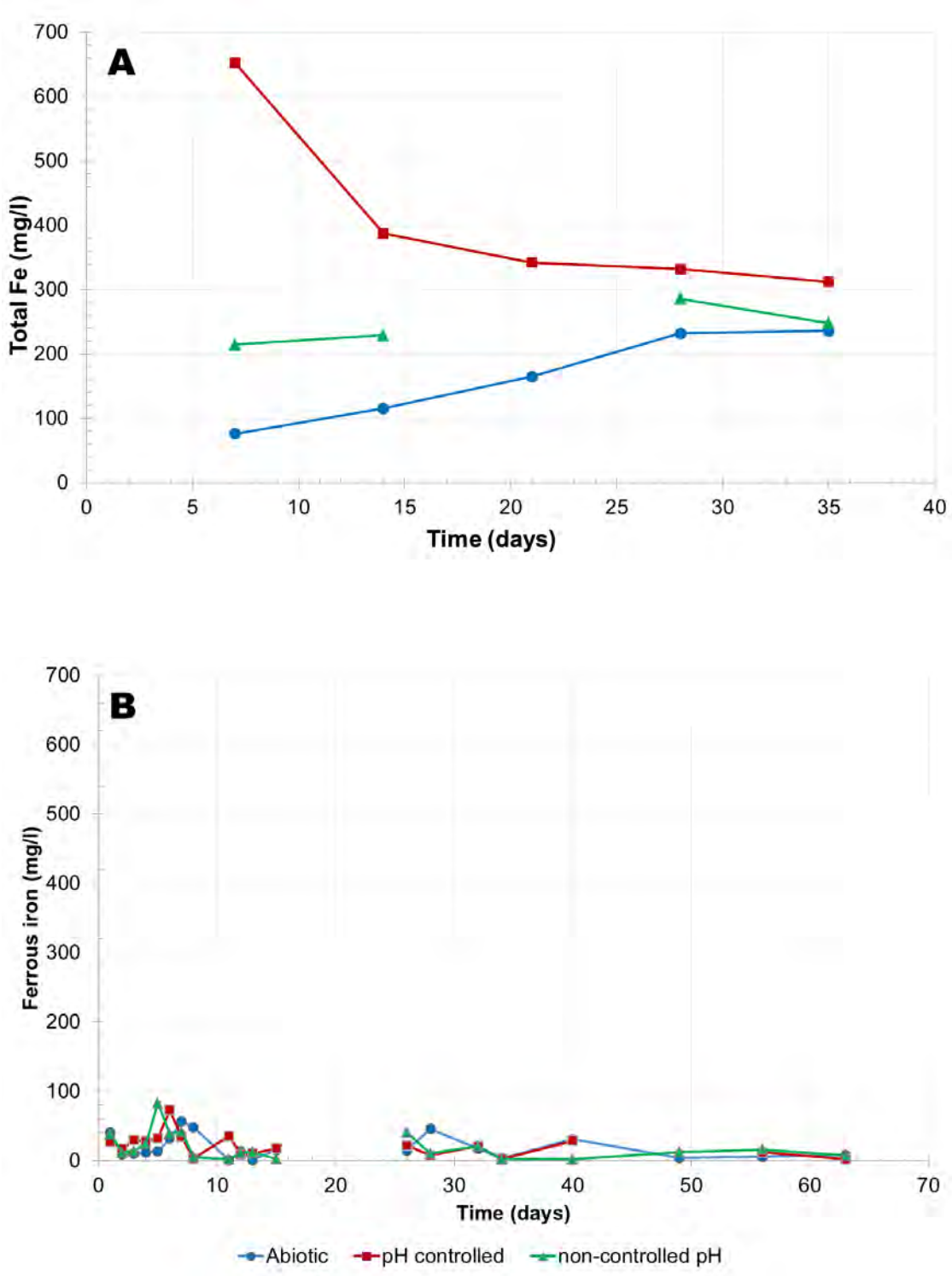

Figure 26: The total iron (A) and ferrous iron (B) profile with time during the biokinetic tests for the gold sample. The missing data points were omitted due to errors encountered in assays. Error bars shown represent standard deviation.

The results in Figure 25A show a higher iron concentration for the controlled pH test (>600 mg/l) than for the abiotic (76 mg/l) and non-controlled pH (214 mg/l) tests. In addition to Fe added during the inoculation stage, the higher Fe concentration for the pH controlled test is probably due to the higher

solubility of Fe^{3+} at the pH values obtained for the pH controlled, than for the other tests, particularly in the earlier stages. The iron concentration decreased after 14 days to more than 300 mg/l for pH controlled test and >200 mg/l for both the abiotic and non-controlled pH tests. The decrease in iron concentration is indicative of the precipitation of Fe-containing secondary minerals (i.e. iron oxyhydroxides and hydroxysulfates). One of the reasons for the consistently lower iron concentration in solution for the abiotic test relative to the biotic pH controlled and non-controlled pH tests is the lower microbial activity, as indicated by the lower redox potentials obtained for this test. The ferrous iron concentration was relatively low (<100 mg/l) for all tests throughout the study. As a result, there are no meaningful trends. The low ferrous iron concentration confirms the catalytic oxidation of ferrous iron into ferric iron in the presence of microbes.

5.2.2. Calcium

The elemental deportment results showed that Ca is mainly hosted by feldspar and sphene, with a minor fraction in the carbonates. The relative reactivity of these minerals from Section 2.3.2 also showed that feldspar (including epidote), sphene and carbonates are slow weathering, inert, very slow weathering and fast dissolving respectively. Figure 26 shows results for the soluble Ca obtained from weekly sampling of the biokinetic tests.

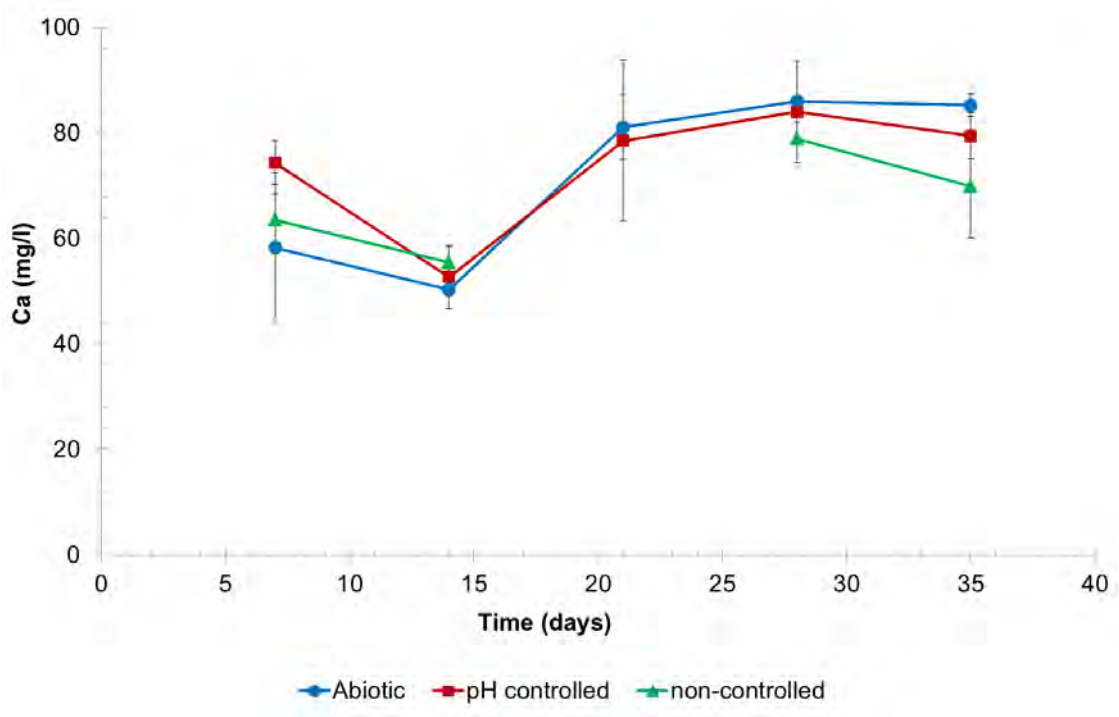

Figure 27: The calcium (Ca) composition from weekly sampling of the biokinetic tests. The missing data points were omitted due to errors encountered in assays. Error bars shown represent standard deviation.

The high concentration of Ca observed at day 7 is consistent with the rapid dissolution of fast dissolving Ca-containing minerals (i.e. carbonates), which corresponds to increasing pH (see Figure 23). The concentration of Ca decreased until 14 days may be indicative of the precipitation of fast dissolving Ca-containing minerals. Thereafter, the Ca concentration showed a slow increase likely due to some dissolution of less reactive silicates. No significant differences in leachate Ca composition are seen related to the test conditions.

5.2.3. Magnesium

The elemental deportment results showed that Mg is hosted by chlorite and mica. The study of Mg represented the leaching behaviour of mica and chlorite. Figure 27 presents the ICP-OES results for the three sets of biokinetic tests.

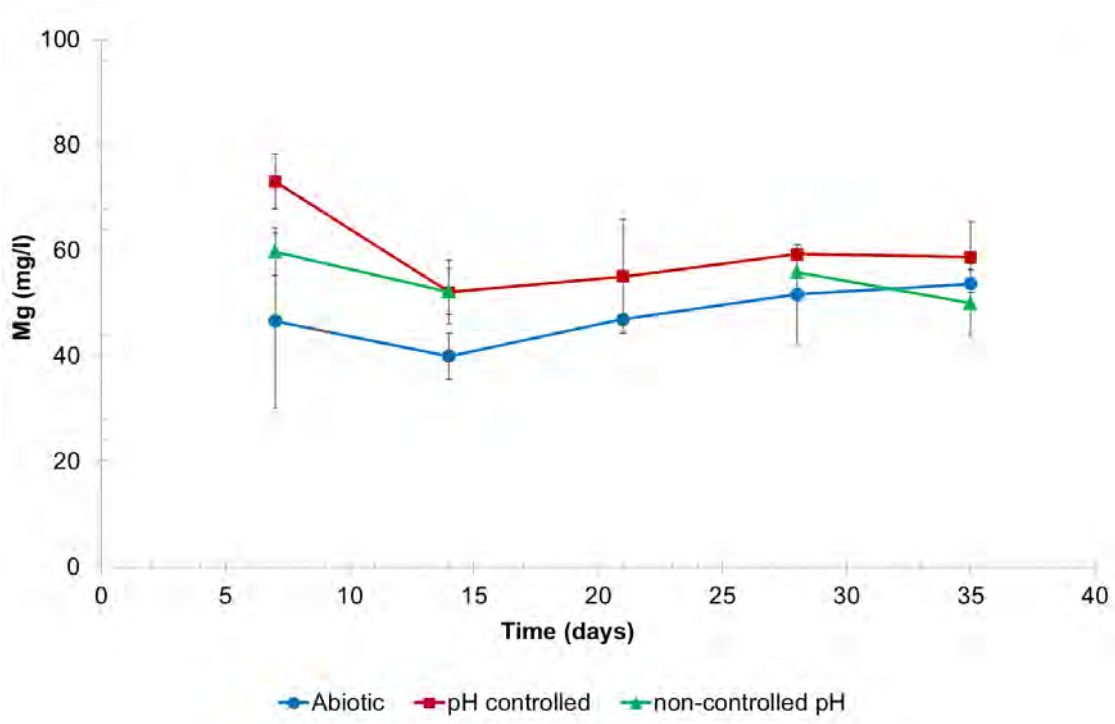

Figure 28: The magnesium (Mg) composition from weekly sampling of the biokinetic tests. The missing data points were omitted due to errors encountered in assays. Error bars shown represent standard deviation.

The high concentration of Mg after day 7 may be due to the more aggressive conditions (low pH) in the earlier stages that caused the dissolution of Mg silicates. The lower concentration in day 14 may be attributed to adsorption or entrainment of Mg in precipitates. Considering the error bars, the concentration of Mg was relatively stable. This suggests a balance between dissolution and precipitation of Mg minerals. The Mg concentration was relatively stable after day 28 which indicated that there were no further reactions of Mg-bearing minerals.

5.2.4. Aluminium

The elemental deportment results showed that Al is hosted by mica and chlorite. The changes observed in Al concentration reflect the leaching behaviour of mica and chlorite and precipitation of secondary minerals such as alunite. Figure 28 presents the results of Al acquired from weekly sampling of the biokinetic tests.

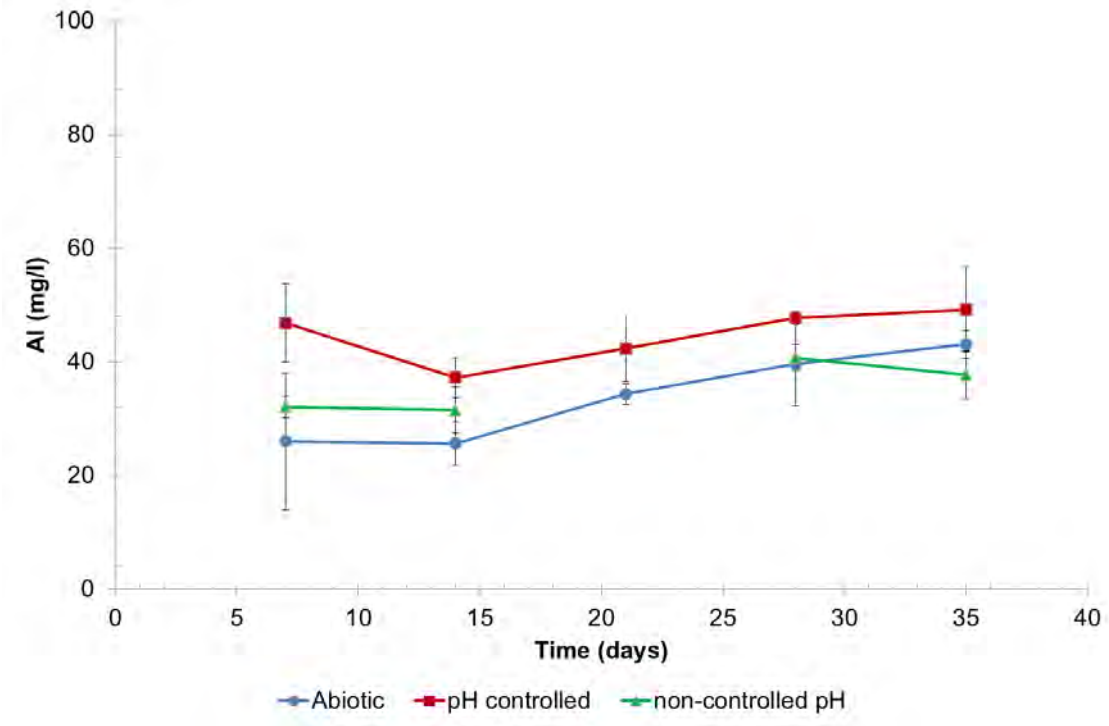

Figure 29: The aluminium (Al) composition from weekly sampling of the biokinetic tests. The missing data points were omitted due to errors encountered in assays. Error bars shown represent the standard deviation.

The leaching behaviour of Al up to day 14 is similar to that observed for Ca and Mg, although elemental deportment revealed that these elements are partially hosted by different minerals. This suggests that the initial low pH also stimulated dissolution of Al silicate, which later precipitated. A slight increase in Al concentration was observed after 21 days. This can be related to the change in pH after day 18, which may be due to dissolution of the slow weathering Al silicates.

5.2.5. Potassium

The element K was studied to evaluate the leaching behaviour of mica and formation of K secondary minerals such as jarosite or alunite. The results obtained from weekly sampling of the three biokinetic tests are presented in Figure 29.

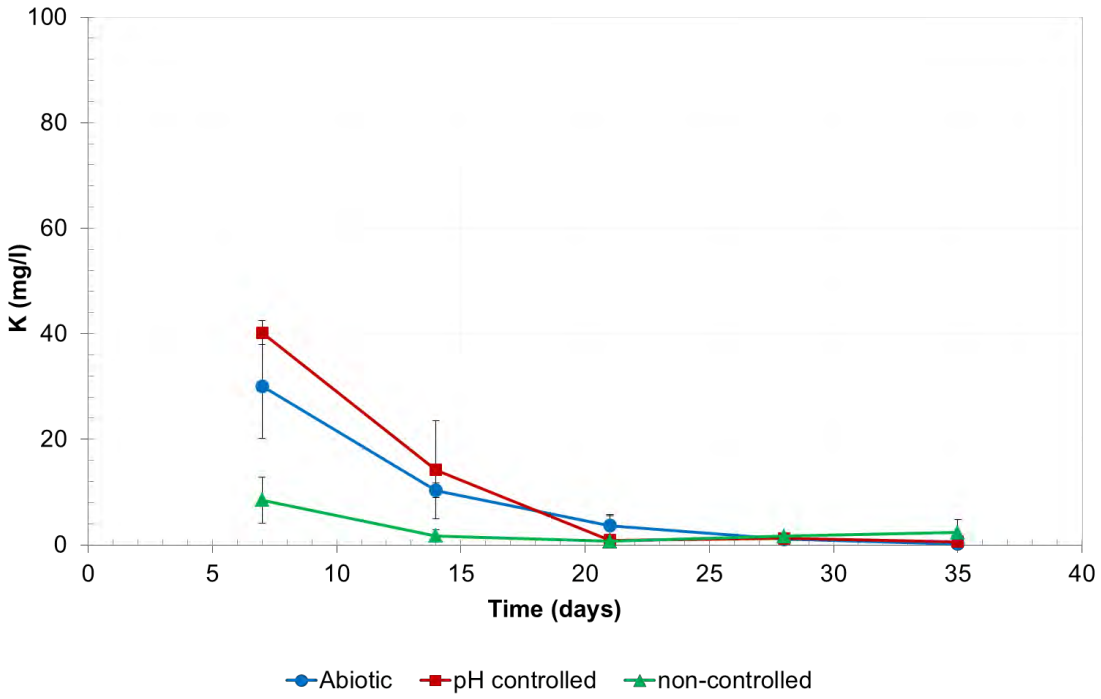

Figure 30: The potassium (K) composition from weekly sampling of the biokinetic tests. The missing data points were omitted due to errors encountered in assays. Error bars shown represent the standard deviation.

The potassium concentration was relatively low throughout the duration of the tests. The K concentration continued to decrease up to <20 mg/l in 21 days for all the tests. This correlates with the decrease in iron concentration after 14 days and thus shows a rapid precipitation of K as a secondary mineral (e.g. jarosite). This was confirmed by the orange colour observed after day 14 (see Figure 30). The K concentration stabilized at approximately 0 mg/l for the rest of the test duration.

Figure 31: Illustration of the colour changes observed in the biokinetic tests.

5.2.6. Silicon

The changes in soluble Si concentration can be considered indicative of leaching behaviour of silicates such as chlorite, feldspar and mica, as well as precipitation of amorphous silica. Figure 31 shows the changes in Si composition in the biokinetic tests on a weekly basis.

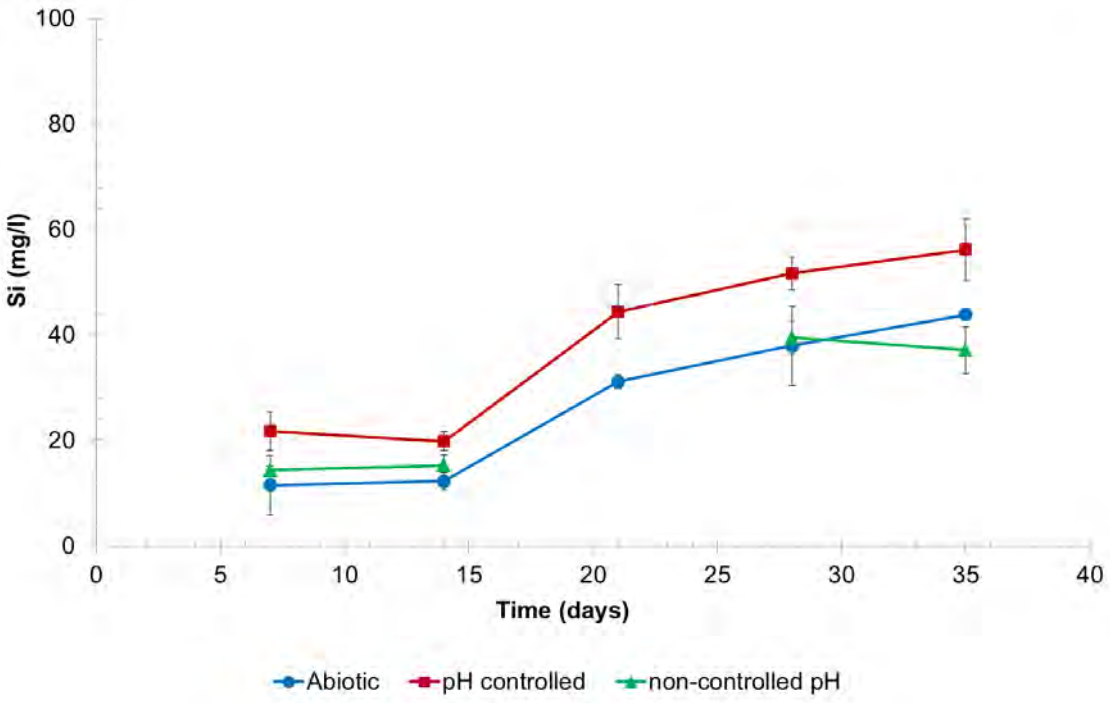

Figure 32: Silicon (Si) composition from weekly sampling of the biokinetic tests. The missing data points were omitted due to errors encountered in assays. Error bars shown represent the standard deviation.

The Si concentration steadily increased after day 14 for all tests throughout the study course. Si concentration was consistently higher for biotic pH controlled test. The increase in Si concentration was indicative of the dissolution of Si-containing minerals. These observations are consistent with pH, Al, Ca and Mg, which confirms the dissolution of Al, Ca and Mg silicates.

5.3. Mineral leach behaviour for biokinetic tests

The solid residues were analysed to determine their chemical composition and bulk mineralogy using XRF, XRD and QEMSCAN. The data obtained was used to evaluate the overall leaching behaviour of certain elements and mineral phases. Bulk mineralogy data obtained from XRD was used to validate information obtained from QEMSCAN. Furthermore, XRD was used to assess the content of hydroxysulfates which were not always positively identified by QEMSCAN. The extent of mineral

leaching was evaluated following the similar principle as in ABA and NAG tests. Categories used to classify the extent of mineral leaching are showed as footnotes in Table 18. Tables 23 and 24 present the extent of mineral leaching for all the biokinetic tests.

Table 23: The extent of minerals leaching for the biokinetic tests. Only major mineral groupings are shown.

Mineral group	Abiotic	pH controlled	Non-controlled pH
Pyrite	Strongly reacted	Strongly reacted	Strongly reacted
Pyrrhotite	Strongly reacted	Strongly reacted	Strongly reacted
Carbonates	Strongly reacted	Strongly reacted	Strongly reacted
Quartz	Unreacted	Unreacted	Unreacted
Feldspar (incl. epidote)	Unreacted	Strongly reacted	Slightly reacted
Mica	Formed	Formed	Unreacted
Chlorite	Moderately reacted	Moderately reacted	Moderately reacted
Fe oxide/hydroxide	Formed	Formed	Slightly reacted
Sulfates (alunite)*		Formed	Formed

*XRD results

Table 24: Extent of elements leaching for the biokinetic tests.

Element	Abiotic	pH controlled	non-controlled pH
Al	Slightly extracted	Slightly extracted	Slightly extracted
Ca	Moderately extracted	Moderately extracted	Moderately extracted
Fe	Slightly extracted	Moderately extracted	Moderately extracted
K	Negative	Negative	Negative
Mg	Slightly extracted	Moderately extracted	Slightly extracted
Si	Not-extracted	Not-extracted	Not-extracted

Table 23 shows that the sulfides were completely oxidized and carbonates were completely dissolved for all the tests. This shows that the prolonged biokinetic test duration allows complete oxidation of

sulfides. Chlorite reacted moderately for all the tests. Mica remained unreacted on the non-controlled pH test whereas formed (or some alteration products with mica-like composition) on the abiotic and the pH controlled tests. Quartz and feldspar remained unreacted or slightly reacted, except for the pH controlled test (feldspar strongly reacted). Other secondary minerals formed are sulfates and Fe oxyhydroxides. The hydroxysulfate minerals identified using XRD are anglesite, jarosite and szomolnokite (see Appendix). This confirms the decrease in K and Fe concentrations in leachates. However, the negative (i.e. formed) K in Table 24 may be attributed to the K added in the basal salt mixture. The net extraction of Si was negligible, suggesting a balance between the dissolution and precipitation reactions. The elements Al, Mg, Fe and Ca were fairly extracted. The difference in Fe extraction on the abiotic compared to the biotic pH controlled and non-controlled tests may be due to the microbial effect on sulfides oxidation. The effects of the biokinetic tests conditions on mineral leaching are further discussed in Chapter 6.

CHAPTER 6

DISCUSSION

This chapter aims at evaluating both the hypotheses and the research questions stated in Chapter 2. The hypotheses seek to evaluate the effect of ANC leach conditions on the final ANC value and further examine leaching behaviour under the ANC (ABA), NAG and biokinetic tests leach conditions. The hypotheses are tested by exploring the key questions, which includes examining the extent of mineral leaching under ABA, NAG and biokinetic test conditions. A better understanding of the leaching behaviour under the different test conditions will assist in interpreting the analytical results (i.e. acid generating potential).

6.1. Mineral leaching behaviour

Both formulated hypotheses require examination of the leaching behaviour of minerals on the different test conditions. Hypothesis 1 is evaluated by examining the effect of different ABA (ANC) leaching conditions on the ANC value as summarised in Table 25. For both tests, the major contributor to ANC were the carbonates, with additional neutralisation capacity provided by the intermediate weathering Mg-silicate chlorite (moderately reacted - Table 18).

Table 25: Comparison between expected and experimental leaching in ANC methods.

ANC method	Expected to react	Actually reacted	ANC (kg H_2SO_4/t)
AMIRA modified Sobek	Carbonates, fast and intermediate weathering silicates	Carbonates (>90%), chlorite (30-60%), mica (0-30%) and Fe oxyhroxides (30-60%)	14.39 ± 0.39
AMIRA modified Skousen	Same as Sobek, excluding Fe and Mn carbonates*		17.43 ± 0.00
Modified Lawrence and Wang	Carbonates and fast weathering silicates	Carbonates (>90%), chlorite (30-60%) and Fe oxyhroxides (0-30%)	4.17 ± 0.66
Paktunc Mineralogical	Carbonates excluding Fe and Mn carbonates	Calcite (100%)	4.89

*dissolution of Fe and Mn carbonates is cancelled during back-titration

According to the literature survey, the Skousen method usually returns a lower ANC compared to the Sobek method due to the peroxide added in the Skousen to cancel the contribution of Fe and Mn carbonates towards ANC value (Skousen *et al*. 1997; Weber *et al*. 2004). In this study, the Skousen method returned a higher ANC than the Sobek method. This can only be justified by examining the leachates after the back-titration stage of both the Sobek and Skousen method. However, the scope of the study was limited to examining the residues and leachates taken after the leaching stage (i.e. before back-titration).

The slightly lower ANC from the Lawrence and Wang method (c.f. Sobek/Skousen) is due to the less aggressive leaching conditions used compared to the Sobek/Skousen method. There is a suggestion of a degree of mica (intermediate weathering) and Fe-oxyhydroxides (slow weathering) reactivity in the Sobek/Skousen method compared to Lawrence and Wang method, although further mineralogical investigation is needed to confirm this with confidence. Overall, the minerals that dissolved in this study are consistent with the minerals reported in the Best Practice Guidelines report, cited from Mills 1997 (Department of Water Affairs and Forestry 2008). Interestingly, the mineralogical ANC calculated based on carbonate dissolution only, is comparable to that of the Lawrence and Wang, even though the latter shows evidence of only partial chlorite reactivity.

Hypothesis 2 evaluates the effect of the biokinetic test on leaching behaviour. Although there was no literature information readily available on the mineral reactivity under the leach conditions of the biokinetic tests, general literature on mineral leaching under microbial conditions was available (e.g. Dopson *et al.* 2009). Table 25 summarises the minerals that reacted in the NAG and biokinetic tests.

Table 26: A summary of the minerals that reacted in the NAG and biokinetic tests.

Method	Minerals reacted	Minerals precipitated	Final pH
Non-controlled pH biokinetic test	Sulfides (>90%), carbonates (100%), chlorite (30-60%), +/- feldspar	Sulfates, Fe-oxyhydroxides	2.1 ± 0.03
pH controlled biokinetic test	Sulfides (>90%), carbonates (100%), chlorite (30-60%), , +/- feldspar	Sulfates, Fe-oxyhydroxides	2.0 ± 0.02
Abiotic biokinetic test	Sulfides (>90%), carbonates (>90%), chlorite (30-60%), , +/- feldspar	Sulfates*, Fe-oxyhydroxides	2.2 ± 0.04
Sequential NAG test	Sulfides (>90%), carbonates (>90%), chlorite (0-30%), feldspar (0-30%) and mica (0-30%)	Sulfates, Fe-oxyhydroxides	4.5 ± 0.02

** Not measured, but inferred*

The elongated period of the biokinetic test allows the complete oxidation of the sulfides under the inoculated test conditions as seen in Table 23 from Chapter 5. The leaching behaviour of the mineral phases was similar for all the tests but the extent of leaching slightly differed. One feature that set the biokinetic test apart from other prediction techniques is that it accelerates the lag time to onset of acid production, by providing conditions that promote microbial activity in a relatively short time (c.f. humidity cells and column leach). The lag time depends on the content of acid neutralising minerals. In this study, microbial activity dominated after the depletion of carbonates (~7 days).

The common denominator between the NAG test and the biokinetic test is that the sulfide oxidation and acid neutralisation reactions take place simultaneously. The solution pH of the NAG is higher than of the biokinetic tests, whereas the test duration is otherwise. The mineral phases reacted in the NAG test are similar to those from the biokinetic test: sulfides, carbonates and chlorite. The key difference is that there was some mica reactivity and that the extent of chlorite reactivity was slightly less in the NAG test compared with the biokinetic tests. It is not clear whether differences in feldspar reactivity between the various biokinetic test conditions are meaningful and can be interpreted with confidence (Table 23). Sulfates and Fe-oxy-hydroxides were precipitated for all test conditions. Unlike the ANC tests, the leaching behaviour of minerals in both the NAG test and the biokinetic test

could not be precisely compared to one study but showed similar trends with what has been reported in literature (Blowes et al. 1998, Hakkou et al. 2008, Bogush et al. 2011).

The acid neutralizing minerals reacted in the NAG and biokinetic tests are similar to those from the Sobek/Skousen ANC test. Considering the fact that intermediate weathering silicates can substantially contribute towards long-term acid buffering; the biokinetic tests can be used to better determine the long-term acid generating potential. The NAG test can be used as part of screening stage to determine whether a sample has a potential to generate acid. The AMIRA modified Sobek and Skousen Incremental ANC methods are more suitable to determine the ANC for samples with significant abundance of reactive silicates. The Lawrence and Wang ANC, and the Paktunc mineralogical ANC are more suitable for sample with carbonates and negligible content of reactive silicates. It is possible that the Paktunc ANC method can be modified to include reactive silicates but an assumption would need to be included relating to the degree of partial reactivity (incongruent leaching).

6.2. Acid generating potential

A suite of prediction tests was conducted to characterize the potential for ARD generation. These tests include static (ABA and NAG), mineralogical techniques (ARDI and $NAPP_{MIN}$) and kinetic (biokinetic test). The main objective of the prediction tests is to evaluate balance between acid generating sulfides and acid neutralising minerals such as carbonates and silicates. The QEMSCAN results showed that the gold sample had 5 wt. % sulfides (predominantly pyrite and pyrrhotite), 0.5 wt. % ‘fast dissolving’ carbonates (mainly calcite), no ‘fast weathering’ silicates, 18 wt. % ‘intermediate weathering’ silicates (chlorite and mica), 2 wt.% ‘slow weathering’ Fe oxyhdroxides, 3 wt. % ‘very slow weathering’ silicates (feldspar) (see Table 15) and 71 wt. % ‘inert’ (quartz and sphene). Both the sulfides and the carbonates were liberated and not associated with each other (see Figure 19). The results obtained from the prediction tests carried out in this study are summarised in Table 27.

Table 27: A summary of the results acquired from the ARD prediction tests.

Parameter	Amount
Total S (wt. %)	1.3 ± 0.9
Sulfide S (wt. %)	1.3 ± 0.04
ARDI (mineralogy)	23.0
MPA (chemical) (kg H_2SO_4/t)	40.7 ± 1.3
MPA (mineralogy) (kg H_2SO_4/t)	64.2
ANC (Skousen) (kg H_2SO_4/t)	17.4 ± 0.002
ANC (Sobek) (kg H_2SO_4/t)	14.4 ± 0.4
ANC (Lawrence and Wang) (kg H_2SO_4/t)	4.2 ± 0.6
ANC (mineralogy) (kg H_2SO_4/t)	4.9
NAPP (Skousen) (kg H_2SO_4/t)	23.3 ± 0.65
NAPP (Sobek) (kg H_2SO_4/t)	26.3 ± 0.65
NAPP (Lawrence and Wang) (kg H_2SO_4/t)	36.5 ± 0.46
NAPP (mineralogy) (kg H_2SO_4/t)	59.4
Single-addition NAG pH	2.5 ± 0.03
Cumulative sequential NAG (kg H_2SO_4/t)	51.6 ± 2.8
Biokinetic test pH at day 63	2.1 ± 0.03
Classification	Potentially Acid Forming

The results from all the tests conducted in this study (Table 27) are consistent in terms of the acid generating potential; the gold sample is potentially acid forming. Both mineralogical techniques, ARDI and $NAPP_{MIN}$, showed that the sample is potentially acid forming. The modified Lawrence and Wang ANC had a very low ANC compared to the AMIRA modified Sobek and Incremental Skousen Siderite correction methods. The Lawrence and Wang ANC was mainly from carbonates and it was relatively comparable to that from Paktunc mineralogical ANC, that was calculated from only carbonates. This suggested that the modified Lawrence and Wang test conducted at room temperature for 24 hours underestimates ANC for samples with reactive silicates. The ANC obtained from the AMIRA modified

Sobek and Incremental Skousen Siderite correction methods may be more representative for samples with reactive silicates such as chlorite.

The single-addition NAG test also showed that the sample is potentially acid forming. In addition to sulfides, the acid neutralising minerals reacted in the sequential NAG are similar to those from AMIRA modified Sobek and Incremental Skousen siderite correction. The ABA and NAG tests results were further compared graphically on the ARD classification plot in Figure 32. All the data points of ABA against NAG also show that the sample is potentially acid forming. The classification criteria for the NAG tests indicates that this sample will be net acid generating, but the biokinetic test shows that the sample will eventually become net acid consuming although it will go through a period of being net acid generating. The acid neutralising carbonates and chlorite reacted in all the tests whereas there is potentially some indication of mica reactivity for selected tests (Sobek ANC, Skousen ANC and sequential NAG). The leaching behaviour of minerals under the different leach conditions supports the consistency of the analytical results (i.e. acid generating potential).

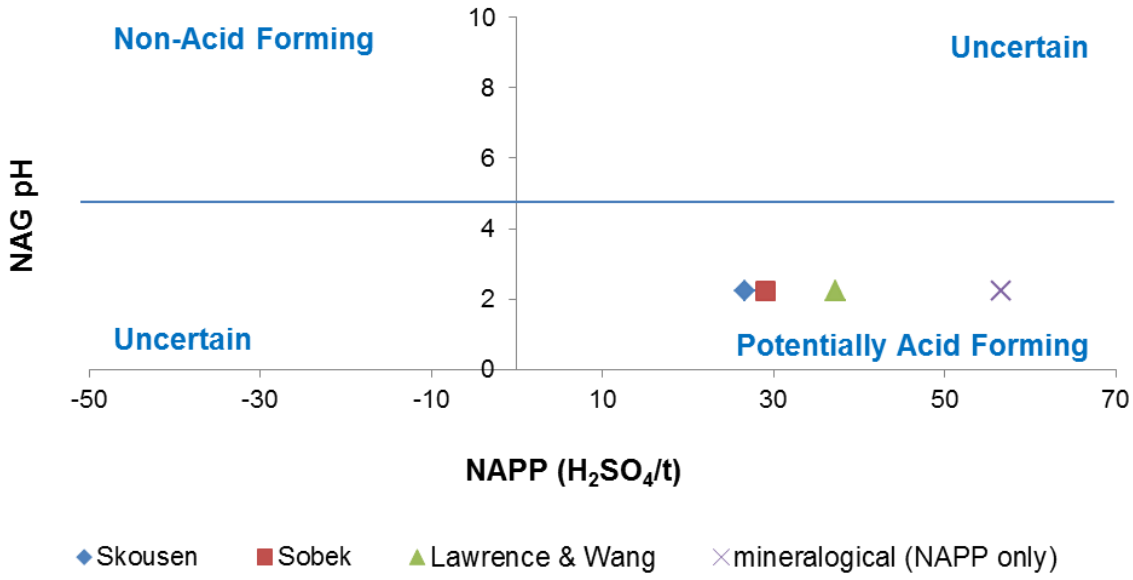

Figure 33: ARD classification plot comparing ABA (NAPP) with NAG pH.

6.3. Role of mineralogy in ARD characterisation

Morin *et al* (1998) encourages the use of a suite of tests that include static (ABA and NAG), kinetic (biokinetic) and mineralogy (ABA_{MIN} and ARDI) when characterising the acid generating potential. Since there is no single test that is capable enough to predict acid generating potential, use of more than one test enhances reliability on the tests. Often when more than one test is used, there are discrepancies that arise. Hence this study aims at providing information on the leaching behaviour of minerals under certain test conditions. The information acquired from studying the leach residues for

chemistry and mineralogy was used to examine the extent of mineral leaching under different prediction test conditions. The understanding of leaching behaviour of minerals under different test conditions can be incorporated in interpreting results generated from ARD prediction tests. That will improve accuracy and reproducibility of prediction tests and subsequently enhance confidence and reliability on these tests. In cases where a sample has similar bulk mineralogy as the gold sample, the information on Table 28 can be used as reference into expected results. Such kind of information will assist in identifying errors and find pointers to the discrepancies arising, if there are any. It must be noted that leaching behaviour is not only influenced by the test conditions, but the sample mineralogy and texture as well. An understanding of such crucial information is of paramount importance when selecting appropriate method.

Table 28: The minerals reacted under certain ARD prediction test conditions.

Method	The gold sample mineralogy	Minerals reacted or partially reacted (incongruent leaching)
Modified Lawrence and Wang ANC	Sulfides, carbonates, chlorite, mica, feldspar (incl. epidote) and quartz	Carbonates and chlorite
AMIRA modified Sobek or Skousen ANC		Carbonates, mica and chlorite
Sequential NAG		Sulfides, carbonates, mica, feldspar and chlorite
Biokinetic tests		Sulfides, carbonates, +/-feldspar and chlorite

Table 28 provides a guideline into the expected leaching behaviour of a sample with bulk mineralogy similar or comparable to that of the gold sample studied. As expected, for the modified Lawrence and Wang ANC method only ‘fast weathering’ carbonates and ‘intermediate weathering’ chlorite dissolved. The AMIRA modified Sobek or Skousen ANC methods dissolve the ‘slow weathering’ mica in addition to the minerals dissolved in modified Lawrence and Wang test. This explains the higher ANC from the AMIRA modified Sobek and Skousen ANC tests. Hypothesis 1 states that the AMIRA modified Sobek method overestimates the effective ANC due to the high-temperature leaching condition that results in the dissolution of the slow weathering silicates such as mica. This study however, showed that the AMIRA modified Sobek ANC provides long-term ANC and the Lawrence and Wang ANC provides short-term ANC. The biokinetic test proved to be capable of generating meaningful results in a reasonable period of time (63 days). The information generated from the biokinetic test compliments the static test results by providing additional data on the microbial activity and long-term net acid

generation. Hypothesis 2, which states that the prolonged test duration of the biokinetic test allow complete reaction of sulfides and acid neutralising minerals, proved positive. The leaching behaviour of residues showed that sulfides and carbonates completely reacted; chlorite moderately reacted on all the tests; Mg-bearing mica type minerals precipitated and feldspar including epidote reacted only in pH controlled biokinetic test. The mineralogy information showed that the biokinetic test is not actually as aggressive as the ANC and the NAG tests, since no mica reacted.

CHAPTER 7

CONCLUSION AND RECOMMENDATIONS

The use of ARD prediction tests to identify ore or waste rock with a risk to generate acid is crucial in mine waste management. However, no single prediction test is capable enough to provide reliable information on ARD formation. It is therefore usual practise to conduct more than one test and cross-check results to ensure that the appropriate conclusions are made. In so doing, the reliability on the tests is improved. In cases where the results from the different tests do not correlate, the representativeness of the different samples, as well as the assumptions behind the test methods will need to be considered. A clear understanding of the behaviour of mine waste under different test conditions will allow the appropriate usage of these tests and so improve their overall reliability. The objective of this study was to use mineralogy to better understand leaching behaviour of minerals under various prediction tests. This objective was achieved by answering the following key questions:

I. What are the mineralogical factors associated with the changes of empirical ANC under different ABA test conditions and how does the empirical ANC compare to the mineralogical ANC?

II. What is the extent of mineral leaching during conventional static and the novel new biokinetic geochemical tests for ARD prediction?

III. How do the results of the mineralogical and above-mentioned geochemical tests compare in terms of characterising ARD potential?

IV. What is the relationship between mineral composition, prediction method and characterisation of ARD potential?

V. In what way can mineralogical analysis be used to enhance the interpretation of ARD characterisation?

The key questions were addressed through experimental work conducted on a South African gold ore sample. The gold ore sample was analysed for chemical composition, bulk mineralogy, texture and acid generating potential. The results obtained from the experimental work are presented in Chapter 4 and 5, and further discussed in Chapter 6. The outcomes of the study will be subsequently presented based on the key questions which had been set out.

7.1. Research outcomes

The research outcomes are discussed by reviewing the hypotheses and the key questions:

Hypothesis I proved true: In addition to carbonates (strongly reacted) and chlorite (moderately reacted), there is an indication of mica reactivity for the AMIRA modified Sobek ANC compared to the Lawrence and Wang ANC method. Further mineralogical investigation is needed to confirm this with more confidence.

Hypothesis II proved true: Carbonates and sulfides reacted completely for the biokinetic tests while chlorite reacted moderately. There was some indication of feldspar reactivity, but it is unclear how this links to the different test conditions.

Key questions:

I. The mineralogical factor associated with the changes in empirical ANC under the different ABA test conditions is: the extent of mineral dissolution of various acid neutralising minerals and the contribution of the acid neutralising minerals towards ANC that govern reactivity of these minerals. Sulfides were completely liberated in this study but this may not always be so for other samples. The mineralogical ANC is relatively lower than the AMIRA modified Sobek or Skousen Incremental ANC, but comparable to the modified Lawrence and Wang ANC.

II. Mainly acid neutralising minerals reacted under the ANC leach conditions. The minerals that reacted are: carbonates and chlorite in AMIRA modified Sobek, Incremental Skousen siderite correction and Lawrence and Wang ANC methods, with the exception of mica in the latter. The sulfides were strongly oxidized, carbonate depleted, chlorite and mica slightly reacted in the sequential NAG test. This proves that both the sulfide oxidation and the dissolution of acid neutralising minerals occurred simultaneously. Then sulfide oxidation reaction dominated creating acidic conditions that stimulated dissolution of slow weathering silicates. Overall, similar minerals reacted under all the different leach conditions showing that the same reactions are taking place. The only notable difference was the extent of leaching.

III. The mineralogical ARDI and $NAPP_{MIN}$ were consistent with the above-mentioned geochemical tests and showed that the sample is potentially acid forming with very little ANC.

IV. This study showed that mineralogy can be used to better understand leaching behaviour of minerals and the controlling reactions in ARD processes as well as in hydrometallurgy applications particularly acid leaching. Use of mineralogy to interpret geochemical test results can be useful in addressing discrepancies encountered and further enhance the level of confidence on the information acquired.

7.2. Concluding remarks

The main objective of this study was to use mineralogy to interpret geochemical ARD prediction tests. This study has shown that the first step towards reliable ARD characterisation is to thoroughly examine the sample for chemical composition, bulk mineralogy and textural properties that affect both the leaching behaviour of minerals and the acid generating potential. The appropriate prediction test must be chosen based on the prospective leaching behaviour of the sample to ensure reliability on the ARD prediction tests. The Lawrence and Wang, and Paktunc mineralogical ANC methods are more suitable for sample with carbonates and negligible contents of silicates. The AMIRA modified Sobek ANC test can be used to determine long-term acid neutralisation in samples that have negligible Fe and Mn carbonate contents in order to avoid interference caused by excess H_2O_2. The AMIRA modified Skousen Incremental ANC method is more suitable for sample containing large quantities of Fe and Mn carbonates. The biokinetic test should be used to determine the long-term net acid generating potential. This study further showed that overall the same minerals reacted under the different leach conditions, but the extent of leaching varied according to the test conditions. In instances where problematic samples are encountered, mineralogy can be used to determine the potential source of error. However the cost of analysis and small sample masses must be taken into consideration when selecting samples for automated mineralogy.

This study also showed the importance of understanding the extent of mineral leaching when interpreting results. The results showed that most mineral phases were partially leached. The incongruent leaching had effect on gathering data on QEMSCAN, since analyses were performed on the surface composition. As a result, the acid leached residues from the ANC and NAG tests had to be treated with different Species Identification Protocol file (QEMSCAN SIP) from the bioleached residues from the biokinetic tests. The information generated on the extent of mineral leaching in the ANC methods can be used to build up a database for leaching behaviour in the ANC test methods. This can minimise errors associated with the common assumption that states “all mineral react completely”. It is also crucial to take note of the pH solution as it affects leaching behaviour. Most importantly, there is no prediction method or technique superior to the other. Each method is more suitable for certain type of samples and provides specific information. Hence mineralogy is used to screen appropriate prediction methods. However different ARD prediction tests should be carefully used to complement each other.

7.3. Recommendations

The future recommendations from this study were made based on the literature survey and the findings of this research:

- This study showed that both the ARDI and the biokinetic test are capable of generating reliable information on the acid generating potential. Considering the cost of QEMSCAN, other mineralogy techniques such as XRD and SEM or even simple ore microscopy can be considered for the evaluation of ARDI.

- The biokinetic test was successful on the controlled laboratory-scale conditions to provide information on the effect of microbial activity on ARD formation. It must be tested and scaled-up on coarser samples in a controlled field-scale environment in order to validate findings from both laboratory- and field-scale. The final pH must account for the initial pH and mineral acid potential. Chemistry and mineralogy should be monitored from day one in order to better understand background concentrations.

- There are many test methods and techniques used to characterize the mine waste for acid generating potential. Each test method is best suitable for a certain type of mineralogy and can only provide meaningful results for certain objectives. The next logical step towards reliable prediction tests to develop a working knowledge of the mineralogy of the ore and how it responds to the tests.

- It was difficult to obtain a good correlation between the mineralogy results acquired through mineral surface analysis of the tests residues. This was due to incongruent leaching of mineral surface from the geochemical tests. In order to optimise accuracy of results, caution must be taken when analysing residues with incongruently leached mineral surfaces (i.e. QEMSCAN SIP must be calibrated). Detailed mineral chemical analyses obtained from electron probe microanalysis would no doubt assist with understand the nature of incongruent leaching.

REFERENCES

AHERN, C.R., MCELNEA, A.E. and SULLIVAN, L.A., 2004. *Acid Sulfate Soils Laboratory Methods Guidelines.* Indooroopilly, Queensland, Australia: Department of Natural Resources, Mines and Energy.

AKABZAA, T. and YIDANA, S., 2012. An Integrated Approach to Environmental Risk Assessment of Cumulatively Impacted Drainage Basin from Mining Activities in South-western Ghana*. Environmental Earth Sciences*, vol. 65, no. 1, pp. 291-312 ISSN 1866-6280. DOI 10.1007/s12665-011-1090-0.

AKCIL, A. and KOLDAS, S., 2006. Acid Mine Drainage (AMD): Causes, Treatment and Case Studies*. Journal of Cleaner Production*, vol. 14, pp. 1139-1145.

AUDRY, S., BLANC, G. and SCHÄFER, J., 2005. The Impact of Sulphide Oxidation on Dissolved Metal (Cd, Zn, Cu, Cr, Co, Ni, U) Inputs into the Lot–Garonne Fluvial System (France)*. Applied Geochemistry*, 5, vol. 20, no. 5, pp. 919-931 ISSN 0883-2927. DOI 10.1016/j.apgeochem.2005.01.006.

BAKER, B.J. and BANFIELD, J.F., 2003. Microbial Communities in Acid Mine Drainage*. FEMS Microbiology Ecology*, 5/15, vol. 44, no. 2, pp. 139-152 ISSN 0168-6496. DOI 10.1016/S0168-6496(03)00028-X.

BENZAAZOUA, M., BUSSIÈRE, B., DAGENAIS, A.-. and ARCHAMBAULT, M., 2004. Kinetic Tests Comparison and Interpretation for Prediction of the Joutel Tailings Acid Generation Potential*. Environmental Geology*, vol. 46, no. 8, pp. 1086-1101 ISSN 0943-0105. DOI 10.1007/s00254-004-1113-1.

BLOWES, D.W., PTACEK, C.J., JAMBO, J.L. and WEISENER, C.G., 2005. 9.05 The Geochemistry of Acid Mine Drainage: In Treatise on Geochemistry*. Environmental Geochemistry*, vol. 9, pp. 149-204.

BLOWES, D.W., JAMBOR, J.L. and HANTON-FONG, C.J., 1998. Geochemical, Mineralogical and Microbiological Characterization of a Sulphide-Bearing Carbonate-Rich Gold-Mine Tailings Impoundment, Joutel, Québec*. Applied Geochemistry*, 8, vol. 13, no. 6, pp. 687-705 ISSN 0883-2927. DOI 10.1016/S0883-2927(98)00009-2.

BOGUSH, A. and LAZAREVA, E., 2011. Behaviour of Heavy Metals in Sulfide Mine Tailings and Bottom Sediment (Salair, Kemerovo Region, Russia)*. Environmental Earth Sciences*, vol. 64, no. 5, pp. 1293-1302 ISSN 1866-6280. DOI 10.1007/s12665-011-0947-6.

BOUZAHZAH, H., BENZAAZOUA, M. and BUSSIÈRE B. A modified protocol of the ASTM normalized humidity cell test as laboratory weathering method of concentrator tailings. WOLKERSDORFER & FREUND, ed. *null*, 2010.

BOWELL, R.J., SAPSFORD, D.J., DEY, M. and WILLIAMS, K.P. Protocols affecting the reactivity of mine waste during laboratory-based kinetic tests BARNHISEL, R.I., ed. *7th International Conference on Acid Rock Drainage*, 2006.

BROADHURST, J.L., BRYAN, C.G., BECKER, M., FRANZIDIS, J-P. and HARRISON, S.T.L. 2013. Characterising the acid generating potential of mine wastes by means of laboratory-scale static and biokinetic tests. IMWA, Reliable Mine Water Technology, Golden CO, USA, pp 275 - 280.

BROADHURST, J.L., HANSEN, Y. and PETRIE, J.G. 2007. Waste characterisation and water-related impact predictions for solid mineral wastes: A new approach. Water Research Commission Report No. 1550/1/07, South Africa.

Brough, C.P., Warrender, R., Bowell, R.J., Barnes, A. and Parbhakar-Fox, A. 2013. The process mineralogy of mine wastes, Minerals Engineering, 52, pp 125 - 135.

BUCKNAM, C.H., WHITE, W.I. and LAPPAKO, K.A. Standardization of mine waste characterisation methods by ADTI-MMS Anonymous *Securing the Future and 8th ICARD*, 2009. BURTON, E.D., *et al*, 2008. A Simple and Inexpensive Chromium-Reducible Sulfur Method for Acid-Sulfate Soils. *Applied Geochemistry*, SEP, vol. 23, no. 9, pp. 2759-2766 ISSN 0883-2927. DOI 10.1016/j.apgeochem.2008.07.007.

CANFIELD, D.E., RAISWELL, R., WESTRICH, J.T., REAVES, C.M. and BERNER, R.A., 1986. The use of Chromium Reduction in the Analysis of Reduced Inorganic Sulfur in Sediments and Shales. *Chemical Geology*, 1/30, vol. 54, no. 1–2, pp. 149-155 ISSN 0009-2541. DOI 10.1016/0009-2541(86)90078-1.

CHAMBER OF MINES OF SOUTH AFRICA, www.bullion.org.za accessed on 19 May 2014.

CHENG, S., JANG, J-H., DEMPSEY, B.A., and LOGAN, B.E., 2011. Efficient recovery of nano-sized iron oxide particles from synthetic acid mine drainage (AMD) water using fuel cell technologies. Water Research, vol. 45, issue 1, pp 303-307.

CHEN, T., YAN, B., LEI, C. and XIAO, X., 2014. Pollution control and metal resource recovery for acid mine drainage. Hydrometallurgy, vol 147-148, pp 112-119

CHIMBGANDA, T., 2012. *An Integrated Approach for the Mitigation of Acid Rock Drainage (ARD) Associated with Pyrrhotite In Nickel Deposits.* Unpublished MSc Thesis, University of Cape Town.

COASTEC RESEARCH INC., 1991. Acid rock drainage prediction manual. Energy, Mines and Resources, Canada, MEND Report 1.16.1 (b)

COETZEE, F., WINDE, F. and WADE, P.W., 2006. *An Assessment of Sources, Pathways, Mechanisms and Risks of Current and Potential Future Pollution of Water and Sediments in Gold-Mining Areas of the Wonderfonteinspruit catchment.* South Africa: Water Research Commission.

CRUZ, R., GONZÁZEL, I. and MONROY, M., 2005. An Experimental Strategy to Determine Galvanic Interactions Affecting the Reactivity of Sulfide Mineral Concentrates. *Hydrometallurgy*, 8, vol. 78, no. 3–4, pp. 198-208 ISSN 0304-386X. DOI 10.1016/j.hydromet.2005.03.006.

CZEREWKO, M.A., CRIPPS, J.C., REID, J.M. and DUFFELL, C.G., 2003. Sulfur Species in Geological materials—sources and Quantification. *Cement and Concrete Composites*, 10, vol. 25, no. 7, pp. 657-671 ISSN 0958-9465. DOI 10.1016/S0958-9465(02)00066-5.

Department of Water Affairs and Forestry, 2008. *G4 Impact Prediction, Best Practice Guidelines.* South Africa

DOLD, B., 2005. *Basic Concepts of Environmental Geochemistry of Sulfide Mine-Waste.*

DOLD, B. and FONTBOTE, L., 2002. A Mineralogical and Geochemical Study of Element Mobility in Sulfide Mine Tailings of Fe Oxide Cu–Au Deposits from the Punta Del Cobre Belt, Northern Chile . *Chemical Geology*, vol. 189, pp. 135-163.

DOPSON, M., LOVGREN, L. and BOSTROM, D., 2009. Silicate mineral dissolution in the presence of acidophillic microorganisms: Implication for heap leaching. Hydrometallurgy, vol. 96, issue 4, pp 288-293.

ELWOOD MADDEN, M.E., MADDEN, S.A., RIMSTIDT, J.D., ZAHRAI, S., KENDALL, M.R. and MILLER, M.A., 2012. Jarosite Dissolution Rates and Nanoscale Mineralogy. *Geochimica Et Cosmochimica Acta*, 8/15, vol. 91, no. 0, pp. 306-321 ISSN 0016-7037. DOI 10.1016/j.gca.2012.05.001.

EVANS, P. and SKOUSEN, J. Effect of digestion method on neutralization potential of overburden samples containing siderite Anonymous *1995 National Meeting of American Society for Surface Mining and Reclamation*, 1995.

FINKELMANN, R.B. and GRIFFIN, D.E., 1986. Hydrogen Peroxide Oxidation: An Improved Method for Rapidly Assessing Acid-Generating Potential of Sediments and Sedimentary Rocks. *Reclamation and Revegetation Research,* vol. 5, pp. 521.

FRIMMEL, H.E., 2009. Geochemical and Geochronological Constraints on the Nature of the Immediate Basement next to Mesoarchaean Auriferous Witwatersrand Basin, South Africa. *Journal of Petrology*, vol. 50, no. 12, pp 2187-2220.

FROSTAD, S., KLEIN, B. and LAWRENCE, R.W., 2002. *Evaluation of Laboratory Kinetic Test Methods for Measuring Rates of Weathering.* Springer Berlin / Heidelberg ISBN 1025-9112.

GOLDICH, S.S., 1938. A Study of Weathering. *Journal of Geology*, vol. 46, pp. 17-58 DOI http://dx.doi.org/10.1086%2F624619.

GONZALEZ-SANDOVAL, M., LIZARAGA-MENDIOLA, L., SANCHEZ-TOVAR, S.A. and DURAN-DOMINGUEZ, M. Humidity Cell Tests: Effect of Air Flow and Cycle Duration in the Quality of Leachates Anonymous *Securing the Future and 8th ICARD*, 2009.

GUNSINGER, M.R., PTACEK, C.J., BLOWES, D.W. and JAMBOR, J.L., 2006a. Evaluation of Long-Term Sulfide Oxidation Processes within Pyrrhotite-Rich Tailings, Lynn Lake, Manitoba. *Journal of Contaminant Hydrology*, 2/10, vol. 83, no. 3–4, pp. 149-170 ISSN 0169-7722. DOI 10.1016/j.jconhyd.2005.10.013.

GUNSINGER, M.R., PTACEK, C.J., BLOWES, D.W., JAMBOR, J.L. and MONCUR, M.C., 2006b. Mechanisms Controlling Acid Neutralization and Metal Mobility within a Ni-Rich Tailings Impoundment. *Applied Geochemistry*, 8, vol. 21, no. 8, pp. 1301-1321 ISSN 0883-2927. DOI 10.1016/j.apgeochem.2006.06.006.

HAKKOU, R., BENZAAZOUA, M. and BUSSIÈRE, B., 2008. *Acid Mine Drainage at the Abandoned Kettara Mine (Morocco): 2. Mine Waste Geochemical Behaviour.* Springer Berlin / Heidelberg ISBN 1025-9112.

HAMMARSTROM, J.M., SEAL II, R.R., MEIER, A.L. and KORNFELD, J.M., 2005. Secondary Sulfate Minerals Associated with Acid Drainage in the Eastern US: Recycling of Metals and Acidity in Surficial Environments. *Chemical Geology*, 2/15, vol. 215, no. 1–4, pp. 407-431 ISSN 0009-2541. DOI 10.1016/j.chemgeo.2004.06.053.

HERELL, M.K., MCRAE, C., SALZSAULER, K. and WAPLES, J.S. Practical Application of Accelerated Methods on Acid Rock Drainage and Metal Leaching Prediction of Mine Materials Anonymous *Securing the Future and 8th ICARD*, 2009.

HESKETH, A., BROADHURST, J.L., BRYAN, C.G., van HILLE, R.P. and HARRISON, S.T.L., 2010. Biokinetic Test for the Characterisation of AMD Generation Potential of Sulfide Mineral Wastes. *Hydrometallurgy*, vol. 104, pp. 459-464.

Inter-Ministerial Committee on Acid Mine Drainage, 2010. *Mine Water Management in the Witwatersrand Goldfields with Special Emphasis on Acid Mine Drainage.* Council of Geoscience, South Africa: Mineral Resources and Water Affairs.

JAMBOR, J.L., DUTRIZAC, J.E. and RAUDSEPP, M. Comparison of measured and mineralogically predicted values of the Sobek neutralisation potential for intrusive rocks Anonymous *7th International Conference on Acid Rock Drainage (ICARD)*, 2006.

JAMBOR, J.L., DUTRIZAC, J., GROAT, L. and RAUDSEPP, M., 2002. Static Tests of Neutralization Potentials of Silicate and Aluminosilicate Minerals. *Environmental Geology*, vol. 43, no. 1, pp. 1-17 ISSN 0943-0105. DOI 10.1007/s00254-002-0615-y.

JAMEISON, H.E. 2011. Geochemistry and Mineralogy of Solid Mine Waste: Essential Knowledge for Predicting Environmental Impact.

JANZEN, M.P., NICHOLSON, R.V. and SCHARER, J.M., 2000. Pyrrhotite Reaction Kinetics: Reaction Rates for Oxidation by Oxygen, Ferric Iron, and for Nonoxidative Dissolution. *Geochimica Et Cosmochimica Acta*, 5, vol. 64, no. 9, pp. 1511-1522 ISSN 0016-7037. DOI http://dx.doi.org/10.1016/S0016-7037(99)00421-4.

JOHNSON, D.B. and HALLBERG, K.B. 2005. A*cid mine drainage remediation options: a review.* Science of the Total Environment. vol. 338 (1-2) pp 3-14.

JURJOVEC, J., PTACEK, C.J. and BLOWES, D.W., 2002. Acid Neutralization Mechanisms and Metal Release in Mine Tailings: A Laboratory Column Experiment. *Geochimica Et Cosmochimica Acta*, vol. 66, no. 9, pp. 1511-1523.

KAARTINEN, T. and WALSTROM, M., 2009. *Development of a European Standard for the Determination of Acid Potential and Neutralization Potential of Sulfidic Waste.*

KAZADI MBAMBA, C., 2011. *Using Froth Flotation to Mitigate Acid Rock Drainage Risks while Recovering Valuable Coal from Ultrafine Colliery Wastes.* Unpublished MSc Thesis, University of Cape Town.

KALINKINA, A.M., KALINKINA, E.V. and VASIL'EVA, T.N., 2003. Effect of Mechanical Activation on Sphene Reactivity. Colloid Journal, Vol. 66, No. 2, pp 160-167. Translated from Kolloidnyt Zhumal, Vol. 66, No. 2, 2004, pp 190-197.

KINGS, S., 2014. One man's home is another man's uranium dump, Mail & Guardian

KLEINMANN, R.I.P., 2000. *Prediction of Water Quality at Surface Coal Mines.* Acid Rock Drainage Initiative, West Virginia University, Morgantown, West Virginia: The National Mine Land Reclamation Centre.

KOMADEL, P. and STUCKI, J.W. 1988. *Quantitative assay of minerals for Fe2+ and Fe3+ using 1,10-phenanthroline: III. A rapid photochemical method*. Clays and Clay Minerals **36**, 379-381.

KOTELO, L.O., 2013. *Characterising the acid mine drainage potential of fine coal wastes. Unpublished MSc Thesis, University of Cape Town.*

KWONG, J.Y.T., 1993. *Prediction and Prevention of Acid Rock Drainage from a Geological and Mineralogical Perspective.* 1.32.1 ed. National Hydrology Research Institute, Canada, S7N 3H5: MEND Report.

LAPPAKO, K., 2002. *Metal Mine Rock and Waste Characterisation Tools: An Overview.* Minnesota Department of Natural Resources, US: Acid Drainage Technology Initiative - Metal Mining Sector.

LAPPAKO, K.A. and LAWRENCE, R.W. Modifications of the net acid production (NAP) test Anonymous *17th Annual British Columbia Mine Reclamation Symposium*, 1993.

LAWRENCE, R.W., RITCEY, G.M, POLING, G.W. and MARCHANT, P.B. Strategies for the prediction of acid mine drainage, COASTECH RESEARCH INC, ed. *13th Annual British Columbia mine Reclamation Symposium*, 1989.

LAWRENCE, R.W. and SCHESKE, M., 1997. *A Method to Calculate the Neutralization Potential of Mining Wastes.* Springer Berlin / Heidelberg ISBN 0943-0105.

LAWRENCE, R.W. and WANG, Y., 1996. *Determination of Neutralization Potential for Acid Rock Drainage Prediction.* Mining and Mineral Engineering, University of British Columbia: MEND Project 1.16.3.

LEHNER, S., SAVAGE, K., CIOBANU, M. and CLIFFEL, D.E., 2007. The Effect of as, Co, and Ni Impurities on Pyrite Oxidation Kinetics: An Electrochemical Study of Synthetic Pyrite. *Geochimica Et Cosmochimica Acta*, 5/15, vol. 71, no. 10, pp. 2491-2509 ISSN 0016-7037. DOI 10.1016/j.gca.2007.03.005.

LI, J., SMART, R.St.C., SCHUMANN, R.C., GERSON, A.R. and LEVAY, G., 2007. A Simplified Method for Estimation of Jarosite and Acid-Forming Sulfates in Acid Mine Wastes. *Science of the Total Environment*, 2/1, vol. 373, no. 1, pp. 391-403 ISSN 0048-9697. DOI 10.1016/j.scitotenv.2006.11.012.

LIFFERINK, M., 2010. Super dump: Mine waste solutions requests assistance: Pelindaba Working Group; Coaliation Against Nuclear Energy.

LOTTERMOSER, B.G., 2010. *Sulfidic Mine Wastes.* Springer Berlin Heidelberg ISBN 978-3-642-12419-8.

MARSDEN, D.D., 1986. The Current Limited Impact of Witwatersrand Gold-Mine Residues on Water Pollution in the Vaal River System. *JOURNAL OF THE SOUTH AFRICAN INSTITUTE OF MINING AND METALLURGY*, vol. 86, no. 12, pp. 481-504.

MILLER, S., 2008. *ACARP Project C15034: Development of ARD Assessment for Coal Process Wastes.* Environmental Geochemistry International, Levay and Co Environmental Services, ACeSSS - University Of South Australia.

MINING TECHNOLOGY MARKET AND CUSTOMER INSIGHT, www.mining-technology.com accessed on 19 May 2014.

MONCUR, M.C., JAMBOR, J.L., PTACEK, C.J. and BLOWES, D.W., 2009. Mine Drainage from the Weathering of Sulfide Minerals and Magnetite. *Applied Geochemistry*, 12, vol. 24, no. 12, pp. 2362-2373 ISSN 0883-2927. DOI 10.1016/j.apgeochem.2009.09.013.

MORIN, K.A. and HUTT, N.M., 2009. On the Nonsense of Arguing the Superiority of an Analytical Method for Neutralization Potential. MDAG.com Internet Case Study 32 on www.mdag.com/case_studies/cs32.html.

MORIN, K.A. and HUTT, N.M., 1999. *Humidity Cells: How Long? How Many? Unpublished Material.*

MORIN, K.A. and HUTT, N.M. Kinetic Tests and Risk Assessment for ARD. Anonymous *5th Annual BC Metal Leaching and ARD Workshop*, 1998.

MORIN, K.A., HUTT, N.M. and FERGUSON, K.D. Measuring Rates of Sulfide Oxidation and Acid Neutralization in Kinetic Tests: Statistical Lessons from the Database Anonymous *Conference on Mining and the Environment*, 1995.

MPEPHU, N.F., 2003. *Rehabilitation of Tailings Dams on the Central Rand; Johannesburg. Unpublished Material.*

NAICKER, K., CUKROWSKA, E. and MCCARTHY, T.S., 2003. Acid Mine Drainage Arising from Gold Mining Activity in Johannesburg, South Africa and Environs*. Environmental Pollution*, 3, vol. 122, no. 1, pp. 29-40 ISSN 0269-7491. DOI 10.1016/S0269-7491(02)00281-6.

NENGOVHELA, A.C., YIBAS, B. and OGOLA, J.S., 2006. Characterisation of Gold Tailings Dams of the Witwatersrand Basin with Reference to their Acid Mine Drainage Potential, Johannesburg, South Africa*. Water SA*, vol. 32, no. 2, pp. 499-506.

NORDSTROM, K.D. 2011. Mine Water: Acid to Circumneutral. *Elements*, Vol. 7, No. 6

NORDSTROM, K.D. and ALPERS, C.N. Negative pH, efflorescent mineralogy, and consequences for environmental restoration at the Iron Mountain Superfund site, California Anonymous *National Academy of Sciences colloquium "Geology, Mineralogy, and Human Welfare"*, 1999.

NWAILA, G., 2014. Application of HPGR and X-Ray CT to investigate the Potential of Witwatersrand Gold ore for Heal Leaching: A Process Mineralogy Approach, Unpublished MSc Thesis, University of Cape Town.

OELOFSE, S.H.H., HOBBS, P.J., RASCHER, R. and COBBING, J.E., 2007. *The Pollution and Destruction Threat of Gold Mining Waste on the Witwatersrand - A West Rand Case Study*

OELOFSE, S., 2008. *Mine Pollution: Acid Mine Decant, Fluent and a Treatment: A Consideration of Key Emerging Issues that may Impact the Environment.* South Africa: Department of Environmental Affairs and Tourism.

OGOLA, J.S. Dispersion of Heavy Metals and their potential Impacts on the Environment: A case study of Gold Tailings Dams in Giyani Belt, Limpopo Province, South Africa WOLKERSDORFER & FREUND, ed. *IMWA "Mine Water and Innovative Thinking"*, 2010.

O'SHAY, T.O., HOSSNER, L.R. and DIXON, J.B., 1990. A Modified Hydrogen Peroxide Oxidation Method for Determination of Potential Acidity in Pyritic Overburden. *J. Environ. Qual.*, vol. 19, pp. 778-782.

PAKTUNC, A.D., 1999a. *Discussion of "A Method to Calculate the Neutralization Potential of Mining Wastes" by Lawrence and Scheske.* Springer Berlin / Heidelberg ISBN 0943-0105.

PAKTUNC, A.D., 1999b. Mineralogical Constraints on the Determination of Neutralization Potential and Prediction of Acid Mine Drainage. *Environmental Geology*, vol. 39, no. 2, pp. 103-112 ISSN 0943-0105. DOI 10.1007/s002540050440.

PARBHAKAR, A., EDRAKI, M., BRADSHAW, D. and WALTERS, S. Development of Mineralogical Characterisation Techniques for Predicting Acid Rock Drainage: A Case Study from an Abandoned Au-Mine, North Australia Anonymous *First Seminar on Environmental Issues in the Mining Industry*. Santiago, Chile, 2009a.

PARBHAKAR, A., EDRAKI, M., BRADSHAW, D. and WALTERS, S., 2009b. *Mineralogical Characterisation Techniques for Predicting Acid Rock Drainage.*

PARBHAKAR-FOX, A., 2012. *Establishing the Value of an Integrated Geochemistry-Mineralogy-Texture Approach for Acid Rock Drainage Prediction.* PhD ed. University of Tasmania.

PARBHAKAR-FOX, A.K., EDRAKI, M., WALTERS, S. and BRADSHAW, D., 2011. Development of a Textural Index for the Prediction of Acid Rock Drainage. *Minerals Engineering*, 10, vol. 24, no. 12, pp. 1277-1287 ISSN 0892-6875. DOI 10.1016/j.mineng.2011.04.019.

PARBHAKAR-FOX, A., EDRAKI, M., BRADSHAW, D. and WALTERS, S., 2012. Development of a Textural Acid Rock Drainage Index for Classifying Acid Formation. In: M.A.T.M. BROEKMANS ed., *Proceedings of the 10th International Congress for Applied Mineralogy (ICAM)*Springer Berlin Heidelberg, pp. 513-521 ISBN 978-3-642-27682-8. DOI 10.1007/978-3-642-27682-8_61.

PARBHAKAR-FOX, A., EDRAKI, M., BRADSHAW, D. and WALTERS, S. Development of a textural acid rock drainage index for classifying acid formation MAARTEN A. T. M. BROEKMANS, ed. *10th International Conference for Applied Mineralogy*, 2012.

PARBHAKAR-FOX, A., LOTTERMOSER, B. and BRADSHAW, D. Cost-effective means for identifying acid rock drainage risks - Integration of the Geochemistry-Mineralogy - Texture Approach and Geometallurgical techniques. In: *The Second AUSIMM International Geometallurgy Conference,* 2013

PLANTE, B., BUSSIÈRE, B. and BENZAAZOUA, M., 2012. Static Tests Response on 5 Canadian Hard Rock Mine Tailings with Low Net Acid-Generating Potentials. *Journal of Geochemical Exploration*, 3, vol. 114, no. 0, pp. 57-69 ISSN 0375-6742. DOI 10.1016/j.gexplo.2011.12.003.

PRICE, W.A., 2009. *Prediction Manual for Drainage Chemistry from Sulphidic Geologic Materials.* CANMET- Mining and Mineral Sciences laboratories, Smithers, British Columbia, VOJ 2NO: MEND Report 1.20.1.

PULLES, W., BANISTER, S. and VAN BILJON, M., 2005. *The Development of Appropriate Procedures towards and after Closure of Underground Gold Mines from a Water Management Perspective.* South Africa: Water Research Commission Report No: 2015/1/05 ed.

ROSNER, T., BOER, T., REYNEKE, R., AUCAMP, P. and VERMAAK, J., 2001. *Preliminary Assessment of Pollution Contained in the Unsaturated and Saturated Zone Beneath Reclaimed Gold-Mine Residue Deposits.* South Africa: Water Research Commission.

RÖSNER, T. and VAN SCHALKWYK, A., 2000. The Environmental Impact of Gold Mine Tailings Footprints in the Johannesburg Region, South Africa. *Bulletin of Engineering Geology and the Environment*, 10/01, vol. 59, no. 2, pp. 137-148 ISSN 1435-9529. DOI 10.1007/s100640000037.

SALOMONS, W., 1995. Environmental Impact of Metals Derived from Mining Activities: Processes, Predictions, Prevention. *Journal of Geochemical Exploration*, 1, vol. 52, no. 1–2, pp. 5-23 ISSN 0375-6742. DOI http://dx.doi.org/10.1016/0375-6742(94)00039-E.

SAPSFORD, D.J., BOWELL, R.J., DEY, M. and WILLIAMS, K.P., 2009. Humidity Cell Tests for the Prediction of Acid Rock Drainage. *Minerals Engineering*, 1, vol. 22, no. 1, pp. 25-36 ISSN 0892-6875. DOI 10.1016/j.mineng.2008.03.008.

SCHUMANN, R., STEWART, W., MILLER, S., KAWASHIMA, N., LI, J. and SMART, R., 2012. Acid–base Accounting Assessment of Mine Wastes using the Chromium Reducible Sulfur Method. *Science of the Total Environment*, 5/1, vol. 424, no. 0, pp. 289-296 ISSN 0048-9697. DOI 10.1016/j.scitotenv.2012.02.010.

SHAW, S.C., GROAT, L.A., JAMBOR, J.L., BLOWES, D.W., HANTON-FONG, C.J. and STUPARYK, R.A., 1998. *Mineralogical Study of Base Metal Tailings with various Sulfide Contents, Oxidized in Laboratory Columns and Field Lysimeters.* Springer Berlin / Heidelberg ISBN 0943-0105.

SKOUSEN, J., RENTON, J., BROWN, H., EVANS, P., LEAVITT, B., BRADY, K., COHEN, L. and ZIEMKIEWICZ, P., 1997. Neutralization Potential of Overburden Samples Containing Siderite. *J. Environ. Qual.*, vol. 26, pp. 673-681.

SMART, R., SKINNER, W.M., LEVAY, G., GERSON, A.R., THOMAS, J.E., SOBIERAJ, H., SCHUMANN, R., WEISENER, C.G., WEBER, P.A., MILLER, S.D., STEWART, W.A., 2002. *ARD Test Handbook. Project P387A Prediction and Kinetic Control of Acid Mine Drainage.* Level 2, 271 William Street Melbourne 3000 Australia: Ian Wark Research Institute, Environmental Geochemistry International Pty Ltd;.

SOBEK, A.A., SCHULLER, W.A., FREEMAN, J.R. and SMITH, R.M., 1978. *Field and Laboratory Methods Applicable to Overburdens and Minesoils.* U.S. Environmental Protection Agency, Cincinnati, Ohio, 45268: EPA-600/2-78-054.

STEWART, W., 2005. *Development of Acid Rock Drainage Prediction Methodologies for Coal Mine Wastes* PhD ed. Ian Wark Research Institute, University of South Australia.

STEWART, W.S., MILLER, S.D. and SMART, R. Advances in acid rock drainage (ARD) characterisation of mine wastes Anonymous *7th International Conference on Acid Rock Drainage (ICARD)*, 2006.

STEWART, W., SCHUMANN, R. and SMART, R. Development of prediction methods for ARD assessment of coal process waste Anonymous *Securing Future and 9th ICARD*, 2009.

STROMBERG, B. and BANWART, S.A., 1999. Experimental Study of Acid-Consuming Processes in Mining Waste Rock: Some Influences of Mineralogy and Particle Size. *Applied Geochemistry*, vol. 14, pp. 1-16.

SULLIVAN, L.A., BUSH, R.T., McCONCHIE, D., LANCASTER, G., CLARK, M., LIN, C. and SAENGER, P., 2004. *Chromium Reducible Sulfur Methods (S_{CR})- Method Code 22B: In Acid Sulfate Soils, Laboratory Methods Guidelines.* Indooroopilly, Queensland, Australia: Department of Natural Resources, Mines and Energy.

THOMAS, J.E., SMART, R.S.C. and SKINNER, W.M., 2000. Kinetic Factors for Oxidative and Non-Oxidative Dissolution of Iron Sulfides. *Minerals Engineering*, 9, vol. 13, no. 10–11, pp. 1149-1159 ISSN 0892-6875. DOI http://dx.doi.org/10.1016/S0892-6875(00)00098-4.

TUTU, H., MCCARTHY, T.S. and CUKROWSKA, E., 2008. The Chemical Characteristics of Acid Mine Drainage with Particular Reference to Sources, Distribution and Remediation: The Witwatersrand Basin, South Africa as a Case Study. *Applied Geochemistry*, 12, vol. 23, no. 12, pp. 3666-3684 ISSN 0883-2927. DOI 10.1016/j.apgeochem.2008.09.002.

VILLENEUVE, M., BUSSIERE, B., BENZAAZOUA, M. and AUBERTIN, M. Assessment of interpretation methods for kinetic tests performed on tailings having a low acid generating potential Anonymous *null*, 2009.

WAPLES, J.S., WICKHAN, M.P., SANDERS, J. and GEAR, J. A Geochemical Testing Program for Reclamation Cover Materials Including Different Kinetic Testing Methods Anonymous *Securing the Future and 8th ICARD*, 2009.

WEBER, P.A., STEWART, W.A., SKINNER, W.M., WEISNER, C.G., THOMAS, J.E. and SMART, R.St.C., 2004a. Geochemical Effects of Oxidation Products and Framboidal Pyrite Oxidation in Acid Mine Drainage Prediction Techniques. *Applied Geochemistry*, 12, vol. 19, no. 12, pp. 1953-1974 ISSN 0883-2927. DOI 10.1016/j.apgeochem.2004.05.002.

WEBER, P.A., THOMAS, J.E., SKINNER, W.M. and SMART, R.S.C., 2004b. Improved Acid Neutralisation Capacity Assessment of Iron Carbonates by Titration and Theoretical Calculation. *Applied Geochemistry*, 5, vol. 19, no. 5, pp. 687-694 ISSN 0883-2927. DOI 10.1016/j.apgeochem.2003.09.002.

WEISENER, C.G. and WEBER, P.A., 2010. Preferential Oxidation of Pyrite as a Function of Morphology and Relict Texture. *New Zealand Journal of Geology and Geophysics*, vol. 53, no. 2-3, pp. 167-176.

WILLIS, J.P., 1999. *Instrumental parameters and data quality for routine major and trace element determinations by WDXRFS.* Information Circular, Department of Geological Sciences, University of Cape Town. pp. 1-12.

YIBAS, B., PULLES, W., LORENTZ, S. and MAIYANA, B., 2011. *Development of Water Balances for Operational and Post-Closure Situations for Gold Mine Residue Deposits to be used as Input to Pollution Prediction Studies for Such Facilities.* South Africa: Water Research Commission.

APPENDIX

APPENDIX A: METHODOLOGY

A.1: Acid Rock Drainage Index

A.1.1: Score allocation for ARDI parameters

ARD Index applied in this study was taken from Parbhakar-Fox (2012)

Parameter A: Sulfide content

Iron sulfide content (%)	ARDI Value
100	10
90	9
80	8
70	7
60	6
50	5
40	4
30	3
20	2
10	1
Contains no sulfides	0

Parameter B: Sulfide Alteration

Degree of Alteration (%fracture/altered)	ARDI value
0 to 10	10
11 to 20	9
21 to 30	8
31 to 40	7
41 to 50	6
51 to 60	5
61 to 70	4
71 to 80	3
81 to 90	2
91 to 100	1

Parameter C: Sulfide Morphology

Meso-scale	Micro-scale	ARDI value
Disseminated >50%	Framboidal <20 μm	10
Disseminated <50%	Framboidal >20 μm	9
Disseminated up to 25%	Anhedral and highly fractured	8
Large crystals >50%	Anhedral	7
Large crystals <50%	Subhedral-anhedral	6
Large crystals < 25%	Subhedral and highly fractured	5
Veins up to 100%	Subhedral	4
Veins <20 mm up to 50%	Euhedral-subhedral	3
Veins up to 25 %	Euhedral and fractured	2
Massive veins	Euhedral	1

Parameter D: Neutralizer Content

		Content around sulfides (%)	ARDI value
Sulfide		100	10
		90	9
		80	8
		70	7
		60	6
		50	5
		40	4
		30	3
		20	2
		10	1
0 sulfide, 0 neutraliser			0
Neutraliser	0 to 20		-1
	21 to 40		-2
	41 to 60		-3
	61 to 80		-4
	81 to 100		-5

Parameter E: Acid former/neutralizer spatial relationship

Contents (%)				ARDI
Sulfide	**Inert (fast weathering)**	**Inert (slow weathering)**	**Primary neutraliser**	
100	0			10
80	20			9
60	40			8
40	60			7
20	80			6
0	100			5
	80	20		4
	60	40		3
	40	60		2
	20	80		1
		100		0
	80		20	-1
	60		40	-2
	40		60	-3
	20		80	-2
	0		100	-1

A.2: ARDI Calculations

ARDI was applied on micro-scale only.

Stage 1:

$$Me = A_{1\text{–}10} + B_{1\text{–}10} + C_{1\text{–}10} + D_{1\text{–}10} + E_{1\text{–}10} = x$$

$$\frac{\sum x}{No.\ of\ \ Me\ \ phases} = X_1$$

Stage 2:

$$Mi = A_{1\text{–}10} + B_{1\text{–}10} + C_{1\text{–}10} + D_{1\text{–}10} + E_{1\text{–}10} = y$$

Me = Meso-scale phase

Mi = Micro-scale phase

A = sulfide content

B = Sulfide Alteration

C = Sulfide Morphology

D = Neutraliser content

E = Association

x or y = Total score (/50)

Σx or Σy = Total score for all phases

X1 = total for Me sample

Y1 = total for Mi sample

$$\frac{\sum y}{No.\ of\ \ Mi\ \ phases} = Y_1$$

Stage 3:

$$\frac{X_1 + Y_1}{2} = ARDI$$

A.2: Chromium Reducible Sulfur Method

1. Weigh accurately 0.500g of dry pulverised sample (-75 μm) into a double-neck round-bottom digestion flask. Include a solution blank in each batch and subject it to the same procedure as the sample.

2. Add 2.0 g of chromium powder and then 10 mL ethanol (95% concentration) to the digestion flask and swirl to wet the sample.

3. Place the digestion flask in the heating mantle and connect to the condenser. The digestion apparatus should be set up in a fume hood.

4. Attach the pressure equalising funnel making sure the gas flow arm is facing the condensers and that the solution tap is shut. Attach Pasteur pipette to the outlet tube at the top of the condenser and insert it into a 100 mL Erlenmeyer flask containing 40 mL zinc acetate solution.

5. Turn on the water flow around the condenser and make sure that all ground glass fittings are tight. Add 60 mL of 6 M HCl to the glass dispenser in the pressure equalising funnel.

6. Connect the N_2 flow to the pressure equalising funnel and adjust the flow to obtain a bubble rate in the zinc acetate solution of about 3 bubbles per second. Allow the N_2 gas to purge the system for about 3 min.

7. Slowly release the 6 M HCl from the dispenser.

8. Wait for 2 min before turning on the heating mantle and adjust the heat so that a gentle boil is achieved. Check for efficient reflux in the condenser. Allow to digest for 20 min.

9. Remove the Erlenmeyer flask and wash any ZnS on the Pasteur pipette into the Erlenmeyer flask with a wash bottle containing deionised water.

10. Measure the sulfide content by UV-Vis following the steps given below:

- Develop a standard calibration curve (Figure B.1) first using a series of known sulfide concentrations.

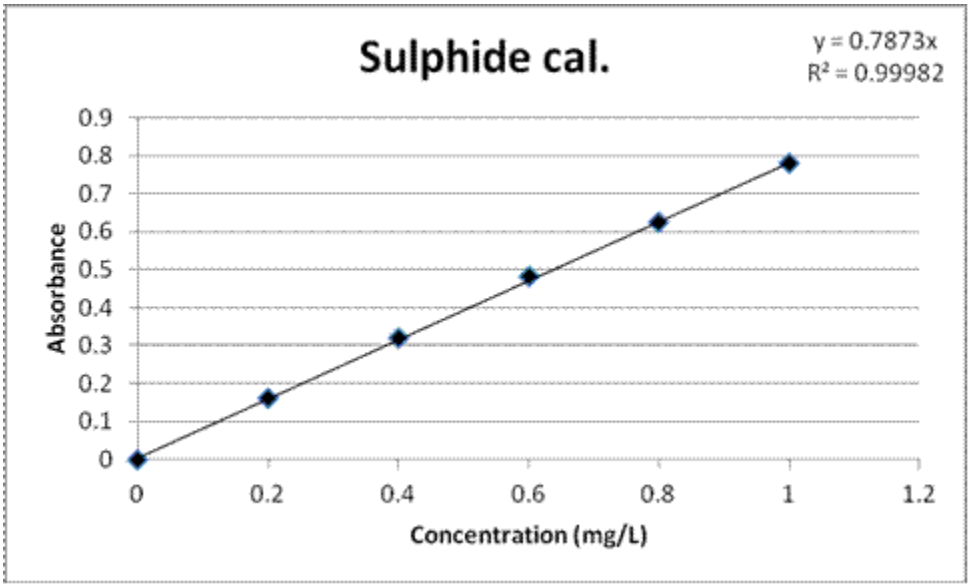

Figure B.1: Standard calibration curve for sulfide

- Use Table B.1 to prepare solutions and to determine which dilution factor to use

Table B.1: Dilution factors for determination of sulphur content by UV-vis

Sulfide concentration (µmole/litre)	Diamine concentration (g/500ml)	Ferric concentration (g/500ml)	Dilution factor (mL:mL)	Path length (cm)
1 – 3	0.5	0.75	1:1	10
3 – 40	2.0	3.0	1:1	1
40 – 250	8.0	12.0	2:25	1
250 - 1000	20.0	30.0	1:50	1

- Pipette 200µL of Zinc Acetate into a test tube
- Add 20µL of sample
- Make up the remaining volume to 5mL with deionised water

- Add 0.5mL of N,N-dimethyl-p-phenylene diamine dihydrochloric
- Add 0.5mL of ferric chloride solution
- Vortex and read at 670nm
- Calculate the concentration of sulfide using the calibration equation and dilution factors

$$[S^{2-}] = \frac{m \times A \times v_1}{v_2 \times v_3 \times M \times 10} \qquad \text{A.1}$$

Where S^{2-} (%) is sulfide concentration, m (L/mg) is gradient of calibration curve, A is absorbance, v_1 (mL) is volume of test tube content, v_2 (µm) is the volume of the sample pipetted into a test tube, v_3 (mL) is final volume of the ZnS solution in 100 mL Erlenmeyer flask, M (g) is the mass of the sample and 10 is units conversion factor.

A.3: KCl extraction

1. Purge a 1M KCl solution with argon gas for 30 minutes prior to conducting the test.
2. Accurately weigh approximately 2.00 g of pulverised sample (-75 µm) into a 125ml plastic bottle.
3. Add 80 ml of purged KCl solution to the bottle.
4. Purge the head space at the top of the bottle with nitrogen or argon gas to remove oxygen.
5. Seal the bottle and shake to mix the contents.
6. Continually mix the contents of bottle in a tumbler for 1 hour.
7. Remove the bottle from the tumbler and filter the sample through a 0.45 µm filter paper.
8. Extract a 30-40ml aliquot of the filtered liquor and titrate with 0.1M NaOH to pH 7.0 to determine acidity (skip this step if pH greater than 7.0).
9. Assay the remaining solution for dissolved S.

A.4: Acid Neutralization Capacity (ANC) tests

A.4.1. Sample and solution preparation

- Leave sample in an open container at room temperature to dry and pulverize it to -75 µm.

- **0.5 M sodium hydroxide:** dissolve 20.0 g of sodium hydroxide pellets in deionized water and dilute to 1 liter. Standardize by placing 50 ml of 0.1 M hydrochloric acid in a beaker and titrate the prepared sodium hydroxide solution to pH 7.
- **0.1 M sodium hydroxide:** dilute 200 ml of the standard 0.5 M sodium hydroxide solution with deionized water up to 1 liter. Standardize by placing 20 ml of 0.1 M hydrochloric acid in a beaker and titrate with the prepared 0.1 sodium hydroxide solution to pH 7.
- **0.5 M hydrochloric acid:** dilute 42 ml of concentrated acid with deionized water up to 1 liter. Standardize by placing 50 ml of anhydrous sodium bicarbonate with known concentration in a beaker and titrate with the prepared HCl solution to pH 7.
- **0.1 M hydrochloric acid:** dilute 200 ml of 0.5 M HCl with deionized water and make up to 1 liter. Standardize by placing 20 ml of anhydrous sodium bicarbonates with known concentration in a beaker and titrate with the prepared HCl solution to pH 7.

A.4.2. ANC calculations and measurements

- Parameters to be measured are final volume, final mass of dried sample, volume of NaOH after back-titrating to pH 7.
- Chemical ANC is calculated by:

$$ANC = \frac{(V_{HCl} - V_{NaOH} \times C) \times 49.0 \times M_{HCl}}{W} \qquad \text{A.2}$$

Where V_{HCl} (ml) is the volume of HCl, V_{NaOH} (ml) is the volume of NaOH, C is the ratio of acid to base added in blanks, 49.0 is a conversion factor for kg H_2SO_4 / ton, M_{HCl} (M) is the concentration of acid and W (g) is the mass of the sample.

- Mineralogical AANC is calculated using the equation:

$$ANC = \sum_{i=1}^{k} \frac{w_a \times 10 \times X_i \times c_i \times n_s}{n_i \times w_i} \qquad \text{A.3}$$

Where w_a is the molecular weight of H_2SO_4,10 is the conversion factor, X_i is the content of mineral in wt. %, c_i is the number of non-oxidisable cations in one formula unit of neutralised mineral i, n_s is the moles of sulfuric acid formed by the oxidation of one mole of sulfide mineral s, n_i is the moles of mineral required to consume n_s, and w_i is the molecular weight the neutralising mineral.

An example for the feed ANC_{MIN}:

Formula	Mineral	X_i	c_i	n_s	w_i	ANC_{MIN}
$CaCO_3$	Calcite	o.5	1	1	100	4.9

A.4.3. AMIRA modified Sobek ANC test

Table A.4.1: AMIRA Fizz Rating

Reaction	Fizz rating	HCl molarity (M)	HCl volume (ml)	NaOH molarity (M)
None	**0**	**0.5**	**4**	**0.1**
Slight	1	0.5	8	0.1
Moderate	2	0.5	20	0.5
Strong	3	0.5	40	0.5
Very strong	4	1.0	40	0.5
Carbonates	5	1.0	60	0.5

1. To determine the amount and concentration of acid to be used in the analysis, the sample is given a "Fizz Rating". This is achieved by placing a small amount of pulverized sample (approximately 0.5 g) on a ceramic plate. One or two drops of 1:3 HCl (approximately 8% HCl) is then added to the sample. The presence of $CaCO_3$ is indicated by a bubbling or audible "fizz" (effervescence). A rating is then given to the scale of reaction obtained as indicated in Table A.4.1.

2. Weigh 2.00 grams of air dried pulverized sample into a clean, dry 250 ml Erlenmeyer flask or beaker. Carefully pipette the required amount of HCl (as indicated in Table A.4.1) into the beaker and add approximately 20 ml of deionized water. Also prepare blanks (in duplicate) by pipetting the same volume and concentration of acid into clean beakers containing no sample and add approximately 20 ml of deionized water. Blanks must be run for each volume and/or concentration of acid used (i.e. for each Fizz Rating used).

3. Place beakers (covered by a watch glass) in a water bath (or hot plate) and heat to 80 to 90^{o}C, swirling the beaker occasionally for 1 to 2 hours or until reaction is complete.

4. Allow the beaker to cool to room temperature. Then add deionized water to give a total volume of approximately 125 ml and measure the pH of the mixture. If the pH is in the range 0.8 to 1.5, then proceed with the titration (Step 5).

NOTE*: If the pH is higher than 1.5, then additional acid is required (except when the test is being run at a fizz rating of 0). For all other fizz ratings (i.e. 1 through 5), if the pH is greater than 1.5 then either additional acid needs to be added to the sample so that the total amount added is equivalent to the next highest fizz rating or the test needs to be re-started on a new sub-sample using the next highest fizz rating.*

If the pH of the mixture is less than pH 0.8, then too much acid may have been added, except when the test is being run at a fizz rating of 5. In such cases it recommended to repeat the test using the next lowest fizz rating.

5. Titrate against standardized NaOH solution (using molarity of NaOH listed in Table A.4.1) with constant mixing. Continue titration to pH 7.0 and record volume of NaOH added. Titrate the "blank" using NaOH as indicated in Table A.4.1.

A.4.4. AMIRA modified Skousen Siderite Correction ANC Method

1. Refer to steps 1 – 4 of AMIRA modified Sobek ANC method
2. Filter digest solution before back titration
3. Back titrate the solution to pH 4.5
4. Add 10 drops of 30% H_2O_2, leave for 15 minutes.
5. Check pH and back titrate to pH 4.5.
6. Repeat steps 9 and 10 until no significant pH change is observed after step 7.
7. Back-titrate to pH 7.
8. Add 10 drops of 30% H_2O_2, leave for 15 min.
9. Check pH and back-titrate to pH 7.
10. Repeat steps 13 and 14 until no significant pH change is observed after step 7.
11. Leave solution for 24 hours.
12. Check pH and adjust with further back titration to pH 7 if required.
13. Add 10 drops of 30% H_2O_2, leave for 24 hours.
14. Repeat steps 16 to 18 over 72 hours.

A.4.5. Modified Lawrence & Wang ANC Method

1. Refer to steps 1 – 2 of AMIRA modified Sobek ANC method
2. Agitate the contents of the flask for 24 hours at room temperature by placing it on an orbital shaker.
3. At the end of the shaking period, check the pulp pH. Refer to step 4 of AMIRA modified Sobek ANC method to ensure appropriate that acid is used.
4. Titrate contents of the flask using 0.1 M or 0.5 M NaOH to pH 7.0. Titrate with NaOH until a constant reading of 7.0 remains for at least 30 seconds.

A.5: Net Acid Generation (NAG) Tests

A.5.1. Sample and solution preparation

- Refer to ANC for sample, 0.5 M NaOH and 0.1 M NaOH preparation
- **15% hydrogen peroxide**: dilute 300 ml of 50% (w/v) hydrogen peroxide with deionised water and make up to 1 litre. Make sure that pH is > 4.5 at all times

A.5.2. NAG calculations and measurements

- Parameters to be measured are final volume, final mass of dried sample, volume of NaOH after back-titrating to pH 7.
- NAG is calculated by:

$$NAG = \frac{49 \times V \times M}{W} \qquad \text{A.3}$$

Where V (ml) is the volume of NAOH, M (M) is the molarity of NaOH and W (g) is the mass of the sample.

A.5.3. Single-Addition NAG Test

1. Weigh 1.25 g sample into 250ml Erlenmeyer flask.
2. Add 125ml 15% H_2O_2, cover, and allow reacting for 24h in a fume hood (make sure the pH is 4.5-6 and record mass of the flask).

3. Measure pre-boil pH.
4. Heat solution until effervescence stops or for a minimum of 2 hours.
5. Allow to cool, make up volume to 125ml with de-ionised water.
6. Record after-boil pH.
7. Filter, retaining solids residue and liquor.
8. Back titrate with NaOH recording volume added at pH 4.5 and pH 7.

A.5.4. Sequential NAG Test

1. Carry out single addition NAG test as stage 1 of sequential NAG
2. Dry solid residue and record its mass
3. Repeat steps 2 to 8 on the dried solid residue.
4. Repeat until no effervescent reaction is seen and NAG pH is > pH 4.5.

A.6: Biokinetic Test

A.6.1. Adaptation of culture

Species used are *Acidithiobacillus ferroxidans* (DSM 584), *Leptospirillum ferriphilum* (ATCC 49881), *Acidithiobacillus caldus* (DSM 8584) and *Sulfobacillus benefaciens* (DSM 19468). The following steps were followed to grow population required to conduct biokinetic tests:

1. Prepare autotrophic basal salts (ABS) solution as follows:
    i. Dissolve 7.5 g $(NH_4)_2SO_4$, 7.5 g $Na_2SO_4.10H_2O$, 2.5 g KCl, 25 g $MgSO_4.7H_2O$, 2.5 g KH_2PO_4 and $Ca(NO_3)_2.4H_2O$ in deionised water and add up to 1 litre.
    ii. Dilute the 50x stock solution to make 1x ABS solution.
    iii. Adjust to pH 2 with H_2SO_4
2. Prepare ferrous medium at a concentration of 5 g/l and a pH of 2.0.
3. Add 3 wt % solids of pyrite.
4. Monitor cultures over 1 to 2 weeks by measuring pH and counting cell.

A.6.2. Test procedure

1. Add 150ml autotrophic basal salts (ABS) solution to 250 ml Erlenmeyer flask.
2. Fit a cotton wool bung, cover with foil and autoclave to sterilise ABS solution.
3. After cooling, weigh in 7.5 g tailings sample to each flask.
4. Inoculate with 7.5 ml mixed culture of iron and sulphur oxidising microorganisms.
5. Measure Redox potential and ensure pH is at 2.0, adjusting with H_2SO_4 if necessary.
6. Weigh each flask and place in shaking incubator at 150 rpm at 37°C.
7. Before sampling, weigh flask. Top up with de-ionised water to account for water loss by evaporation.
8. Record pH, redox, ferrous and total iron concentrations every 2-4 days.

Ferrous and total iron concentrations are determined by 1-10 phenanthroline method. The analysis was conducted using the Helios UV-Vis spectrophotometer at a wavelength of 510 nm and the solution concentration of each sample was calculated using a standard calibration curve (Figure F.1).

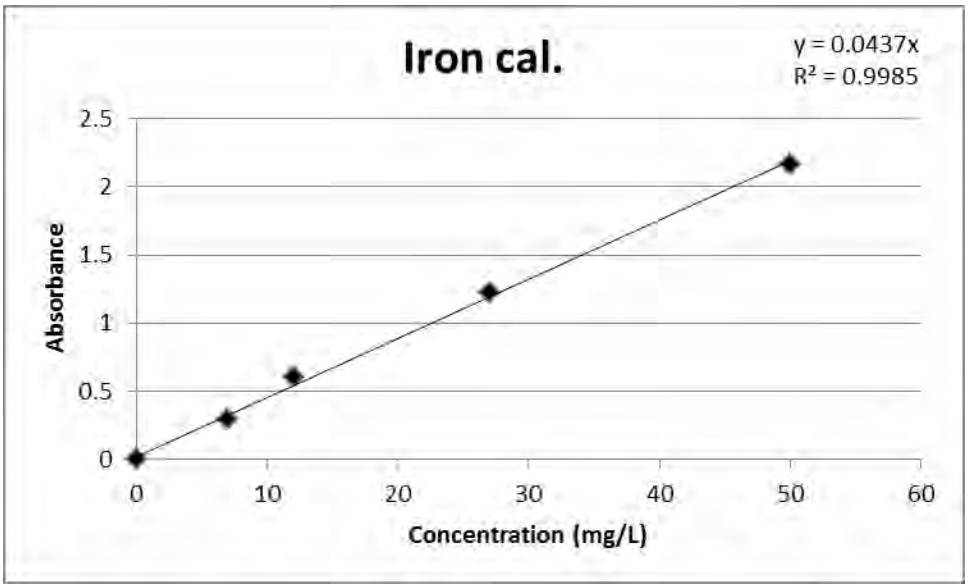

Figure A.6.1: Standard calibration curve for ferrous iron

- Pipette 200 µl of deionised water into a test tube
- Pipette 2 ml ammonium acetate buffer solution
- Pipette 2 ml 1-10 phenanthroline

- Pipette 20 µl sample
- Vortex and run at 510 nm
- For total iron, add a spatula tip amount of hydroxylamine
- Vortex and run at 510 nm
- Calculate both ferrous and total iron concentration using gradient of the standard concentration curve:

$$y = 0.0437x \qquad \text{A.4}$$

Where y is absorbance, 0.0437 (L/mg) is gradient of standard calibration curve and x (mg/L) is iron concentration.

APPENDIX B: EXPERIMENTAL RESULTS

B.1. Feed characterization

B.1.1: Elemental composition of the feed for all the size fractions in wt. %.

Element		Combined	-150/+106	-106/+75	-75/+38	-38/+0
Al	QEMSCAN	4.1	2.3	2.1	2.0	5.5
	XRF	4.4	2.7	2.7	2.9	5.8
Ca	QEMSCAN	0.5	0.5	0.4	0.6	0.6
	XRF	0.6	0.6	0.5	0.6	0.6
Fe	QEMSCAN	4.2	3.7	3.3	4.1	4.6
	XRF	3.0	3.0	2.9	2.9	3.1
K	QEMSCAN	1.2	0.8	0.7	0.6	1.6
	XRF	1.5	0.8	0.9	0.9	2.0
Mg	QEMSCAN	0.5	0.4	0.3	0.4	0.6
	XRF	0.6	0.6	0.4	0.4	0.6
S	QEMSCAN	2.2	2.2	1.9	2.5	2.3
	LECO S	1.3	1.1	1.4	1.7	3.2
Si	QEMSCAN	36.8	39.4	40.3	39.4	34.5
	XRF	37.1	39.2	39.6	39.4	35.3
Ti	QEMSCAN	0.3	0.3	0.3	0.3	0.3
	XRF	0.2	0.2	0.2	0.2	0.2

B.1.2: QEMSCAN Bulk mineralogy of the feed for all size fractions in wt. %

Mineral	Combined	-150/+106	-106/+75	-75/+38	-38/+0
Pyrite	2.3	2.8	1.9	2.4	2.1
Pyrrhotite	2.5	1.8	2.1	2.9	2.7
Other sulfides	0.2	0.1	0.2	0.3	0.3
Sulfates	<0.1	<0.1	<0.1	<0.1	<0.1
Carbonates	0.5	0.4	0.4	0.6	0.6
Quartz	70.7	78.3	80.9	78.9	64.0
Feldspar	3.1	3.2	2.7	3.0	3.2
Mica	12.8	6.8	6.4	5.5	17.8
Chlorite	5.0	3.8	3.2	3.9	6.1
Sphene	0.8	0.9	0.8	1.0	0.8
Fe oxides/hydroxides	1.6	1.6	1.3	1.3	1.8
Others	0.4	0.3	0.3	0.3	0.5

B.1.3: Elemental deportment of the feed in mass %

Element/Mineral	Al	Ca	Fe	K	Mg	Si	S
Pyrite	-	-	25	-	-	-	54
Pyrrhotite	-	-	36	-	-	-	42
Other sulfides	-	-	1	-	-	-	3
Sulfates	-	-	-	-	-	-	-
Carbonates	-	35	-	-	1	-	-
Quartz	-	-	-	-	-	86	-
Feldspar	9	26	-	11	-	2	-
Mica	81	-	5	89	16	8	-
Chlorite	7	11	24	-	83	2	-
Fe oxides/hydroxides	2	-	8	-	-	-	-
Sphene	1	23	-	-	-	-	-

B.1.4: Sulfur speciation and MPA results

Total sulfur	Sulfides	Sulfates	MPA
1.38	1.37	0.008	41.96
1.29	1.29	0.009	39.34
1.33	1.33	0.014	40.81
1.33		0.012	

B.1.5: ANC tests results

Skousen		Sobek		Lawrence and Wang	
pH after heating	ANC	pH after heating	ANC	pH after 24 hours	ANC
2.34	17.43	2.25	14.12	1.96	3.70
2.30	17.43	2.30	14.67	2.00	4.63

B.1.6: NAG test results

Stage 1		**Stage 2**		**Stage 3**	
pH after boiling	NAG	pH after boiling	NAG	pH after boiling	NAG
2.58	24.42	4.39	5.88	4.02	12.15
2.60	25.14	4.26	7.645	3.97	15.64
2.58	23.47	4.38	9.18	4.04	13.69

B.1.7: The pH results for all the biokinetic tests

Days	Abiotic	pH controlled	Non-controlled pH
0	1.96 ± 0.17	1.94 ± 0.04	1.98 ± 0.09
1	2.58 ± 0.20	1.99 ± 0.05	2.21 ± 0.14
2	2.73 ± 0.18	2.01 ± 0.06	2.29 ± 0.28
3	2.78 ±0.16	2.02 ± 0.05	2.38 ± 0.13
4	2.84 ± 0.15	1.99 ± 0.06	2.49 ± 0.04
5	2.88 ± 0.15	2.00 ± 0.06	2.40 ± 0.04
6	3.01 ± 0.13	2.00 ± 0.05	2.27 ± 0.07
7	2.60 ± 0.04	1.95 ±0.09	2.23 ± 0.06
8	2.59 ± 0.11	1.99 ± 0.05	2.19 ± 0.16
11	2.40 ± 0.10	1.97 ± 0.04	2.20 ± 0.07
12	2.30 ± 0.08	1.97 ± 0.04	2.17 ± 0.08
13	2.36 ± 0.12	1.97 ± 0.05	2.16 ± 0.06
14	2.23 ± 0.11	1.86 ± 0.03	2.04 ± 0.06
15	2.25 ± 0.11	2.06 ± 0.02	2.09 ± 0.06
18	2.10 ± 0.06	1.91 ± 0.04	1.97 ± 0.06
21	2.17 ± 0.06	2.09 ± 0.05	2.07 ± 0.06
26	2.03 ± 0.04	1.89 ± 0.03	1.98 ± 0.03
28	2.15 ± 0.04	2.11 ± 0.01	2.08 ± 0.03
32	2.00 ± 0.01	1.87 ± 0.03	1.95 ± 0.03
34	2.08 ± 0.04	2.06 ± 0.02	2.03 ± 0.03
40	2.18 ± 0.06	2.10 ± 0.01	2.12 ± 0.04
49	2.17 ± 0.04	1.98 ± 0.02	2.12 ±0.03
56	2.18 ± 0.04	2.00 ± 0.01	2.12 ± 0.04
63	2.17 ± 0.04	1.98 ± 0.02	2.12 ± 0.03

B.1.8: The redox potential results for all the biokinetic tests

Days	Abiotic	pH controlled	Non-controlled pH
0	443 ± 5	454 ± 15	458 ± 3
1	359 ± 1	434 ± 35	475 ± 9
2	347 ± 3	563 ± 119	634 ± 68
3	349 ± 26	625 ± 83	680 ± 12
4	349 ± 14	654 ± 91	677 ± 13
5	419 ± 36	669 ± 111	702 ± 7
6	413 ± 8	686 ± 69	701 ± 6
7	511 ± 36	678 ± 81	691 ± 9
8	595 ± 33	675 ± 94	703 ± 1
11	698 ± 6	679 ± 116	719 ± 5
12	699 ± 3	676 ± 105	711 ± 6
13	698 ± 18	677 ± 83	710 ± 10
14	698 ± 18	680 ± 78	709 ± 10
15	708 ± 4	685 ± 63	714 ± 6
18	709 ± 2	707 ± 22	714 ± 4
21	703 ± 24	707 ± 10	720 ± 6
26	698 ± 15	703 ± 12	711 ± 3
28	706 ± 1	708 ± 4	711 ± 5
32	713 ± 7	712 ± 8	715 ± 5
34	693 ± 18	698 ± 4	704 ± 5
40	706 ± 9	704 ± 3	707 ± 7
49	705 ± 3	710 ± 4	706 ± 2
56	697 ± 5	695 ± 4	694 ± 1
63	697 ± 5	711 ± 2	697 ± 4

B.1.9: Ferrous iron results for all the biokinetic tests

Days	Abiotic	pH controlled	Non-controlled pH
1	41.0 ± 2.4	27.2 ± 1.3	38.3 ± 3.4
2	9.0 ± 0.3	17.0 ± 1.8	12.3 ± 2.0
3	10.5 ± 0.4	29.9 ± 3.2	13.7 ± 1.9
4	11.7 ± 0.7	27.7 ± 1.8	24.8 ± 2.1
5	13.7 ± 0.6	32.9 ± 2.2	83.1 ± 1.7
6	32.4 ± 2.2	73.0 ± 2.5	38.7 ± 1.6
7	56.6 ± 1.9	34.2 ± 0.3	41.9 ± 1.7
8	47.9 ± 0.1	3.2 ± 0.4	5.2 ± 0.5
11	0.9 ± 0.1	35.5 ± 2.4	2.1 ± 0.01
12	13.3 ± 1.6	9.1 ± 1.3	11.3 ± 1.6
13	1.4 ± 0.01	10.9 ± 1.8	11.9 ± 1.5
15	15.8 ± 2.1	17.8 ± 3.1	2.4 ± 0.1
21	27.6 ± 3.6	35.0 ± 0.8	69.7 ±1.4
26	14.9 ± 2.0	21.9 ± 1.4	41.1 ± 3.2
28	45.8 ±1.8	7.6 ± 1.4	10.1 ± 1.6
32	17.6 ± 2.4	21.3 ± 1.7	21.1 ± 1.8
34	3.1 ± 0.1	2.7 ± 0.1	2.2 ± 0.03
40	31.0 ± 0.2	28.8 ± 0.1	2.1 ± 0.05
49	4.1 ± 0.1	62.2 ± 4.9	12.7 ± 1.7
56	5.8 ± 0.02	11.9 ± 0.5	16.1 ± 1.0
63	8.5 ± 0.8	2.4 ± 0.1	7.6 ± 0.9

B.1.10: Results from the weekly elemental analysis of the biokinetic tests leachates

Day	Abiotic	pH controlled	Non-controlled pH
		Ca	
7	58.3 ± 14.1	74.4 ± 4.2	63.6 ± 5.0
14	50.4 ± 1.4	52.8 ± 6.0	55.5 ± 2.9
21	81.1 ± 6.1	78.6 ± 15.2	96.9 ± 5.5
28	86.1 ± 7.7	84.0 ± 1.9	79.0 ± 4.6
35	85.3 ± 2.1	79.5 ± 4.4	69.9 ± 9.8
		Fe	
7	76.2 ± 41.2	652.2 ± 191.0	214.4 ± 48.6
14	115.3 ± 26.0	387.3 ± 31.7	229.0 ± 58.4
21	164.9 ± 36.7	342.1 ± 27.4	325.9 ± 43.7
28	231.8 ± 37.2	332.0 ± 30.8	285.6 ± 29.5
35	235.9 ± 37.5	312.1 ± 24.0	247.8 ± 24.9
		K	
7	30.1 ± 9.9	40.2 ± 2.3	8.5 ± 4.3
14	10.3 ± 1.4	14.2 ± 9.3	1.7 ±.2
21	3.7 ± 2.1	3.5 ± 4.6	0.6 ± 0.5
28	1.1 ± 0.03	1.2 ± 0.8	1.6 ± 0.4
35	0.18 ± 0.2	0.6 ± 0.2	2.3 ± 2.4
		Mg	
7	46.7 ± 16.6	73.1 ± 5.2	59.8 ± 4.5
14	40 ± 4.4	52.1 ± 6.0	52.2 ± 4.3
21	47 ± 1.0	55.1 ± 10.8	66.4 ± 3.5
28	51.7 ± 9.5	59.4 ± 0.8	55.9 ± 3.5
35	53.7 ± 3.8	58.8 ± 6.7	50.0 ± 6.4

B.1.10: Continued

Day	Abiotic	pH controlled	Non-controlled pH
		Ca	
7	11.6 ± 5.6	21.8 ± 3.7	14.4 ± 0.8
14	12.3 ± 1.7	19.9 ± 1.8	15.3 ± 2.1
21	31.2 ± 1.3	44.4 ± 5.1	43.5 ± 3.0
28	38.0 ± 7.5	51.7 ± 3.2	39.5 ± 3.2
35	43.9 ± 0.9	56.2 ± 5.9	37.2 ± 4.4

B.2. Residues and leachates characterisation

B.2.1: Sulfates content of residues from XRD in wt. %

Mineral	Lawrence and Wang	Sobek/ Skousen	Sequential NAG	pH-controlled	Non-controlled pH
Alunite	nd	nd	nd	<1	<1
Anglesite	< 1	< 1	< 1	< 1	< 1
Jarosite	1	1	1	2	2
Szomolnokite	2	2	2	3	3

B.2.2: Bulk mineralogy of the feed and solid residues from all the tests in wt. %

			ANC tests		NAG test	Biokinetic tests		
Mineral	**Instrument**	**Feed**	**Lawrence and Wang**	**Sobek/Skousen**	**Sequential**	**Abiotic**	**pH-controlled**	**non-controlled pH**
Pyrite	QEMSCAN	2.3	1.5	1.7	0.1	0.1	<lld	<lld
	XRD	0.9	1.0	0.9	<lld	<lld	<lld	<lld
Pyrrhotite	QEMSCAN	2.5	2.2	2.3	0.1	0.1	<lld	<lld
	XRD	1.6	0.6	0.5		<lld	<lld	<lld
Other sulfides	QEMSCAN	0.2	0.6	0.3	0.1	<lld	0.1	<lld
	XRD	nd	nd	nd	nd	nd	nd	nd
Sulfates	QEMSCAN	<0.1	0.2	0.2	<0.1	<0.1	<lld	0.1
	XRD	<0.1	4.4	4.5	4.3	nd	5.7	5.6
Carbonates	QEMSCAN	0.5	<lld	<lld	<lld	<lld	<lld	<lld
	XRD	0.2	0.7	0.7	0.8	nd	0.5	0.4
Quartz	QEMSCAN	70.7	64.5	70.9	70.9	68.6	69.6	75.4
	XRD	68.0	70.3	71.2	72.8	nd	62.0	66.6
Feldspar	QEMSCAN	3.1	8.6	6.4	2.7	3.0	0.8	3.4
	XRD	3.9	3.5	4.0	4.1	nd	4.9	4.7
Mica	QEMSCAN	12.8	16.8	13.3	13.5	21.5	24.1	13.2
	XRD	17.3	13.5	13.0	10.3	nd	22.3	19.2
Chlorite	QEMSCAN	5.0	3.0	3.1	4.7	3.4	2.2	3.2
	XRD	5.1	3.5	3.1	3.3	nd	5.7	5.2
Sphene	QEMSCAN	0.8	0.6	0.5	0.7	0.9	0.1	0.8
	XRD	0.3	1.2	1.2	0.9	nd	0.3	0.3
Fe oxyhydroxides	QEMSCAN	1.6	1.3	1.1	6.3	2.3	2.7	1.4
	XRD	nd	nd	nd	nd	nd	nd	nd
Others	QEMSCAN	0.4	0.6	0.3	0.8	0.2	0.4	0.1
	XRD	2.6	1.8	2.3	3.9	nd	19	1.7
XRD GOF		4.52	9.09	8.92	9.73		4.05	3.89
Final mass			2.3	2.3	2.1	7.3	7.2	7.2

B.2.3: Elemental composition of solid residues from all the tests in wt. %

			ANC tests		NAG tests	Biokinetic tests		
Element	**Instrument**	**Feed**	**Lawrence and Wang**	**Sobek/Skousen**	**Sequential**	**Abiotic**	**pH-controlled**	**non-controlled pH**
Al	QEMSCAN	3.1	5.4	4.0	4.0	4.9	5.7	3.7
	XRF	4.4	5.3	5.4	4.8	5.2	5.2	5.4
Ca	QEMSCAN	0.5	0.2	0.2	0.6	0.3	0.3	0.1
	XRF	0.6	0.3	0.3	0.3	0.3	0.3	0.3
Fe	QEMSCAN	4.1	3.6	3.5	4.5	1.7	1.2	1.0
	XRF	3.0	2.5	2.3	2.2	2.4	1.9	2.2
K	QEMSCAN	1.2	1.3	1.8	1.3	1.4	1.3	1.1
	XRF	1.5	1.3	1.3	1.1	1.9	1.9	1.9
Mg	QEMSCAN	0.5	0.4	0.4	0.5	0.5	0.4	0.3
	XRF	0.5	0.4	0.5	0.5	0.5	0.4	0.5
S	QEMSCAN	2.2	2.0	2.0	0.2	0.1	0.1	<lld
	LECO S	1.3	nd	nd	nd	nd	nd	nd
Si	QEMSCAN	36.8	35.5	37.3	37.1	38.0	40.0	37.7
	XRF	37.1	36.9	37.3	37.3	36.6	37.0	36.8

B.2.4: Elemental composition of the static tests leachates in ppb

Elements	Lawrence and Wang	Sobek or Skousen	Sequential NAG
Al	12986 ± 380	20961 ± 2469	3816 ± 70
Ca	32461 ± 2807	34133 ± 3364	17485 ± 1826
Fe	33296 ± 774	48774 ± 4071	5564 ± 1839
K	5356 ± 123	4720 ± 469	3524 ± 280
Mg	6040 ± 392	9668 ± 873	2561 ± 692
Final volume (ml)	125	125	250

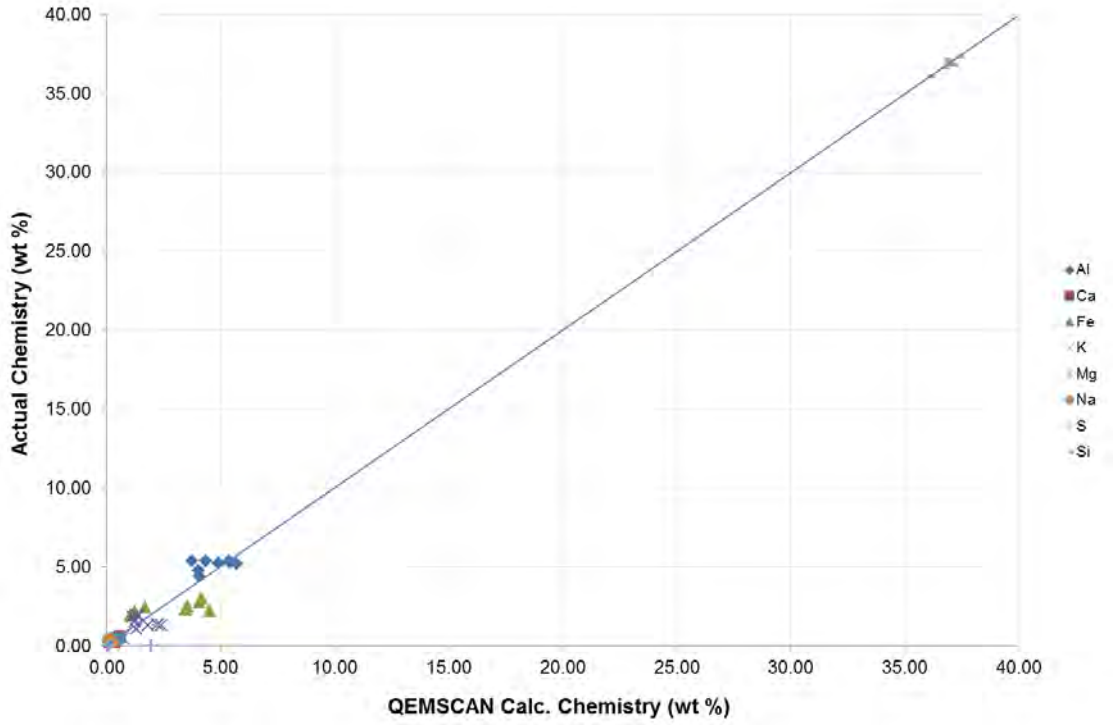

B.2.5: Graph showing the correlation between XRF chemical assay and QEMSCAN data for the major elements present in the solid residues. The x=y shows 1:1 relation.

B.3. Mineral leaching

B.3.1: Mas balance calculations

Conversion of wt. % into g

$$mass\ in\ sample(g) \quad = \quad \frac{wt\% \times final\ mass\ of\ sample(g)}{100\%}$$

%reacted on solid residues

$$\%reacted = 100\% - (\frac{mass\ in\ residue\ (g)}{mass\ in\ feed\ (g)} \times 100\%)$$

%extracted into leachates

$$\%extracted = \frac{mass\ in\ leachate\ (g)}{mass\ in\ feed\ (g)} \times 100\%$$

B.3.2: Extent of elements leaching on the Lawrence and Wang ANC method

Elements	Residues			Classification	Leachates		Classification
	Mass in feed, g	Mass in residue	Extent of reaction, %		Mass in leachate, g	Extent of reaction, %	
Al	0.149	0.123	18	Slightly extracted	0.002	1	Slightly extracted
Ca	0.013	0.006	54	Moderately extracted	0.004	30	Moderately extracted
Fe	0.076	0.059	23	Slightly extracted	0.004	6	Slightly extracted
K	0.042	0.030	29	Slightly extracted	0.001	2	Slightly extracted
Mg	0.015	0.011	30	Slightly extracted	0.001	5	Slightly extracted
Si	0.887	0.859	3	Not-extracted	nd	nd	

B.3.3: Extent of mineral leaching on the Lawrence and Wang ANC method

Mineral Phase	QEMSCAN			XRD			Classification[1]
	Mass in feed, g	Mass in residue, g	Extent of reaction, %	Mass in feed, g	Mass in residue, g	Extent of reaction, %	
Pyrite	0.056	0.034	40	0.024	0.023	2	Moderately reacted
Pyrrhotite	0.061	0.052	15	0.040	0.014	64	Slightly reacted
Carbonates	0.013	<0.001	96	0.006	0.016	-166	Strongly reacted
Quartz	1.767	1.505	15	1.701	1.638	4	Unreacted
Sphene	0.021	0.013	39	0.009	0.028	32	N/A
Feldspar	0.078	0.201	-157	0.097	0.094	2	Formed
Mica	0.320	0.392	-22	0.432	0.314	27	Formed
Chlorite	0.125	0.070	44	0.128	0.080	37	Moderately reacted
Fe oxides/hydroxides	0.040	0.031	24	nd	nd	nd	Slightly reacted
Sulfates	0.001	0.006	-761	<0.001	0.078	undefined	Formed

[1] Classification interpreted on the basis of the relative abundance of the mineral masses in the initial sample (confidence in the results), as well as the extent of mineral reaction from both QEMSCAN and XRD (recognising inherent shortcomings of each dataset)

B.3.4: Extent of elements leaching on the AMIRA modified Sobek and Skousen ANC methods

Elements	Residues			Leachates		Classification
	Mass in feed, g	Mass in residue, g	Extent of reaction, %	Mass in leachate, g	Extent of reaction, %	
Al	0.149	0.124	16	0.003	2	Slightly extracted
Ca	0.013	0.006	55	0.004	32	Moderately extracted
Fe	0.076	0.054	29	0.006	8	Slightly extracted
K	0.042	0.029	31	0.001	1	Slightly extracted
Mg	0.015	0.009	42	0.001	8	Moderately extracted
Si	0.887	0.864	3	nd	nd	Slightly extracted

B.3.5: Extent of mineral leaching on the AMIRA modified Sobek and Skousen Incremental ANC methods

	QEMSCAN			XRD			
Mineral Phase	Mass in feed, g	Mass in residue, g	Extent of reaction, %	Mass in feed, g	Mass in residue, g	Extent of reaction, %	Classification
Pyrite	0.056	0.040	30	0.024	0.022	6	Slightly reacted
Pyrrhotite	0.061	0.054	12	0.040	0.012	70	Slightly reacted
Carbonates	0.013	<0.001	98	0.006	0.015	-145	Strongly reacted
Quartz	1.767	1.642	7	1.701	1.647	3	Unreacted
Sphene	0.021	0.012	42	0.009	0.027	-216	N/A
Feldspar	0.078	0.144	-85	0.097	0.081	16	Formed
Mica	0.320	0.307	4	0.432	0.300	31	Slightly reacted
Chlorite	0.125	0.071	43	0.128	0.071	45	Moderately reacted
Fe oxides/hydroxides	0.040	0.025	38	nd	nd	nd	Moderately reacted
Sulfates	0.001	0.005	-400	<0.001	0.086	undefined	Formed

B.3.6: Extent of elements leaching on the sequential NAG test

Elements	Residues			Leachates		Classification
	Mass in feed, g	Mass in residue, g	Extent of reaction, %	Mass in leachate, g	Extent of reaction, %	
Al	0.149	0.114	24	0.001	1	Slightly extracted
Ca	0.013	0.008	38	0.004	33	Moderately extracted
Fe	0.076	0.053	29	0.001	2	Slightly extracted
K	0.042	0.025	40	0.001	2	Moderately extracted
Mg	0.015	0.012	25	0.001	4	Slightly extracted
Si	0.887	0.892	-1	nd	nd	Not-extracted

B.3.7: Extent of mineral leaching on the sequential NAG test

Mineral Phase	QEMSCAN			XRD			Classification
	Mass in feed, g	Mass in residue, g	Extent of reaction, %	Mass in feed, g	Mass in residue, g	Extent of reaction, %	
Pyrite	0.056	0.003	96	0.024	<0.001	100	Strongly reacted
Pyrrhotite	0.061	0.002	97	0.040	<0.001	100	Strongly reacted
Carbonates	0.013	0.001	95	0.006	0.016	-155	Strongly reacted
Quartz	1.767	1.482	16	1.701	1.522	10	Slightly reacted
Sphene	0.021	0.015	30	0.009	0.018	-114	N/A
Feldspar	0.078	0.057	27	0.097	0.085	12	Slightly reacted
Mica	0.320	0.283	12	0.432	0.215	50	Slightly reacted
Chlorite	0.125	0.098	22	0.128	0.068	47	Slightly reacted
Fe oxides/hydroxides	0.040	0.132	-227	nd	nd	nd	Formed
Sulfates	0.001	0.001	-7	<0.001	0.085	Undefined	Formed

B.3.7: Extent of elements leaching on the abiotic biokinetic test

Element	Mass in feed. g	Mass in residue, g	Extent of reaction, %	Classification
Al	0.446	0.379	15	Slightly extracted
Ca	0.040	0.018	54	Moderately extracted
Fe	0.227	0.176	22	Slightly extracted
K	0.127	0.136	-7	Not-extracted
Mg	0.046	0.034	26	Slightly extracted
Si	2.660	2.659	0	Not-extracted

B.3.8: Extent of mineral leaching on the abiotic biokinetic test

	QEMSCAN			
Mineral Phase	Mass in feed, g	Mass in residue, g	Extent of reaction, %	Classification
Pyrite	0.169	0.006	96	Strongly reacted
Pyrrhotite	0.184	0.004	98	Strongly reacted
Carbonates	0.038	0.001	98	Strongly reacted
Quartz	5.302	4.979	6	Unreacted
Sphene	0.063	0.063	1	N/A
Feldspar	0.234	0.221	6	Unreacted
Mica	0.961	1.558	-62	Formed
Chlorite	0.376	0.244	35	Moderately reacted
Fe oxides/hydroxides	0.121	0.165	-36	Formed
Sulfates	0.002	0.001	27	Slightly reacted

B.3.9: Extent of elements leaching on the pH controlled biokinetic test

Element	Mass in feed. g	Mass in residue, g	Extent of reaction, %	Classification
Al	0.446	0.372	17	Slightly extracted
Ca	0.040	0.018	55	Moderately extracted
Fe	0.227	0.138	39	Moderately extracted
K	0.127	0.133	-5	Negative
Mg	0.046	0.030	34	Moderately extracted
Si	2.660	2.653	0	Not-extracted

B.3.10: Extent of mineral leaching on the pH controlled biokinetic test

	QEMSCAN			XRD			
Mineral Phase	Mass in feed, g	Mass in residue, g	Extent of reaction, %	Mass in feed, g	Mass in residue, g	Extent of reaction, %	Classification
Pyrite	0.169	<0.001	100	0.071	<0.001	100	Strongly reacted
Pyrrhotite	0.184	<0.001	100	0.119	<0.001	100	Strongly reacted
Carbonates	0.038	<0.001	100	0.018	0.034	-82	Strongly reacted
Quartz	5.302	4.984	6	5.102	4.446	13	Unreacted
Sphene	0.063	0.008	87	0.026	0.020	21	N/A
Feldspar	0.234	0.059	75	0.290	0.352	-22	Moderately reacted
Mica	0.961	1.722	-79	1.295	1.596	-23	Formed
Chlorite	0.376	0.161	57	0.385	0.407	-6	Moderately reacted
Fe oxyhydroxides	0.121	0.194	-59	nd	nd	nd	Formed
Sulfates	0.002	<0.001	100	<0.001	0.165	undefined	Formed

B.3.11: Extent of the elements leaching on the non-controlled pH biokinetic test

Element	Mass in feed. g	Mass in residue, g	Extent of reaction, %	Classification
Al	0.446	0.386	13	Slightly extracted
Ca	0.040	0.019	53	Moderately extracted
Fe	0.227	0.157	31	Moderately extracted
K	0.127	0.137	-8	Not-extracted
Mg	0.046	0.034	27	Slightly extracted
Si	2.660	2.651	0	Not-extracted

B.3.12: Extent of mineral leaching on the non-controlled pH biokinetic test

Mineral Phase	QEMSCAN			XRD			Classification
	Mass in feed, g	Mass in residue, g	Extent of reaction, %	Mass in feed, g	Mass in residue, g	Extent of reaction, %	
Pyrite	0.169	<0.001	100	0.071	<0.001	100	Strongly reacted
Pyrrhotite	0.184	0.003	98	0.119	<0.001	100	Strongly reacted
Carbonates	0.038	<0.001	100	0.018	0.027	-48	Strongly reacted
Quartz	5.302	5.428	-2	5.102	4.792	6	Unreacted
Sphene	0.063	0.058	9	0.026	0.022	15	N/A
Feldspar	0.234	0.245	-4	0.290	0.335	-16	Formed
Mica	0.961	0.959	0	1.295	1.382	-7	Unreacted
Chlorite	0.376	0.228	40	0.385	0.374	3	Moderately reacted
Fe oxides/hydroxides	0.121	0.102	16	nd	nd	nd	Slightly reacted
Sulfates	0.002	0.005	100	<0.001	0.144	undefined	Formed